

The Investigation of Freezing-Thawing Effects on Physico-mechanical Properties of Cohesive Soils

Donma-Çözölme Sürecinin Kohezyonlu Toprak Zeminlerin Fiziko-Mekanik Özellikleri Üzerine Etkisinin İncelenmesi

PARISA ADELI GHAREH VIRAN

ASSOC PROF. DR. ADİL BİNAL
Supervisor

Submitted to Institute of Sciences of Hacettepe University
As a Partial Fulfillment to the Requirements
For the Award of the Degree of Master of Science
In Engineering Geology

2015

The topic of the thesis work is “**The Investigation of Freezing-Thawing Effects on Physico-mechanical Properties of Cohesive Soils**” by **PARISA ADELI GHAREH VIRAN** has been approved as a thesis for the degree of **MASTER OF SCIENCE IN ENGINEERING GEOLOGY** by the below mentioned Examining Committee Members.

Prof. Dr. Candan GÖKÇEOĞLU
Head

Assoc. Prof. Dr. Adil BİNAL
Supervisor

Prof. Dr. Murat ERCANOĞLU
Member

Assoc. Prof. Dr. Dilek TÜRER
Member

Assoc. Prof. Dr. Aykut AKGÜN
Member

This thesis has been approved as a thesis for the degree of **MASTER OF SCIENCE IN ENGINEERING GEOLOGY** by Board of Directors of the Institute for Graduate Studies in Science and Engineering.

Fatma SEVİN DÜZ
Director of the Institute of
Graduate Studies in Science

ETHICS

In this thesis study, prepared in accordance with the spelling rules of Institute of Graduate Studies in Science of Hacettepe University,

I hereby declare:

- All the information and documents have been obtained based on the academic rules,
- All audio-visual and written information and results have been presented according to the rules of scientific ethics,
- In case of using others Works, related studies have been cited by the scientific standards,
- All cited studies have been fully referenced,
- No distortion have been made in the data set,
- No part of this thesis has been presented in our University or any other University.

27/07/2015

PARISA ADELI GHAREH VIRAN

ABSTRACT

THE INVESTIGATION OF FREEZING-THAWING EFFECTS ON PHYSICO-MECHANICAL PROPERTIES OF COHESIVE SOILS

Parisa ADELI GHAREH VIRAN

Master of Science, Department of Engineering Geology

Supervisor: Assoc. Prof. Dr. Adil BINAL

July 2015, 104 pages

An apprehending of freezing and thawing effects on cohesive soil is considerable for many construction and environmental subjects. This paper relates the effects of freezing and thawing on physico-mechanical behavior of clayey soils. The capital city of Turkey, Ankara, is located in sequence of lacustrine sediments. At places these sediments contain fine grain soils. Collected undisturbed samples were high plasticity clay and clayey sand that were obtained from the bottom of a construction zone at about 1m depth under the ground surface. Total of 64 molded samples were prepared with constant water content to reflect the moisture condition in the active surface layer. CH and SC soil were analyzed in the laboratory, and found to have the plastic limits (PL) of 33.01% and 22.56%, the liquid limits (LL) of 75.05% and 36.97%, and the plasticity indexes (PI) of 42.04% and 14.41%. The soil samples were classified as “CH” and “SC” by the unified soil classification system. Soil samples for all tests were placed in a refrigerator with a temperature of 18°C for twenty-four hours. Then, they have been removed from the refrigerator and was placed in a room with temperature 21°C and 80% RH humidity for twenty-four hours. As a result, one freezing and thawing cycle was achieved between -18°C (24 hours) and 21°C (24 hours), and it took two days.

Freezing and thawing (FT) sequences were selected as 1, 3, 7, 14 and 21. After each FT sequence, Atterberg limits, sieve analysis, shear strength and consolidation tests were carried out in accordance with ASTM standards. Liquid and plastic limits of soil samples, suddenly, were decreased after first FT cycle. That state is a sign of the change of clay mineral orientation due to freezing and thawing process. The soil classification of clayey sand was changed from "SC" to "SM" after first FT cycle. Furthermore, the coefficient of consolidation and permeability of CH soil had been increased by rising in FT cycles up to 7 and then continue to decline as well as these values of clayey sand start to decrease after 14 FT cycles. The cohesion and internal friction angle increase about 37% and 10.5% for CH soil and SC soil decrease about 80% and 10.5% in value after FT tests.

Keywords: Frozen Soil, Freezing and Thawing Test, Atterberg Limits, Shear Strength, Consolidation, Cohesive soils.

ÖZET

Donma-Çözülme Sürecinin Kohezyonlu Toprak Zeminlerin Fiziko-Mekanik Özellikleri Üzerine Etkisinin İncelenmesi

Parisa ADELİ GHAREH VİRAN

Yüksek Lisans, Jeoloji Mühendisliği Bölümü

Tez Danışmanı: Doç. Dr. Adil BİNAL

Temmuz 2015, 104 sayfa

Son senelerde Türkiye'nin doğu illeri kış aylarında daha fazla kar yağışı almaya başlamış ve sıfırın altında geçen gün sayısı artmıştır. Bunun doğal bir sonucu olarak toprak don derinliği her geçen sene giderek artmaktadır. Özellikle, Erzurum, Kars, Ağrı ve Ardahan illerinde don penetrasyon derinliği yaklaşık 1.5 metreye ulaşmış ve geçmiştir. Yeraltı su seviyesinin yeryüzüne yakın olduğu ovalık alanlarda don etkisi toprağın daha derin kısımlarına kadar ulaşabilmektedir. Bunun sonucu olarak ovalık alanlarda kurulan yerleşim yerlerinde özellikle sığ temellere sahip üstyapılarda (Karayolu, demiryolu, havaalanı vb.) ve alt yapılarda (Kanalizasyon, su şebekesi vb.) önemli hasarlar meydana gelebilmektedir. Kış aylarında donan toprak zemin, ilkbahar aylarına doğru erimekte ve donma-çözülme etkisiyle toprak yapısında meydana gelen değişiklikler toprağın fiziko-mekanik özelliklerinde de değişikliklere neden olmaktadır. Toprağın üst kısmında don etkisiyle hacimsel artışlar meydana gelmekte ve toprak gözenekli bir yapı kazanmaktadır. İlkbahar aylarında toprağın gözeneklerindeki suyun erimesi sonucu toprak aşırı doymun hale gelmesine bağlı olarak efektif gerilim düşmekte, toprak çok yüksek oranda dayanım kaybetmekte ve sıvı davranışa yakın bir davranış göstermektedir.

Soğuk iklime sahip ÷lkelerde yapılan alıřmalar g÷stermiřtir ki, donma-÷z÷lme evrim sayısı arttıkka toprak zeminlerin dayanımları azalmakta ve toprak daha g÷zenekli bir yapıya sahip olmaktadır (Huang, 1983; Chen vd. 1994; Thevanayagam vd. 2002; Coop, 1991; Allman ve Atkinson, 1992, Georgiannou vd. 1990; Jafari and Shafiee, 2004). Toprağın g÷zenekliliğindeki artışa ve dayanımındaki azalmaya paralel olarak sığ temellere sahip yapılarda problemler g÷r÷lmektedir. Özellikle yol yapılarında, ökmeler ve ukurlar oluşmaktadır.

Tez kapsamında, Ankara ilinin farklı iki lokasyonundan (Dumlupınar ve iğdem mahalleleri) toprak örnekleme yapılmıřtır. Laboratuvar ortamında araziden getirilen toprak örneklerinin Atterberg limitleri, tane boyu, özgül ağırlığı, makaslama dayanımı ve konsolidasyon özellikleri belirlenmiřtir. XRD analizleri ile örneklerin ierdiği kil türleri saptanmıřtır. SEM görüntüleme yöntemi ile toprak örneklerinin yapısı belirlenmiřtir.

Donma-÷z÷lme evrimlerini gerekleřtirmek iin, ilk olarak toprak örneklerinin nem ierikleri saf su ile arttırılmıřtır. Doygun hale gelen toprak örnekleri -18°C sıcaklığındaki derin dondurucu iine yerleřtirilmiř ve 24 saat bekletilmiřtir. Daha sonra, dondurucudan ıkarılan örnekler sabit oda sıcaklığında (21°C) ve nemde (% 80 RH) 24 saat beklemeye bırakılmıřtır. Sonuç olarak, donma ve ÷z÷lme (D) evrimleri -18 °C (24 saat) ve 21 °C (24 saat) arasında gerekleřtirilmiř ve bir donma-÷z÷lme evrimi iki gün sürmüřtür. D evrim sayıları 1, 3, 7, 14 ve 21 olarak seilmiřtir. Uygulanan donma ve ÷z÷lme yöntemi tüm deney türleri iin aynıdır. D evrimlerinden sonra, özgül ağırlık belirleme, kıvam limitleri tayini, elek analizleri, konsolidasyon, doğrudan makaslama deneyleri, XRD analizi ve SEM görüntülemeleri yapılmıřtır.

Tez kapsamında sahadan alınan toprak örnekleri seilen D evrimine tabi tutulmuş ve ilk donma ve ÷z÷lme evriminden sonra bu örneklerin fiziksel ve dayanım özelliklerinin aniden azaldığı gözlemlenmiřtir. Ayrıca, kohezyonlu zeminlerin farklı fiziko-mekanik özellikler gösterdiği 7 ve 14 D evrimi arası eşik değeri olarak belirlenmiřtir. Elde edilen bu sonuçlara göre, hafif yapıların inřasından önce, inřaat sahasından alınacak toprak örneklerinin, arazinin donma ÷z÷lme evrim sayısına göre D deneylerine tabi tutulması oldukça önemlidir. Duraylılık analizleri de bu sonuçlara göre gerekleřtirilmelidir.

Anahtar Kelimeler: Donma ve Çözölme, Kıvam Limitleri, Makaslama Dayanımı, Konsolidasyon, Kohezyonlu topraklar.

ACKNOWLEDGEMENTS

I am immensely thankful to God for being an imperceptible driving force throughout my life. I wish to express my deep appreciation and gratitude to my advisor Assoc. Prof. Dr. Adil Binal for believing in me, his guidance, motivation, tremendous knowledge and insightful comments helped me throughout my masters.

I gratefully acknowledge Prof. Dr. Candan Gökçeoğlu, Prof. Dr. Murat Ercanoğlu, Assoc. Prof. Dr. Dilek Türer and Assoc. Prof. Dr. Aykut Akgün for being a part of my committee. Special thanks to my teachers' and friends Otgon Namki, Nazlı Tunar Özcan and Dr. Gülseren Dağdelenler, who have supported me in the true sense of the word, listening to me and guiding me. I will always cherish the good moments we had together. I would like to thank geotechnical laboratory's Responsible Prof. Dr. Murat Ercanoğlu and technician Özgür Erol for his enormous help and for making the work environment amiable. I also benefited a great deal by the help of in setting up the laboratory instruments.

I will be eternally indebted to my mother and father for everything which cannot be put into words, despite their physical absence their love and backing has helped me in the successful completion of my study at Turkey. Finally, I am thankful to everybody at Hacettepe University who made my programme successful and memorable.

CONTENTS

	<u>Page</u>
ABSTRACT	i
ÖZET	iii
ACKNOWLEDGEMENTS.....	vi
CONTENTS.....	vii
TABLES.....	ix
FIGURES	x
SYMBOLS AND ABBREVIATIONS.....	xiii
1. INTRODUCTION.....	1
2. LITERATURE REVIEW	3
2.1. Permafrost Soil.....	3
2.2. Geomechanical Properties of Permafrost Soil.....	3
3. STUDY AREA AND SAMPLING	12
3.1. Location and Transportation.....	12
3.2. Climate	12
3.3. Geological conditions of the area	16
4. MATERIALS	20
4.1. CH Soil	20
4.2. Clayey Sand Soil (SC).....	23
5. METHODS AND RESULTS	26
5.1. Specific Gravity and Density.....	27
5.1.1. Sample Preparation.....	27
5.1.2. Test Results	28
5.2. Atterberg Limits	29
5.2.1. Sample Preparation.....	29
5.2.2. Test Results	30
5.3. Grain Size Analyses	36
5.3.1. Sample Preparation.....	36
5.3.2. Test Results	37
5.4. Clay Activity.....	42

5.5. Shear Strength	44
5.5.1. Sample Preparation.....	44
5.5.2. Test Results	44
5.6. Consolidation.....	48
5.6.1. Sample Preparation.....	48
5.6.2. Test Results	48
5.7. XRD Analyses	51
5.8. Scanning Electron Microscopy (SEM) Studies	54
6. CONCLUSIONS AND RECOMMENDATIONS	59
REFERENCES.....	61
Appendix A. Unified Soil Classification System (USCS).....	67
Appendix B. Atterberg Limit Changes	68
Appendix C. Grain size distribution	70
Appendix D. Direct Shear Box Test.....	76
Curriculum vitae	88

TABLES

	<u>Page</u>
Table 2.1. Cohesion and frictional angle for soils tested (Czurda and Homann,1997).	8
Table 4.1. Some properties of CH	22
Table 4.2. Some properties of SC	25
Table 5.1. ASTM standards used in tests.....	27
Table 5.2. Specific Gravity of CH and SC soils.	28
Table 5.3. Atterberg limits values (%).....	31
Table 5.4. Atterberg limit changes (%)	31
Table 5.5. Changes in the ratio of grain size depending on FT cycles	38
(a) CH and (b) SC soils.	38
Table 5.6. Shear strength parameters.....	45
Table 5.7. Change (%) in shear strength parameters.....	45
Table 5.8. The percentages of CH soil's minerals	51
Table 5.9. The percentages of SC soil's minerals	51

FIGURES

	<u>Page</u>
Figure 2.1. Loss of weight (%) of the specimens (Aubert and Gasc-Barbier, 2012).	4
Figure 2.2. Stress–strain behavior of clay soils experienced freeze–thaw cycles under different confining pressure (200 to 800 kPa) (Wang et al. 2007).	5
Figure 2.3 The variations of the coefficient of consolidation with freeze-thaw (Wang and Bhuwani, 2010).	6
Figure 2.4. Effects of soil moisture content at freezing and the number of freezing and thawing cycles on aggregate stability in different types of soils (AD: air dry; FC: Field capacity; NS: Near saturation) (Taskin and Ferhan, 2003).....	7
Figure 2.5. (a) Moisture-cohesion curves and (b) moisture-internal friction curves before and after frozen-thaw with 95% soil compaction (Guo and Shan, 2011)	9
Figure 2.6. SEM images and binary images.....	10
Figure 3.1. The sampling area.....	13
Figure 3.2. The average rainfall and temperature of Ankara between 1944-2006 years (Anonim 2006).....	14
Figure 3.3. Frost index and frost depth penetration map of Turkey (Republic Of Turkey General Director of Highways, 2008).	15
Figure 3.4. Stratigraphic Columnar Section of Ankara (Kasapoğlu, 1980).	18
Figure 3.5. 1: 100 000 scale geological map of the Ankara valley and around (Akyürek et al. 1997)	19
Figure 4.1. Plasticity chart of soil sample	20
Figure 4.2. Sieve Analysis of CH soil	21
Figure 4.3. Failure envelope of CH.....	21
Figure 4.4. XRD analyses of CH (S: Smectite, I: Illite, K: Kaolin, Q: Quartz, F: Feldspar, Ca: Calcite).....	22
Figure 4.5. Sieve analysis of SC	23
Figure 4.6. Failure envelope of SC.....	24
SC composes of quartz, feldspars, calcite and clay minerals (Figure. 4.7).	24
Figure 4.7. XRD analyses of SC (Q: Quartz, F: Feldspar, Ca: Calcite)	24

Figure 5.1. Isoline map of the freeze-thaw severity index of Turkey (numbers indicated freeze and thaw cycles) (Binal A, 2008).	26
Figure 5.2. Specific Gravity Test	28
Figure 5.3. The relationship between FT cycles and Liquid Limit changes of.....	32
(a) CH and (b) SC soils.	32
Figure 5.4. The relationship between FT cycles and Plastic Limit changes.....	33
of (a) CH and (b) SC soils.	33
Figure 5.5. The relationship between FT cycles and Plasticity Index changes.....	34
of (a) CH and (b) SC soils.	34
Figure 5.6. Plasticity chart for CH soil.	35
Figure 5.7. Plasticity chart for SC soil.....	35
Figure 5.8. Total mass of samples that passing No. 4 sieve	36
Figure 5.9. Hydrometer analysis procedure.....	37
Figure 5.10. Grain size distribution for CH soil	39
Figure 5.11. Grain size distribution for SC soil	40
Figure 5.12. Variation of fine particles (a) Clay, (b) Silt	41
Figure 5.13. Variation of coarse particles (a) Sand, (b) Gravel.....	41
Figure 5.14. Clay activity for (a) CH and (b) SC soils.	43
Figure 5.15. Cohesion (c) of (a) CH and	46
(b) SC soils after FT cycles.	46
Figure 5.16. Internal friction angle (Φ) of (a) CH and.....	47
(b) SC soils after FT cycles.	47
Figure 5.17. Coefficient of Consolidation (C_v) of a) CH and b) SC soils.....	49
Figure 5.18. Coefficients of permeability (k) of	50
a) CH and b) SC soils.....	50
Figure 5.19. XRD analyses of (a) CH and (b) SC soils (Q: Quartz, F: Feldspar,	53
Ca: Calcite).....	53
Figure 5.20. SEM micrographs of CH a) Fresh, b) one FT cycle, c) 3 FT cycles, d) 7 FT cycles, e) 14 FT cycles and f) 21 FT cycles.....	54
Figure 5.21. SEM micrographs of SC a) Fresh, b) one FT cycle, c) 3 FT cycles, d) 7 FT cycles, e) 14 FT cycles and f) 21 FT cycles.....	55

Figure 5.22. Converting the SEM views of CH soil into black and white color; a) for fresh sample, b) for sample exposed 3 FT cycles, c) after 7 FT cycles, d) 14 FT cycles e) 21 FT cycles.....	57
Figure 5.23. The determination of white and black colors to investigate cracks propagation in CH soil; a) for white color represented voids, b) for black color symbolized particles.	58
Figure 5.24. The determination of white and black colors to investigate cracks propagation in SC soil; a) for white color represented voids, b) for black color symbolized particles.	58

SYMBOLS AND ABBREVIATIONS

Gs	Specific Gravity
ρ	Density
Φ^0	Internal Friction Angle
c	Cohesion
Cv	Coefficient of Consolidation
k	Coefficient of Permeability
PI	Plasticity Index
LL	Liquid Limit
PL	Plastic Limit
Ac	Clay Activity
FT	Freezing-Thawing
F	Feldspar
I	Illite
Q	Quartz
S	Smectite
Ca	Calcite
K	Kaoline
CH	High Plasticity Inorganic Clay
SC	Clayey Sand
MH	High Plasticity Inorganic Silt
USCS	Unified Soil Classification System
XRD	X Ray Diffraction Analysis
SEM	Scanning Electron Microscopy

1. INTRODUCTION

The design and construction of earth structures influenced seasonally by subzero temperatures requires the determination of mechanical properties of the construction materials under appropriate thermal conditions. Water saturated materials exhibit a zone of partially frozen soil at the frozen-unfrozen soil interface. To define the critical failure surface and governing shear strength in this zone, the effects of partial freezing on the mechanical behavior as a freezing front advances, must be well understood (Hohmann and Czurda, 1997). The researchers which were conducted in the countries with cold climate have indicated that the increase in the number of freezing and thawing cycles weakens soil strength while creating high porosity in the soil (Huang, 1983; Chen, et al., 1994; Thevanayagam et al. 2002; Coop, 1991; Allman and Atkinson, 1992; Georgiannou et al., 1990; Jafari and Shafiee, 2004).

In recent years, the eastern part of Turkey has begun to take more precipitation in the winter. Simultaneously soil frost depth increased with year. Frost depth in the city of Erzurum has reached about 1 m. The soil and ground pores water freezes in winter and melts by starting spring. Changes occurring in the soil that caused by freezing and thawing, have an important effects on soil physico-mechanical properties. In studies conducted in countries with cold climates, it was determined that by increasing number of freeze-thaw cycles, soils lose their cohesion and become a porous structure. In parallel with the loss of soil strength, it was observed that engineering structures with shallow foundation having problems, with collapse and pits formed in the road construction.

The aim of this thesis is that subjected clay and clayey sand samples to repeated number of freeze-thaw cycles in laboratory to determine the changes in the physical properties and mechanical parameters. For this aim, the cohesive soil samples have been collected from the regions with colder climates. In the laboratory, grain size, porosity, density, specific gravity, natural moisture content and clay content of soil samples obtained from the field have been determined. Types of clay were examined with the XRD analysis as well as fabric of soil samples were determined by SEM imaging. To determine the initial mechanical parameters of the soil samples, Atterberg limits, direct shear, and consolidation tests have been performed.

After detecting the initial physical-mechanical parameters of samples, they have been performed on a certain number of freeze-thaw cycles. At the end of the cycles, physico-mechanical properties have been determined again. The results obtained from tests before and after the freeze-thaw cycles, have been compared with each other and the changes in results have been determined. Also, the changes occurring in the soil structure that have been subjected to freeze-thaw have been observed by SEM imaging.

2. LITERATURE REVIEW

2.1. Permafrost Soil

Permafrost is frozen soil, permanently. Its classification is based on temperature, not moisture or ground cover. The ground must remain below 0°C for at least two years to be considered permafrost (Turetsky et al., 2007).

2.2. Geomechanical Properties of Permafrost Soil

Wang et al. (2015) investigated the subgrade fill material from the Nagqu Logistics Center Yard (NLCY). They thoroughly analysed the thaw subsidence properties and dynamic properties in the laboratory tests. Samples with a higher degree of compactness displayed heave while during those with a lower level of compactness shown compressive strain deformation after repeated freezing and thawing cycles. Furthermore, the dynamic modulus increases and the damping ratio decreases as the confining pressure and compactness increase.

Aubert and Gasc-Barbier (2012) worked own conventional method for cycles of freezing- thawing, which the samples immersed used. Samples saturated by placing them in a humid environment (Relative Humidity: RH 95% and 20°C) for one week and then subjected to cycles of freezing - thawing without any re-wetting between cycles. The variation of weight and compressive wave velocity showed that freezing-thawing cycles led to the desiccation of the samples. The subsequences of these cycles on the characteristics of the soil blocks were thus those of a conventional desiccation of specimens and, in particular, their hardening. This hardening highlighted by the study of the mechanical characteristics of the clayey soil blocks (Figure 2.1)

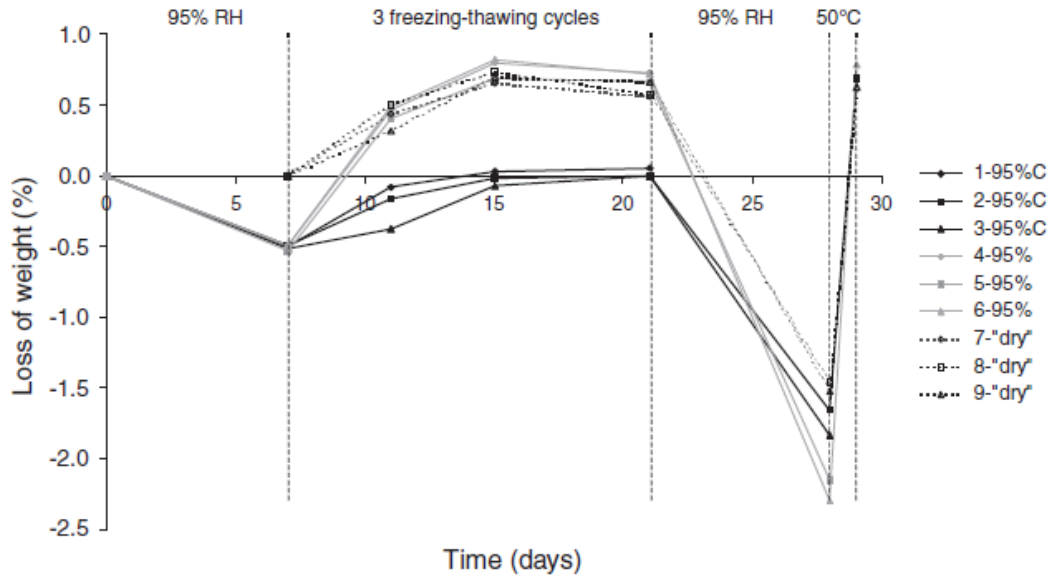


Figure 2.1. Loss of weight (%) of the specimens (Aubert and Gasc-Barbier, 2012).

Wang et al. (2007) in their work on Qinghai-Tibet clays applied to 21 of freezing-thawing cycles in the temperature range of -7°C to $+14^{\circ}\text{C}$. As well as in the lateral pressure range of 200 to 800 kPa. After seven cycles of freezing-thawing, increase of volume, decreases of water content and cohesion, and no changes of angle of internal friction determined. In the other way by increasing the freezing and thawing cycle's samples start to behave hardening-strain to softening-strain (Figure 2.2).

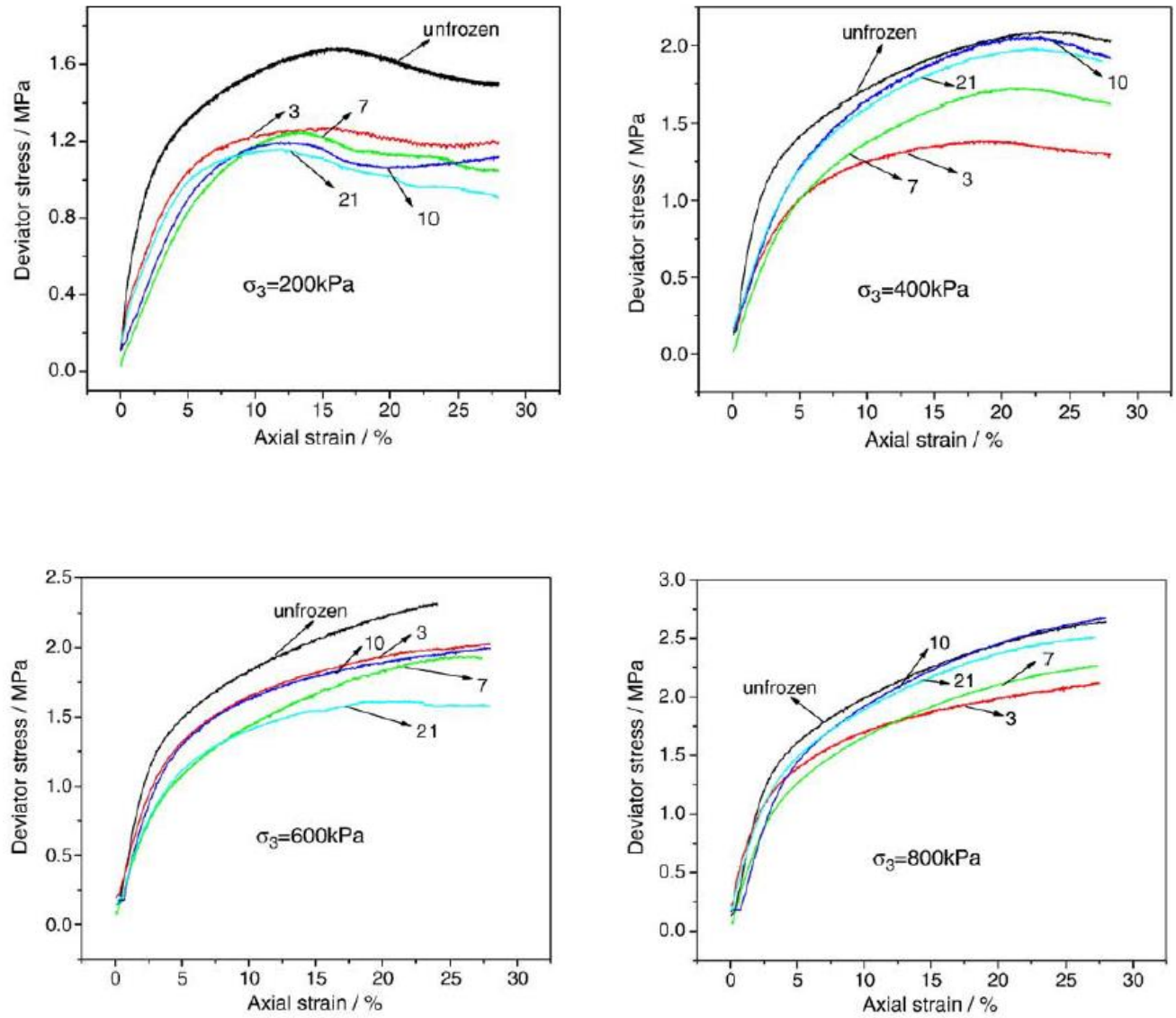


Figure 2.2. Stress–strain behavior of clay soils experienced freeze–thaw cycles under different confining pressure (200 to 800 kPa) (Wang et al. 2007).

In the study of Yıldız et al. (2012), they subjected 6% lime-stabilized clay samples that have high and low plasticity up to 14 freeze-thaw cycles (28days) in temperature range of -10 °C to +22 °C. Results of this study indicated that the hydraulic conductivity of the samples increased by 1000 times, but only after the third cycle, hydraulic conductivity increased by 10 to 20 times in clays that toughened. After 28 days, the strength of the soils that have high plasticity 15 times as well as have low plasticity increased three times. In the other hand, the strength of both stabilized clays decreased 10–15% at the end of the freeze-thaw cycles.

Wang and Bhuwani, (2010) in their research in Canada, took soil samples obtained from the bottom of the active layer of permafrost zone at an about one-meter depth. They were tested samples in the laboratory conditions which reflected the natural conditions. As to this study, the values of consolidation and hydraulic conductivity coefficient increased due to an increased number of freeze-thaw cycles (Fig. 2.3).

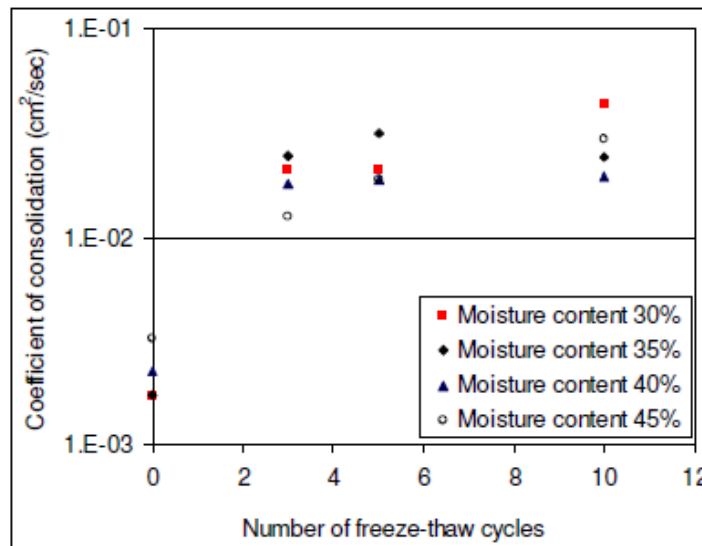


Figure 2.3. The variations of the coefficient of consolidation with freeze-thaw (Wang and Bhuwani, 2010).

Taskin and Ferhan (2003) study about effect of freezing and thawing on soil stability that formed from different mother rocks and grain size groups with varying water content, periods of freezing (3-6-9) and freezing temperatures (-4°C and -18°C). The initial stability of materials decreased from 28.6 % to 51.7 % with the effect of freezing-thawing depending on the soil type. In general, by increasing the number of cycles of freezing from 3 to 6, wet aggregate stability increased and decreased after that point. The percentage of water stable aggregates in all types of soils at -18°C degrees is less than -4°C (Fig. 2.4).

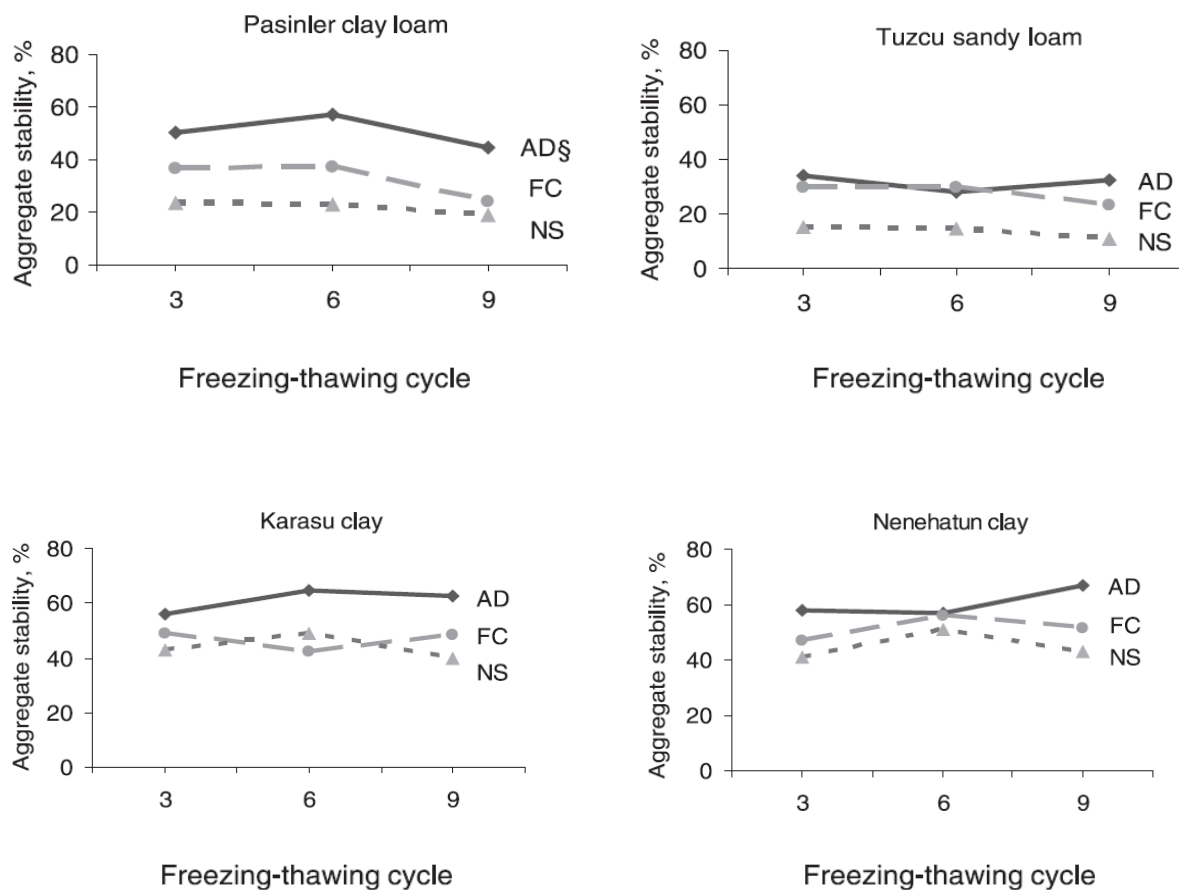


Figure 2.4. Effects of soil moisture content at freezing and the number of freezing and thawing cycles on aggregate stability in different types of soils (AD: air dry; FC: Field capacity; NS: Near saturation) (Taskin and Ferhan, 2003).

Wang et al. (2006) have done ultrasonic measurements and dilatation on frozen clay, frozen loess and frozen sand of Peking, which performed on cylindrical samples under different freezing temperatures. Their measurements shows that the influence of grain size and temperature of freezing soil on propagation of ultrasonic wave velocity at frozen soil is due to the variation of unfrozen water which adjusted by the above-mentioned factors under the other conditions being equal. The results show that ultrasonic wave velocity and dynamic mechanical parameters of frozen soil depends on soil type and freezing temperature. P-waves and dynamic elasticity modulus of soil decrease with increasing temperature. Dynamic Poisson's ratio increases with increasing temperature and decreases when grain size becoming coarse.

Czurda and Homann (1997) in their study give a testing procedure for five clayey soil that describes series of direct shear tests for investigating effect of different freezing conditions on the shear strength of the clayey soils. It can be concluded from the obtained results that changes in the shear strength of frozen soil with time and temperature is due to changes in ice cohesion, and frictional resistance may be regarded as essentially constant (Table 2.1).

Table 2.1. Cohesion and frictional angle for soils tested (Czurda and Homann,1997).

Soil	Shear parameter	System of freezing			
		unfrozen	closed system	open system	
				depth 7–9.5 cm	depth 4.5–7 cm
Kaolin/Hirschau	ϕ (°)	18.8	66.2	21.0	25.2
	c (kPa)	10.8	189.0	13.4	10.9
Tixoton	ϕ (°)	10.5	45.0	22.4	19.6
	c (kPa)	96.3	112.5	63.7	78.2
Maulbronn	ϕ (°)	34.0	46.0	28.0	28.5
	c (kPa)	24.0	152.5	13.4	22.6
Wiesloch UN	ϕ (°)	11.0	46.8	19.9	21.2
	c (kPa)	43.0	160.0	27.5	51.9
Wiesloch D	ϕ (°)	11.0	48.3	17.0	17.0
	c (kPa)	45.0	132.0	30.2	54.7

Aldaoood. A., et al., (2014) investigate the effect of freeze-thaw cycles on the mineralogical and mechanical behaviour of soils stabilized with gypsum. Laboratory research related to this study consists of fine-grained soils with different gypsum contents (0, 5, 15 and 25%). Soil samples stabilized with 3% lime, at 20 °C and cured for 28 days. A series of unconfined compression and the wave velocity tests carried out. pH, electrical conductivity, water content and volume changes estimated. The analysis shows that freezing-thawing cycles reduce unconfined compressive strength of soil samples. Gypsum soil samples lose significant amounts of their strength after a few number of freezing and thawing cycles. Also, during periods of applied water content increase and cause significant changes in the volume of gypsum in the soil. Water content during the applied cycles increases and induces substantial volume changes with the gypsum content in the soil.

Guo and Shan (2011) investigated the effect of freeze-thaw cycles and water content on soil cohesion and internal friction angle by using triaxial test for 1, 2 and 5 freezing and thawing cycles. Results show that, when soil water content is less than optimum water content, soil cohesion increases with increasing moisture, and while soil water content is bigger than the optimum water content, soil cohesion decline with increasing moisture and the peak value of soil cohesion is near the optimum water content. Besides, the internal friction angle of soil decreases with the increasing moisture (Fig.2.5).

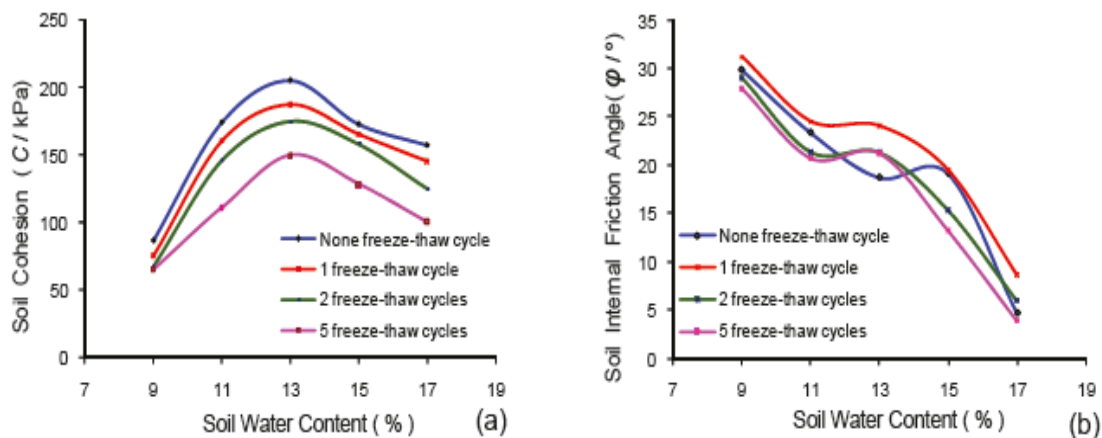


Figure 2.5. (a) Moisture-cohesion curves and (b) moisture-internal friction curves before and after frozen-thaw with 95% soil compaction (Guo and Shan, 2011)

Cui et al., (2014) were investigated mechanical characteristics and quantitatively analysis of the scanning electron microscope (SEM) images of silty clay before and after freezing and thawing. Undisturbed soil samples have been frozen for 12 hours at -20°C in deep freeze. Then sealed and conserved in plastic bags and thawed for 72 hours in water at room temperature. Results show that after freezing and thawing, the equivalent diameter of particle decreased and soil becomes looser because the cementation body between soil particles damaged when pore water frozen to ice, so it cause disintegration and dispersion of the soil particles (Figure 2.6).

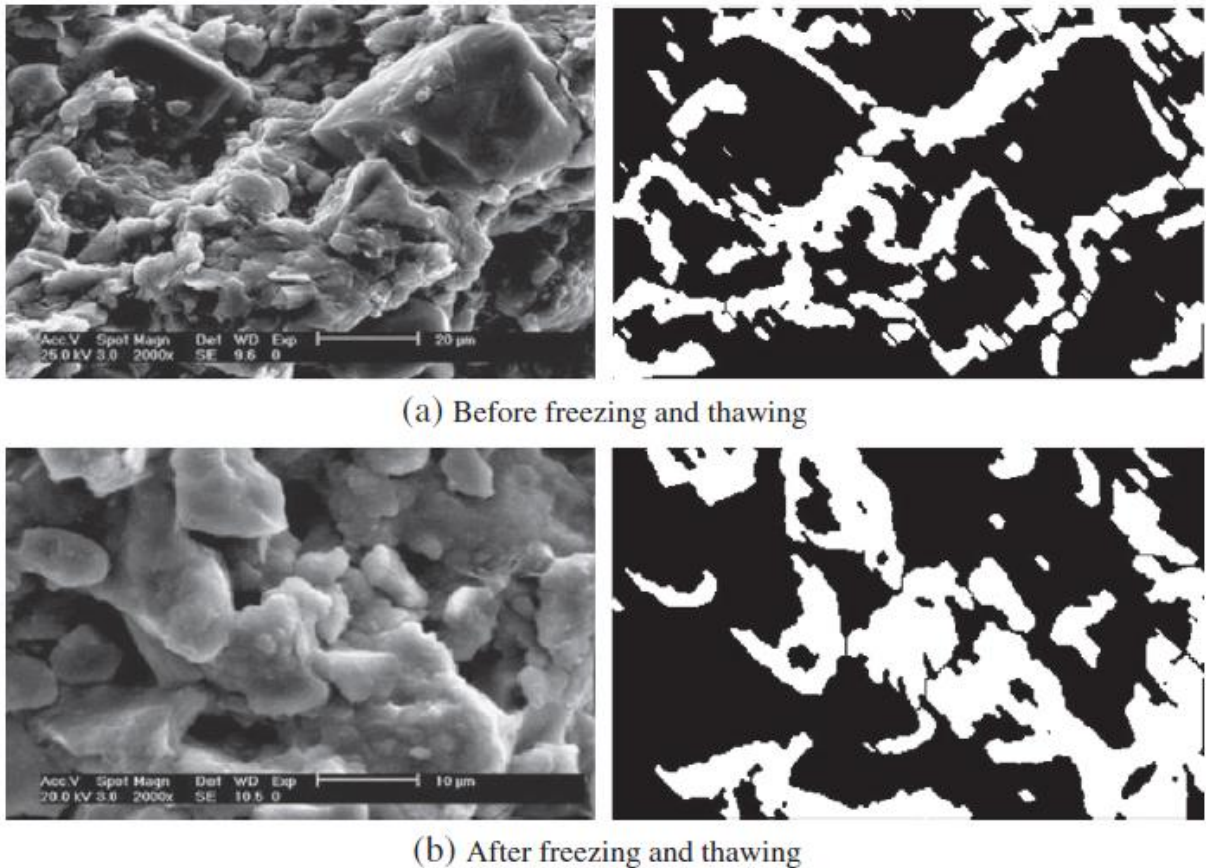


Figure 2.6. SEM images and binary images.

When the temperatures rise above freezing the ice within the soil melts, leaving behind a void space that the ice occupied. The changes in pressure and void space caused by freeze-thaw cycles can have a direct impact on the physical characteristics of a soil, resulting in a change in the soils' hydrologic properties (Flerchinger et al., 2005).

Freeze events reduce the permeability of soils, by filling void spaces within the soil with ice, which results in a decrease in the infiltration capacity of the soil while frozen (Flerchinger et al., 2005). There is also a reduction in the soil aggregate stability of soils after freeze-thaw cycles. There is a larger reduction in stability with increased soil moisture at the time of freezing (Lehrsch et al., 1991; Oztas and Fayetorbay, 2003). This reduction in soil aggregate stability can also influence a soil's infiltration rate and hydraulic conductivity (Lehrsch et al., 1991).

The infiltration rate of a soil during freeze-thaw cycles is also limited due to differential pressures in the soil during freezing (Watanabe et al., 2011). Investigation of the relationship between unfrozen water content and pressure head within soils performed using ceramic soil column studies by Watanabe et al. (2011). Their study investigated three different soils (sand, loam, and silt loam) in soil columns outfitted with thermocouples, time domain reflectometry and tensiometers. Their column was 35 cm tall and had a diameter of 7.8 cm, and was made of ceramic to insulate the columns, and limit temperature interaction between the soil and the surrounding air during freeze-thaw cycles. Freeze-thaw cycles generated by two temperature control units placed at the base and the top of the column. Top down freezing cycles generated in the column by setting the bottom temperature control unit to 2°C and the top unit to either -8°C or -10°C (depending on the mixture). Watanabe et al.'s (2011) study tested five soil columns with different durations of freezing. Their study concluded that there excess water present in the soil after the freezing front passed through it, though the magnitude of excess water dependent on the soil mixture type. The excess water after the freezing front passes could be because during thaw events the ice within the soil often melts more rapidly than it can be reabsorbed into the surrounding media, this can result in a supersaturated soil that has a much higher (approximately 14 times) chance of surficial soil erosion due to the loss of shear strength within the soil (Flerchinger et al., 2005).

3. STUDY AREA AND SAMPLING

3.1. Location and Transportation

For this study the soil blocks have been taken from two different construction areas of Ankara:

Fifteen soil blocks were supplied from an area that is near the south of Eskişehir highway (Soğütözü district) with depth of 1 m and khaki-grey color. As well, the color of Ankara Clay (CH) the sampling area is generally grey-brown or brown, and another fifteen soil blocks were supplied from West of Konya highway (Çiğdem districts) with depth of 1 m and khaki-grey color (Fig. 3.1).

3.2. Climate

Ankara has continental climate which are winters less rainy and cold and summers are hot and dry. The most rainfall is in spring season. Significant differences in temperature seen between summer and winter seasons and between day and night. Respectively the hottest months are July (average 23.1 °C) and August (average 23.3 °C), while the coldest months are January (average 0.3 °C) and February (average 1 °C). The average humidity of forty-five years is 60%. The average rainfall and temperature of Ankara between 1944-2006 years were 32.76 and 11.79 ° C (Anomim 2006) (Figure 3.2). Frost depth in Ankara varies between 60 and 80 cm. Therefore, to obtain undisturbed and unfrozen samples, soil samples were taken from the depth of 1 m. Frost index and frost depth penetration of Turkey shows in the figure 3.3 (Republic of Turkey General Director of Highways, 2008).

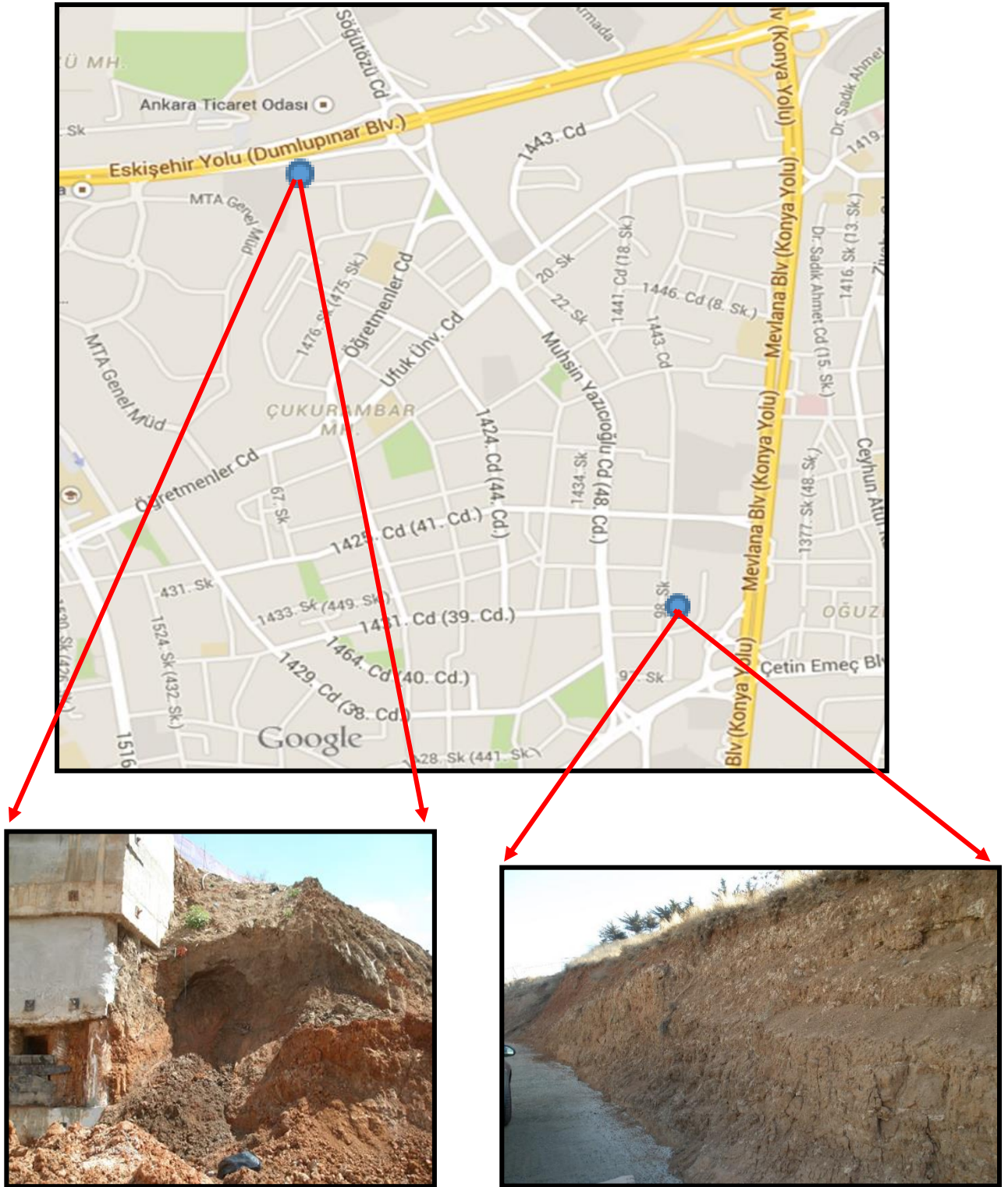


Figure 3.1. The sampling area

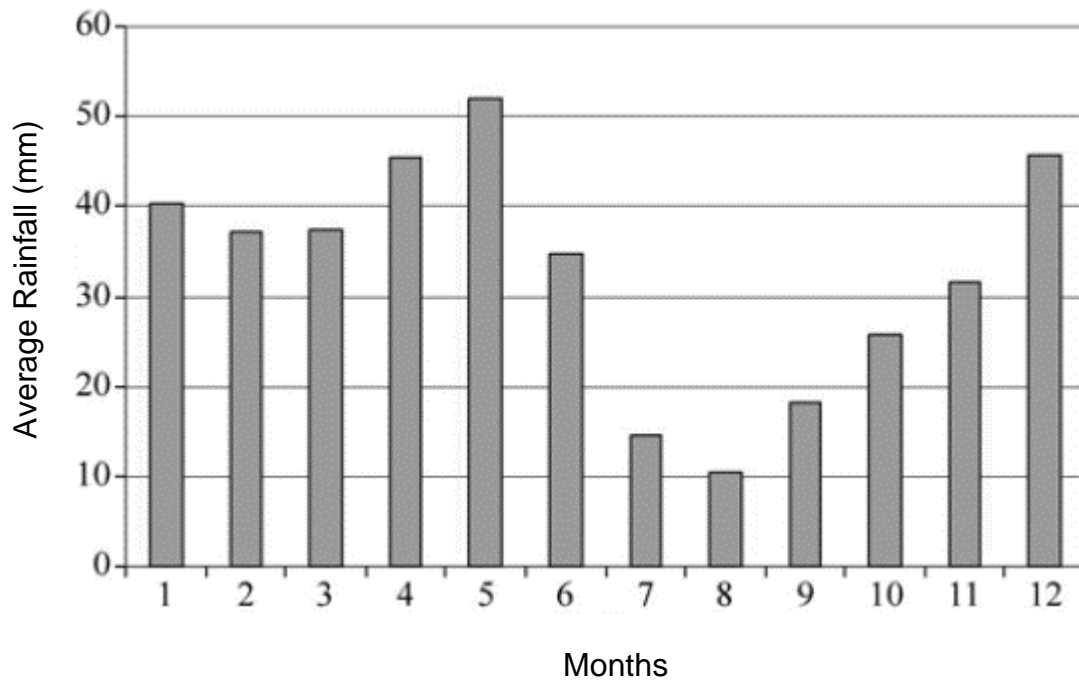
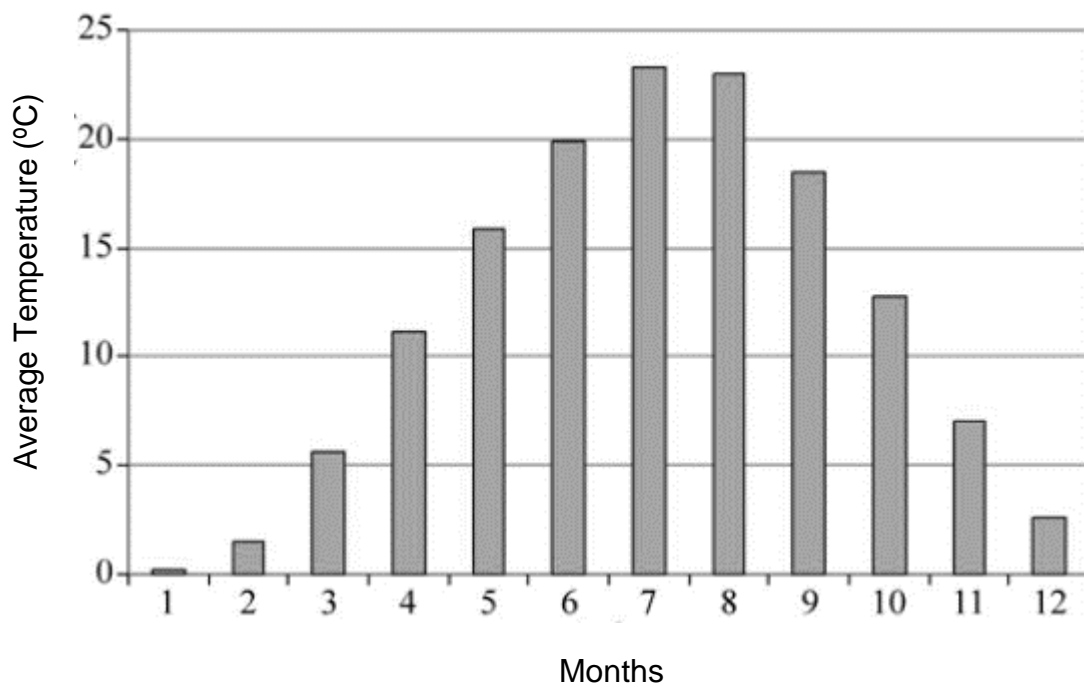


Figure 3.2. The average rainfall and temperature of Ankara between 1944-2006 years (Anonim 2006).

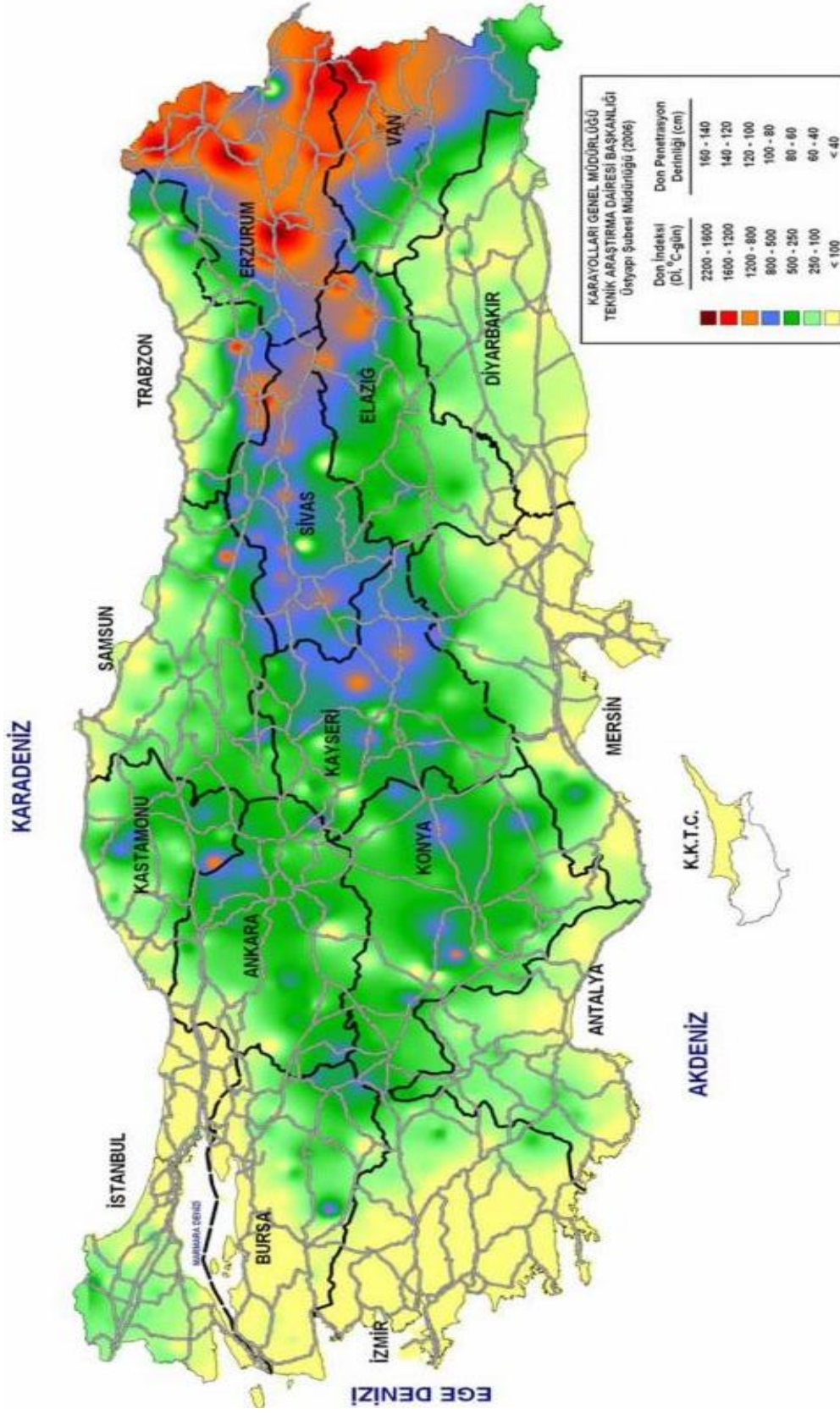


Figure 3.3. Frost index and frost depth penetration map of Turkey (Republic Of Turkey General Director of Highways, 2008).

3.3. Geological conditions of the area

Ankara region based on sequences of rock that made by epimetamorphic schist rocks. (Dager et al., 1963; Erentöz, 1975; Batman et al., 1978). Epimetamorphic schists consist of green chlorite glaucophane schists, pink sericitic schists, and phyllites-micaceous clayey schists-graphitic schists in order to younger that usually observed in the east and southeast of Ankara and around the middle Imrahor and down Imrahor (Erol, 1956). Ankara region's generalized stratigraphic sequence was shown on Figure 3.4-5.

A complex series of greywacke and metagreywacke with interbedded greenish brown schist which contained old limestone blocks of Permo-Carboniferous and Triassic, set on epimetamorphic schists (Kasapoğlu, 1980).

According to Erol (1986), the greywacke near the schist outcrops in deep was harder and mixed with extrusion, towards the top limestone, light greenish-brown more likely to be the younger, fractured, uneven layer, crumble and easily broken layer type. Especially, in the south of Ankara plains in the heights of Lodumlu Çankaya and northern outskirts of Çaldağ, many of this type of greywacke seen in the city's east, Seyrantepe and Topraklık district, so it was indicated that along the İncesu and Dikmen valleys to the south gradually transition to dark, hard and laminar type of layer.

Old Liassic unit developed on the top of this unit, which contained a vague mismatch base of conglomerate, sandstone-siltstone and fossiliferous Calcareenites. The age of ammonite limestones, silty-sandy-clayey limestones and plaques limestone with nodular limestone was about Dogger, Malm and Lower Cretaceous (Erol, 1956; Erentöz, 1975; Kasapoğlu, 1980)

"Ophiolitic melange" that consists of Lower and Upper Cretaceous serpentines, radiolarites, spilite basalt, diabase, limestone, sandstone, mudstone, marl, flint, gabbro and olistostromes, and its upper mismatch flysch series which includes conglomerate sandstone, siltstone, marl and olistostromes (Erol, 1956; Dağcı et al., 1963; Norman, 1972) located on the old unit.

Marine origin in the northern and southern part of Ankara includes large areas of old Paleocene and Eocene sediments. Conglomerate, sandstone, siltstone, marl and

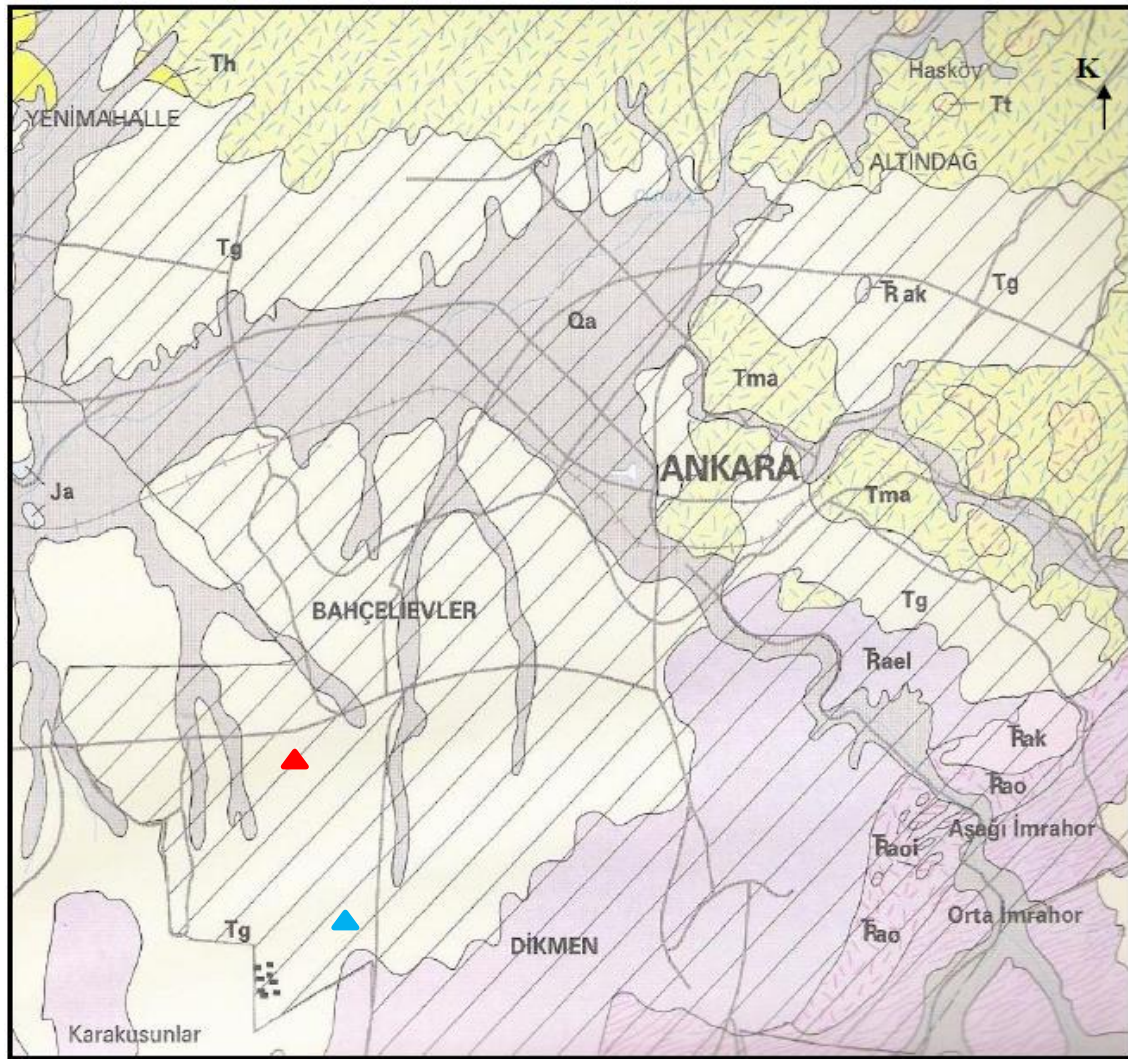
limestone represented Paleocene as well as fossiliferous sandy limestones represented the Eocene (Kiper, 1983). Miocene siliceous clayey lacustrine sediments, marl, claystone, conglomerate, andesites, basalts, agglomerates and tuffs located on the Oligocene lagoon and evaporate sedimentary environment (Chaput, 1931; Erol, 1956).

Upper Pliocene rivers and lakes sediments placed over of underlying rocks (Erentöz, 1975; Kasapoğlu, 1980) and the most distinctive feature was the inclusion of white concretions which developed in the vertical direction in some areas of Ankara represented the gravelly, sandy and clayey alluvial sediments, which coming on the Quaternary underlying units (Erol, 1956; Kasapoğlu, 1980).

Ankara Clay consists of a sequence of lacustrine sediments that comprises the surface of the Ankara Valley and extends in places down to 100 m. These expansive soils are found in central, western, and southern parts of Ankara, the capital of Turkey (Ordemir et al., 1977).

Eratem Era	System Period	Series Epoch	Lithological symbol	EXPLANATIONS
CENOZOIC	Quaternary			Alluvium (gravel, sand, silt)
	TERTIARY	Neogene		Loosely cemented conglomerate, red sandy silty clay, red clay and limestone nodules
				pink marl and clay mixed with lava pebbles and tuffs
		Miocene		schist-clayey lacustrine limestone, marl and claystone, conglomerate, andesites, basalts, agglomerates and tuffs
		Paleogene	Oligocene	conglomerate, sandstone, marl, gypsum
			Eocene	fossiliferous sandy limestones and sandstones
			Paleocene	Flysches (conglomerate, sandstone, siltstone, marl, limestone)
MESOZOIC	Cretaceous	Upper		Flysches (conglomerate, sandstone, siltstone, marl and olistostromes)
		Lower		Ophiolitic melange (serpentine, radiolarite, spilite, basalt, diabase, limestone, sandstone, mudstone, marl, flint, gabbro and olistostromes)
	Jurassic	Upper	Malm	Amonitl limestone, silty-sandy-clayey limestones and nodular limestone plaque
		Middle	Dogger	
		Lower	Lias	
	Triassic			Nixed-Block Series : pillow blocks made of spilite-basalt, greywacke and metagreywacke containing teryas and Permo Carboniferous limestone blocks
PALEOZOIC	Permian-Carboniferous			epimetamorphic schists (phyllit, graphite schist, chlorite schist, mica schist, quartzite)

Figure 3.4. Stratigraphic Columnar Section of Ankara (Kasapoğlu, 1980).



	Sampling location 1		Sampling location 2
Qa	Alluvium, Sand, Gravel.	Ja	Akbayır Formation; white cream and red silica tape and nodular limestone.
Tg	Gölbaşı Formation, conglomerate, Sandstone, Mudstone, Silt, Clay.	TRak	Keçikaya Formation; Grey and white limestone.
Tt	Tekke Volcanic; Andesite, Trachyandesite, Tuff, agglomerate.	TRao	Ortaköy Formation; spilite, diabase, Tuff, Volkarenit Agglomerate
Tma	Mamak Formation; agglomerate, Tuff, Andesite.	TRaoi	Imrahor Member Limestone; primitive associated with volcanic limestone
Th	Hançili Formation; Sandstone, Siltstone, Marl, Clayey Limestone, Tuff, Gypsum, oil shale.	TRael	Elmadag Formation; muscovite - quartz schist, sericite-quartz schist, phyllite, calcschist, metavolcanics metaconglomerate.

Figure 3.5. 1: 100 000 scale geological map of the Ankara valley and around (Akyürek et al. 1997)

4. MATERIALS

Thirty blocks of undisturbed high plasticity clay soil (CH) and clayey sand (SC) were obtained from the Söğütözü and Çiğdem districts. Properties of them were explained separately below:

4.1. CH Soil

The dense and cohesive soil was analyzed in the laboratory for its properties like water content, natural unit weight, Atterberg limits, grain size analyses, consolidation, direct shear test, XRD analyses and SEM study, and found to have a plastic limit (PL) of 33.01%, a liquid limit (LL) of 75.05% and plasticity index (PI) of 42.04% (Fig. 4.1). The soil sample was classified as “CH” by the unified soil classification system. It includes 62.50% clay, 22.00% silt, 11.24% sand and 4.26% gravel-sized materials (Fig. 4.2).

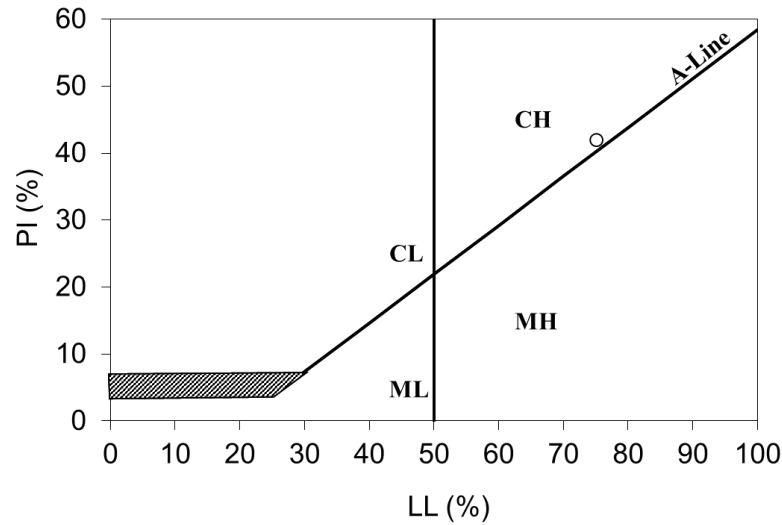


Figure 4.1. Plasticity chart of soil sample

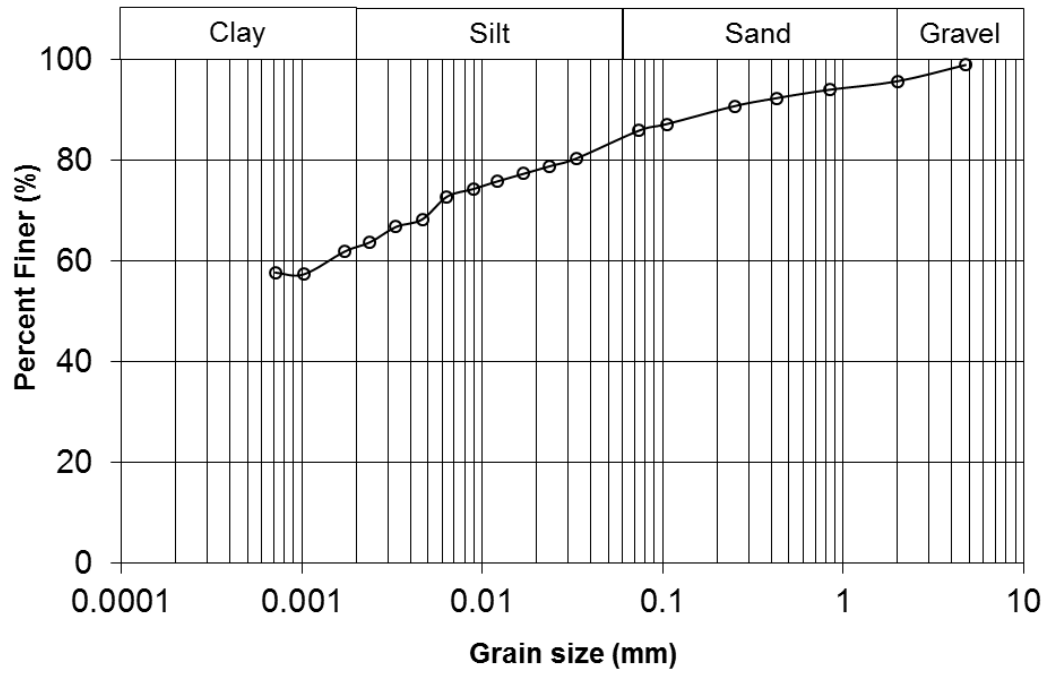


Figure 4.2. Sieve Analysis of CH soil

Shear strength parameter was calculated as cohesion (c) of 10.95 kPa and internal friction angle (ϕ^0) of 27.71 using the direct shear box test apparatus (Fig. 4.3).

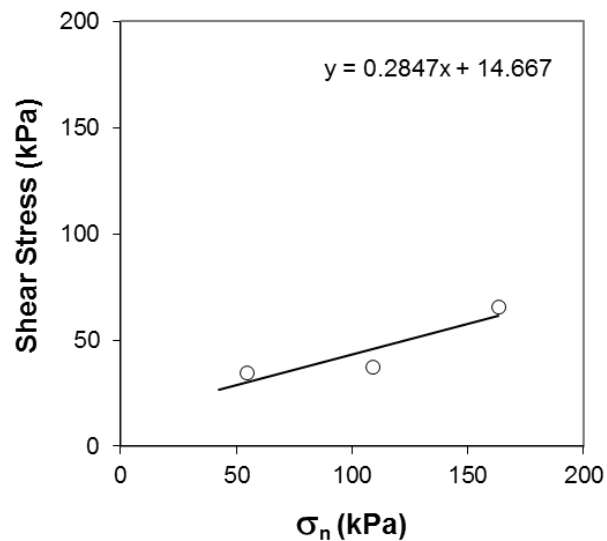


Figure 4.3. Failure envelope of CH

As to XRD-analysis, CH includes smectite, illite, kaolin, quartz, feldspar and calcium minerals (Fig. 4.4.). Some properties of CH was summarized in Table 4.1.

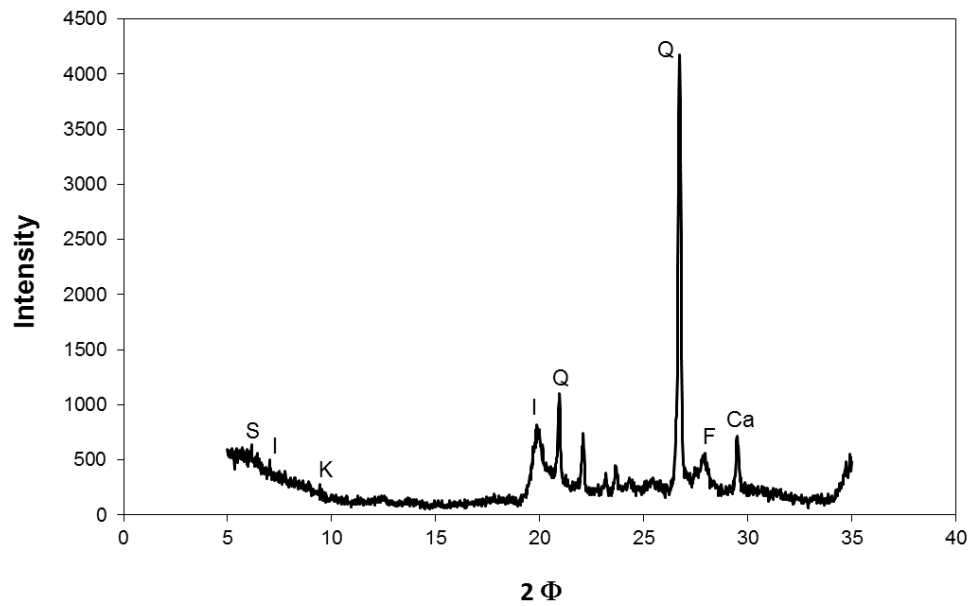


Figure 4.4. XRD analyses of CH (S: Smectite, I: Illite, K: Kaolin, Q: Quartz, F: Feldspar, Ca: Calcite)

Table 4.1. Some properties of CH

Natural water content, w_n (%)	39.09
Natural unit weight, g_n (KN/m ³)	19.7
Liquid limit, w_L (%)	75.05
Plasticity index, PI (%)	42.04
Specific gravity, G_s	2.73
Gravel (%)	4.26
Sand (%)	11.24
Silt (%)	22
Clay (%)	62.5
% finer than no.200	85.74
Activity, A_c	0.67

4.2. Clayey Sand Soil (SC)

The second soil sample have disturbed structure because of its sand mixture and low natural water content. It was analyzed in the laboratory and found to have a plastic limit (PL) of 22.56%, a liquid limit (LL) of 36.97% and plasticity index (PI) of 14.41%. It includes 16.80% clay, 26.20% silt, 56.10% sand and 0.30% gravel-sized materials.

According to unified soil classification system (USCS), the percentage of material passing under No. 200 sieve was 46% and amount of material remaining on the sieve was 54%, therefore, the soil sample inters into the coarse-grained class. The percentage of material remaining on the sieve No. 4 was 0.18% therefore it has called sand soil sample. Plasticity index of the soil sample (PI) was determined as 14.41%. Because of the PI value was more than 4%, the second symbol of soil sample was determined as "C" (See appendix A), so soil samples was named as SC.

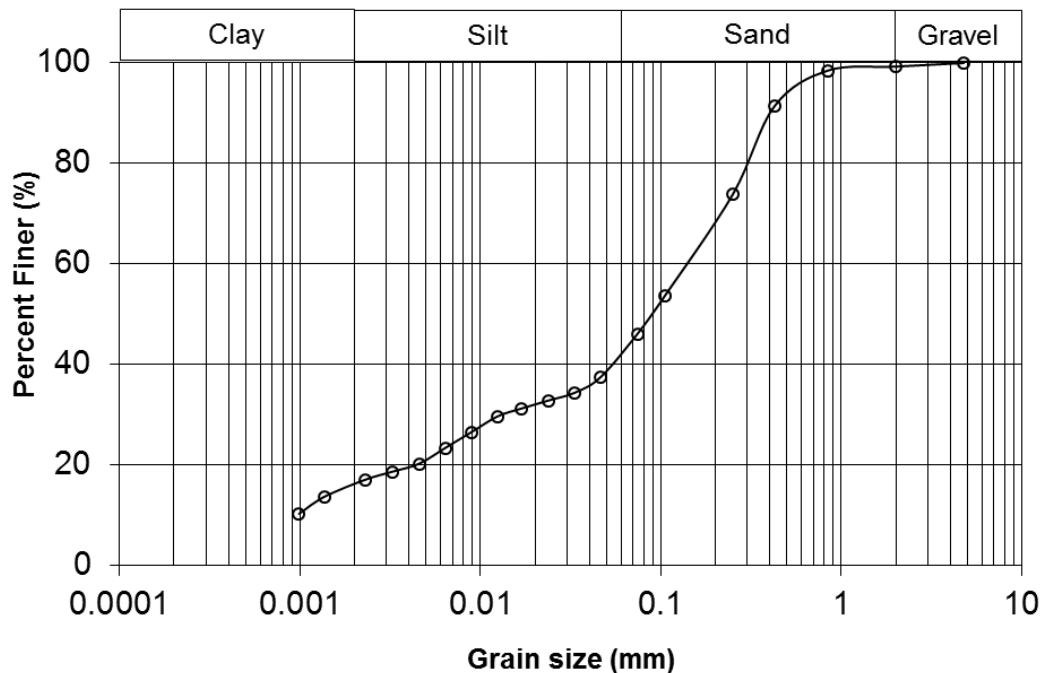


Figure 4.5. Sieve analysis of SC

Shear strength parameter was calculated as cohesion (c) of 19.68 kPa and internal friction angle (ϕ^0) of 49.81 using the direct shear box test apparatus (Fig. 4.6). Some properties of SC was presented in Table 4.2.

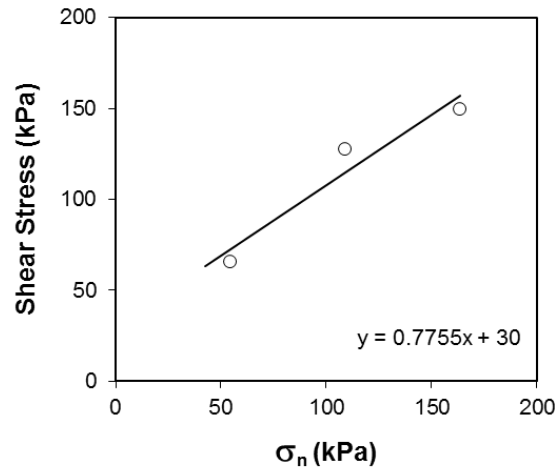


Figure 4.6. Failure envelope of SC

SC composes of quartz, feldspars, calcite and clay minerals (Figure. 4.7).

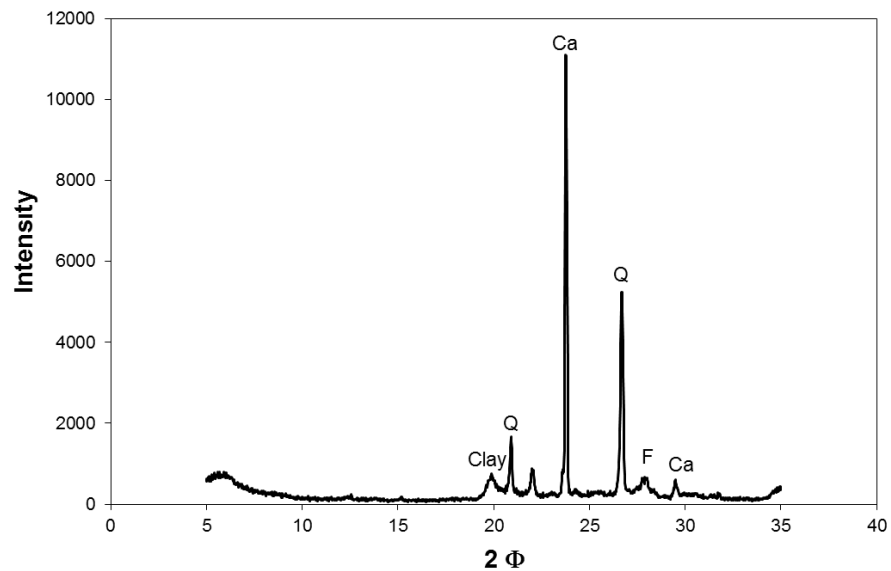


Figure 4.7. XRD analyses of SC (Q: Quartz, F: Feldspar, Ca: Calcite)

Table 4.2. Some properties of SC

Natural water content, w_n (%)	8.7
Natural unit weight, g_n (KN/m ³)	14.5
Liquid limit, w_L (%)	36.97
Plasticity index, PI (%)	14.41
Specific gravity, G_s	2.48
Gravel (%)	0.30
Sand (%)	56.10
Silt (%)	26.20
Clay (%)	16.80
% finer than no.200	45.70
Activity, A_c	0.85

5. METHODS AND RESULTS

Collected samples that were prepared (saturated, molded) for Atterberg limits, consolidation and direct shear tests were placed into a freezer that has -18°C temperature. Samples have been waited in it for twenty-four hours. Then, they have been removed from the freezer and allowed to stand for twenty-four hours at a constant room temperature (21°C) and humidity (80% RH). As a result, one freezing and thawing (FT) cycle was achieved between -18°C (24 hours) and 21°C (24 hours), and it took two days. FT sequences were selected as 1, 3, 7, 14 and 21. Explained freezing and thawing procedure that applied for all test samples is the same. After each FT sequence, Atterberg limits, sieve analyses, consolidation, direct shear strength tests, XRD analyses and SEM viewing have been carried out according to ASTM standards (Table 5.1)

The number of FT, in accordance to map of freezing and thawing number of Ankara, have been selected as 21 cycles. Therefore, experiments were conducted at 21 FT cycles (Binal A, 2008).

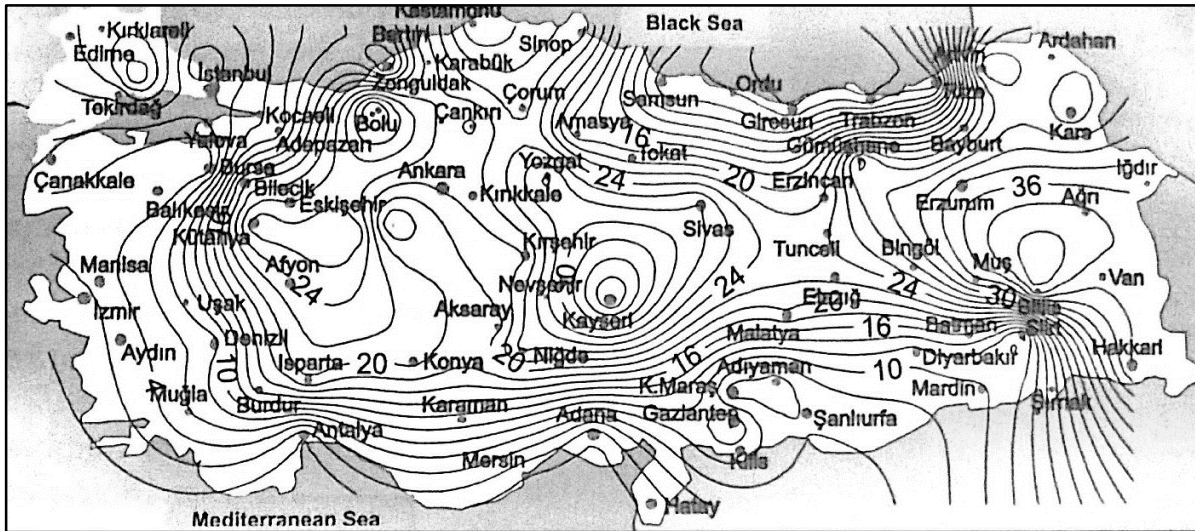


Figure 5.1. Isoline map of the freeze-thaw severity index of Turkey (numbers indicated freeze and thaw cycles) (Binal A, 2008).

Table 5.1. ASTM standards used in tests

Water content	D4656-07	Specific Gravity	D854-14
SEM view	E986-04	Density	D792-13
Sieve analysis	C136M-14	Consolidation	D2435M-11
Shear strength	D3080M-11	XRD analysis	D3906-03
Plastic limit	D4318-05	Liquid limit	D4318-05

5.1. Specific Gravity and Density

Specific Gravity (G_s) is defined as the density of a soil divided by the density of water at a specified temperature.

The density (ρ) of a soil is the ratio of its mass to its unit volume. Density procedure Eq.5.1. is used for determination of the bulk of density of soil samples (Figure 5.2).

$$\text{Bulk Density (g/cm}^3\text{)} = \frac{M_d}{V} \quad (\text{Equation 5.1.})$$

M_d = Mass of dry soil sample (dry weight) (gram)

V = soil volume (cm³)

5.1.1. Sample Preparation

Disturbed soil samples were used for Atterberg limits tests. First, samples were saturated with distilled water. For this, soil that was located in a nylon bag, spray with distilled water. Nylon bag contain wet soil was locked and placed into the deep freeze to start FT cycles.



Figure 5.2. Specific Gravity Test

5.1.2. Test Results

The specific gravity of the particles was determined for both CH and SC soils, using standard methods on representative samples after every FT cycles. The determined G_s values are illustrated in table 5.1. These are each an average of three readings having scatter of about ± 0.005 . The G_s values vary between 2.39 and 2.74 for CH and 2.46 and 2.49 for SC, the lowest values are often for 3, 7 and 14 FT cycles (Table 5.2).

Table 5.2. Specific Gravity of CH and SC soils.

	CH	SC
FT Cycles	Specific Gravity (G_s)	Specific Gravity (G_s)
0	2.74	2.49
1	2.71	2.46
3	2.39	2.47
7	2.39	2.49
14	2.40	2.47
21	2.73	2.49

5.2. Atterberg Limits

A fine grained soil can exist in any of several states; each state depends on the amount of water content in the soil system.

Liquid limit: The liquid limit test is carried out to measure the water content of a soil at the limit between plastic and liquid states of consistency by recording a series of water contents, each corresponding to a number of blows close to 25 in special device used for the test. A semi-logarithmic graph is then drawn relating number of blows and water content; the water content corresponding to 25 blows is read off.

Plastic limit: Plastic limit is the water content at which the soil begins to crumble when rolled down to a diameter of 3 mm.

The plasticity Index: The plasticity index is simply the numerical variation between the liquid limit and the plastic limit and shows that the magnitude of the range of water content over which the soil stays plastic (Eq. 5.2).

$$PI = LL - PL \quad \text{(Eq. 5.2.)}$$

It is the measure of the cohesion qualities of the resulting from the clay content. Also it gives some indication of the value of swelling and shrinkage which will result in the wetting and drying of that fraction tested. The plasticity index is nothing but a determination that gives the amount of water content which should be added in order to change a soil from its plastic limit to its liquid limit. Normally the behavior of all the soils and more specifically clays considerably differs with the presence of water so one needs a reference index to show the effects.

5.2.1. Sample Preparation

Water content is one of the most essential factors in soil frost process so after determining the initial water content, for more accurate results, samples were saturated with distilled water.

For saturation, these samples distilled water spray have been used, then sprayed soils were placed in plastic bags and samples have been placed inside the deep freeze since to start FT cycles.

$$\% \text{ Change} = \frac{\text{Data after FT Test} - \text{Original Data}}{\text{Original Data}} * 100 \quad (\text{Eq. 5.3.})$$

5.2.2. Test Results

The result of the liquid limit and plastic limits of the samples were determined as well as recorded in table 5.3 and 5.4.

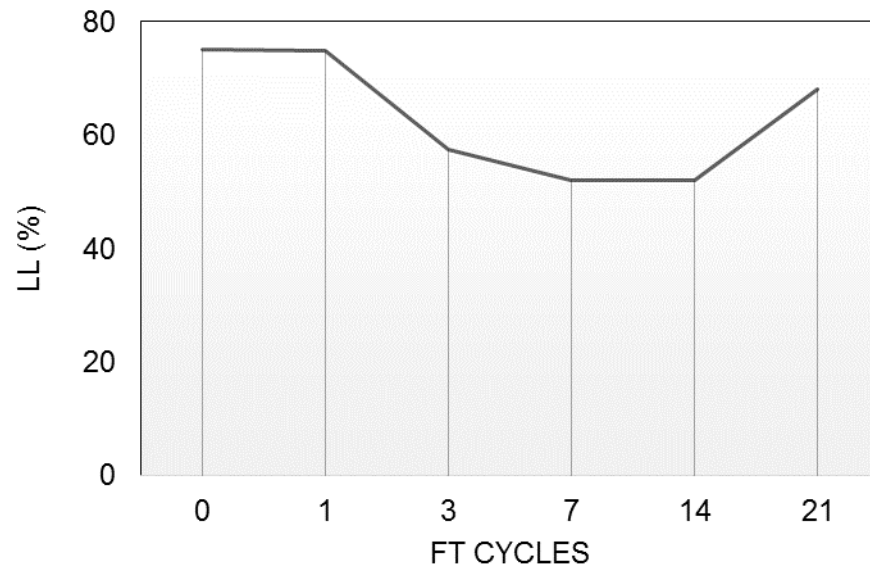
As the results show values of liquid (LL) and plastic limit (PL) decrease until seven FT cycle, then, they start to increase. As well, the same inference was observed on the plasticity index (Fig 5.3-5).

Table 5.3. Atterberg limits values (%)

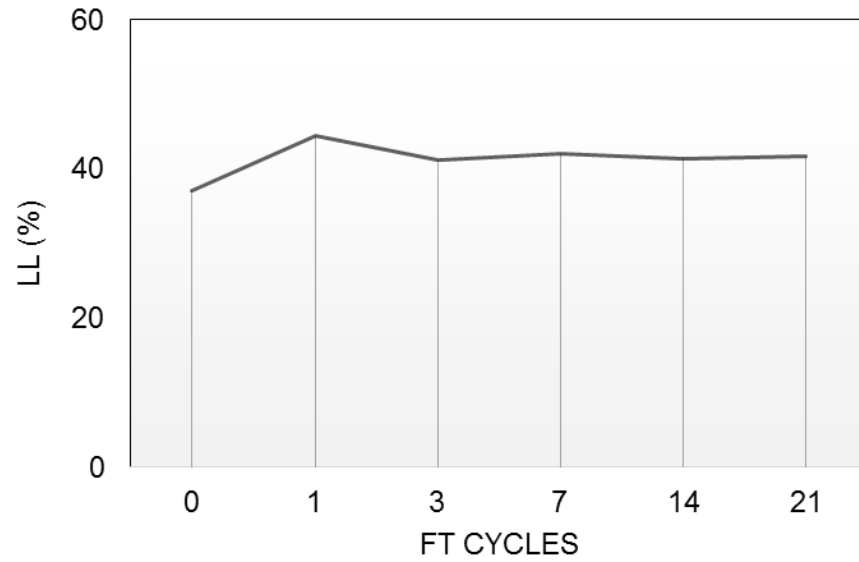
FT Cycles	CH			SC		
	LL	PL	PI	LL	PL	PI
0	75.05	33.02	42.04	36.97	22.57	14.40
1	74.84	38.32	36.73	44.45	22.70	14.27
3	57.46	38.20	36.85	41.03	20.17	16.80
7	51.92	32.48	42.58	42.00	26.03	10.94
14	51.95	32.76	42.29	41.24	24.30	12.67
21	67.98	37.73	37.33	41.58	24.25	12.72

Table 5.4. Atterberg limit changes (%)

FT Cycles	CH			SC		
	LL	PL	PI	LL	PL	PI
1	-0.29	1	2	20.23	0.59	0.93
3	-23.45	10.00	11.00	10.99	-10.63	-16.66
7	-30.82	40.46	32.92	13.60	15.34	24.05
14	-30.78	48.83	41.06	11.56	7.67	12.02
21	-9.42	47.25	39.57	12.47	7.44	11.67

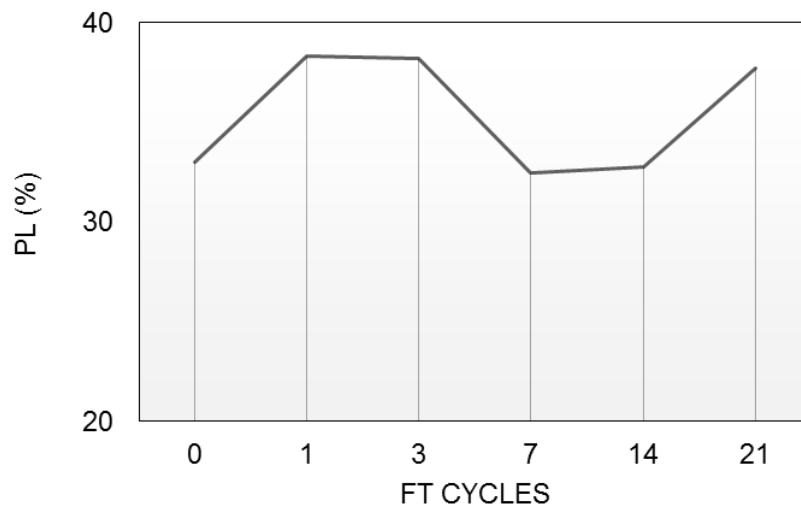


(a)

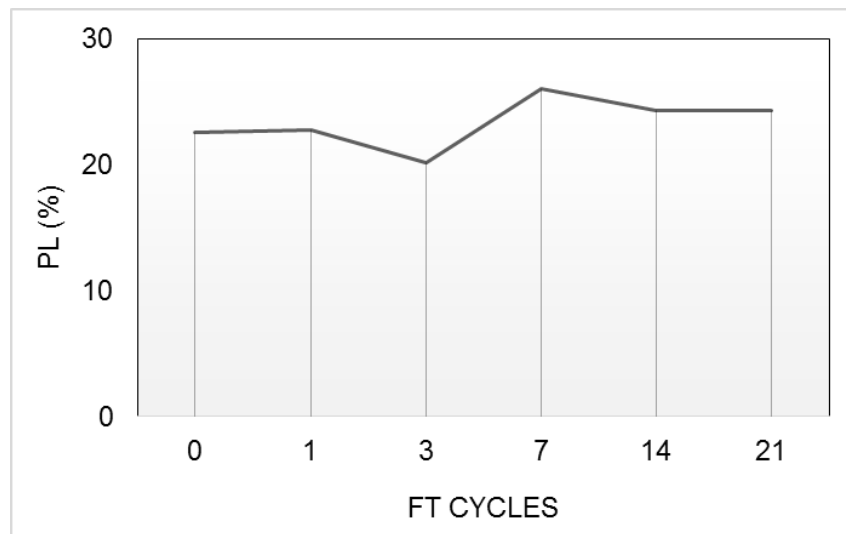


(b)

Figure 5.3. The relationship between FT cycles and Liquid Limit changes of
(a) CH and (b) SC soils.

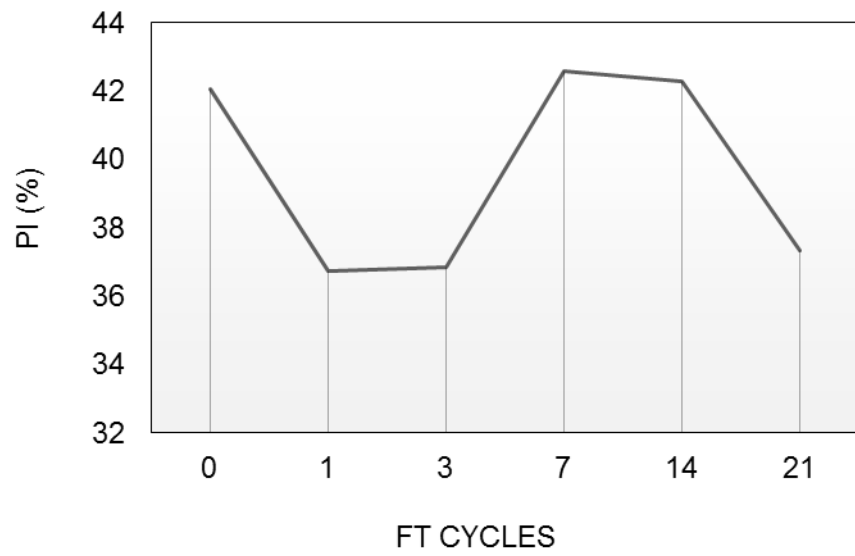


(a)

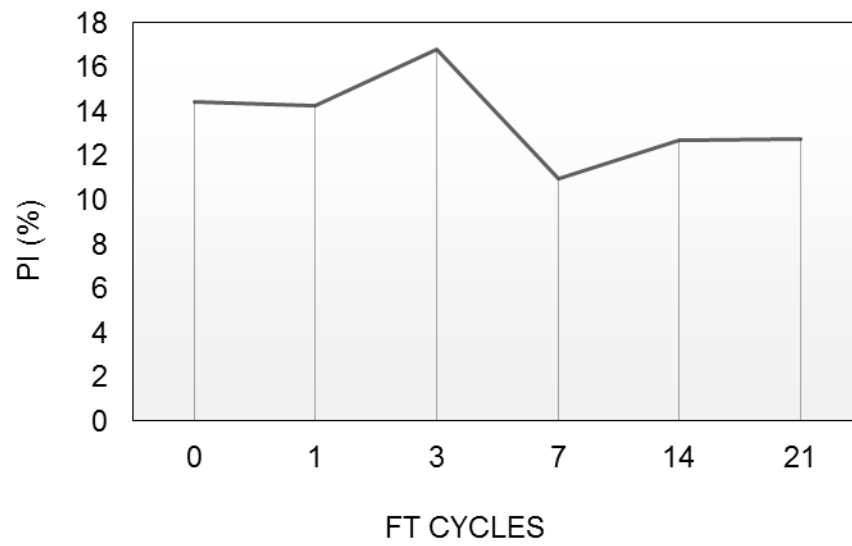


(b)

Figure 5.4. The relationship between FT cycles and Plastic Limit changes of (a) CH and (b) SC soils.



(a)



(b)

Figure 5.5. The relationship between FT cycles and Plasticity Index changes of (a) CH and (b) SC soils.

Results show that FT cycles are very effective within the Atterberg limits of the soil. The unified soil classification of the CH soil was changed from “CH” to “MH” after first FT cycle (Fig. 5.6). However, PL was inclined from 33.02% to 37.73% as well as LL was declined from 75.05% to 67.98% at 21 FT cycle.

It had been observed that, the second symbol of clayey sand was changed from “C” to “M” after first FT cycle (Fig. 5.7). However PL was declined from 42.03% to 37.32% as well as LL was inclined from 36.97% to 41.58% at first FT cycle.

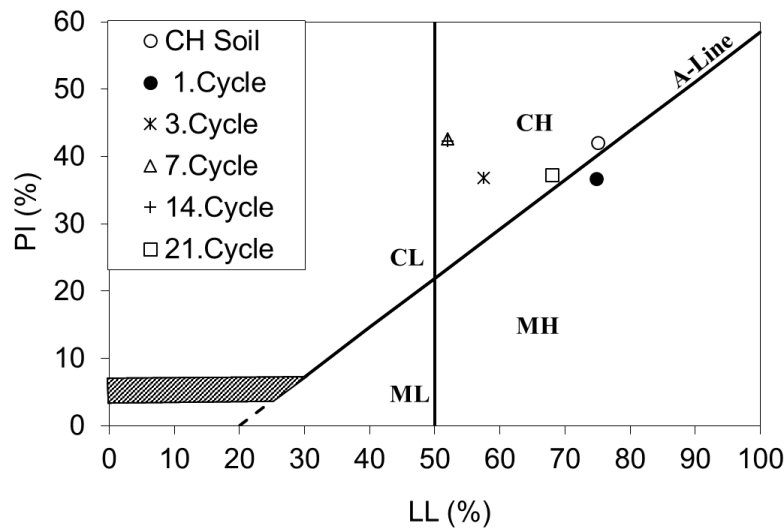


Figure 5.6. Plasticity chart for CH soil.

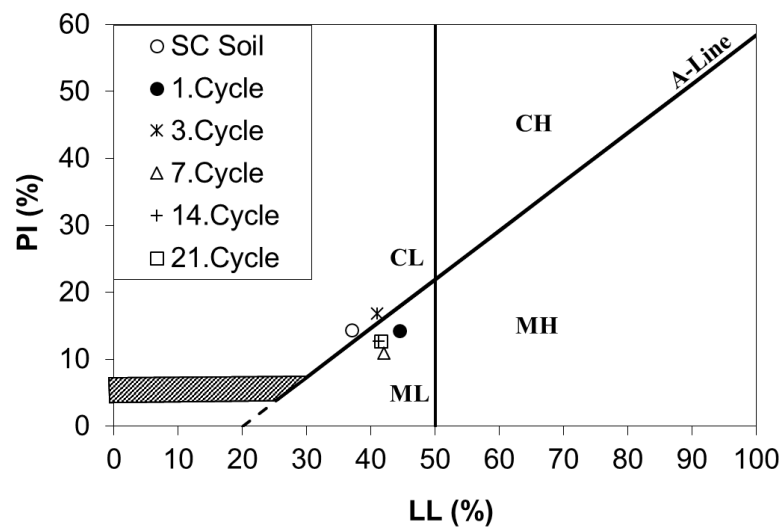


Figure 5.7. Plasticity chart for SC soil.

5.3. Grain Size Analyses

Grain size analysis is the determination of the size range of particles present in a soil, represented as a percentage of the total dry weight.

Generally there are two methods used to find the particle size distribution of soil:

- 1) Sieve analysis - it's used for particle sizes larger than 0.075 mm in diameter.
- 2) Hydrometer analysis - it's used for particle sizes smaller than 0.075 mm in diameter.

5.3.1. Sample Preparation

As it mentioned above water content is one of the most essential factors in soil frost process so after determining the initial water content, for more accurate results, samples were saturated with distilled water. For saturate these samples distilled water spray have been used, then sprayed soils were placed in plastic bags and samples have been placed inside the deep freeze since to start FT cycles.



Figure 5.8. Total mass of samples that passing No. 4 sieve



Figure 5.9. Hydrometer analysis procedure

5.3.2. Test Results

Grain size distribution tests of the soil samples were used to classify the soils in accordance with the unified soil classification system (USCS) and to define grain size distribution indices for each soil sample.

The average grain size distribution curves for the two soils, according to sieve analysis and hydrometer data, are shown in Figures 5.10-11. Graphs of grain size distribution for each sample are shown in Appendix C. Table 5.5 provides a summary of the grain size distribution indices including clay, silt, sand and gravel.

Table 5.5. Changes in the ratio of grain size depending on FT cycles
(a) CH and (b) SC soils.

	Clay	Silt	Sand	Gravel
0	0.63	0.22	0.11	0.04
1	0.59	0.26	0.12	0.03
3	0.59	0.28	0.11	0.03
7	0.55	0.30	0.12	0.03
14	0.53	0.31	0.12	0.04
21	0.57	0.31	0.10	0.02

(a)

	Clay	Silt	Sand	Gravel
0	0.17	0.26	0.56	0.30
1	0.19	0.33	0.48	0.38
3	0.14	0.30	0.57	0.22
7	0.18	0.31	0.51	0.25
14	0.17	0.26	0.57	0.11
21	0.17	0.26	0.57	0.30

(b)

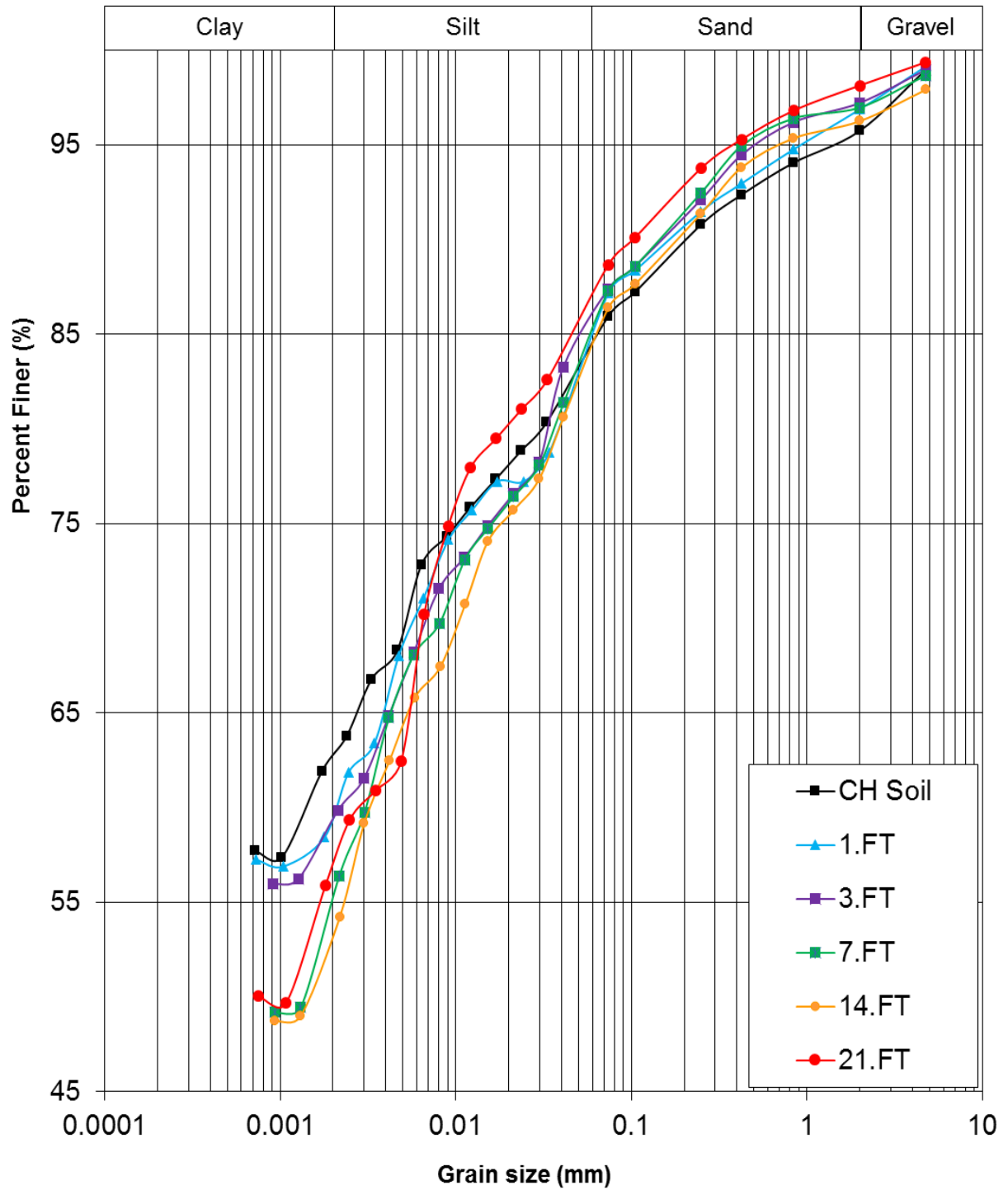


Figure 5.10. Grain size distribution for CH soil

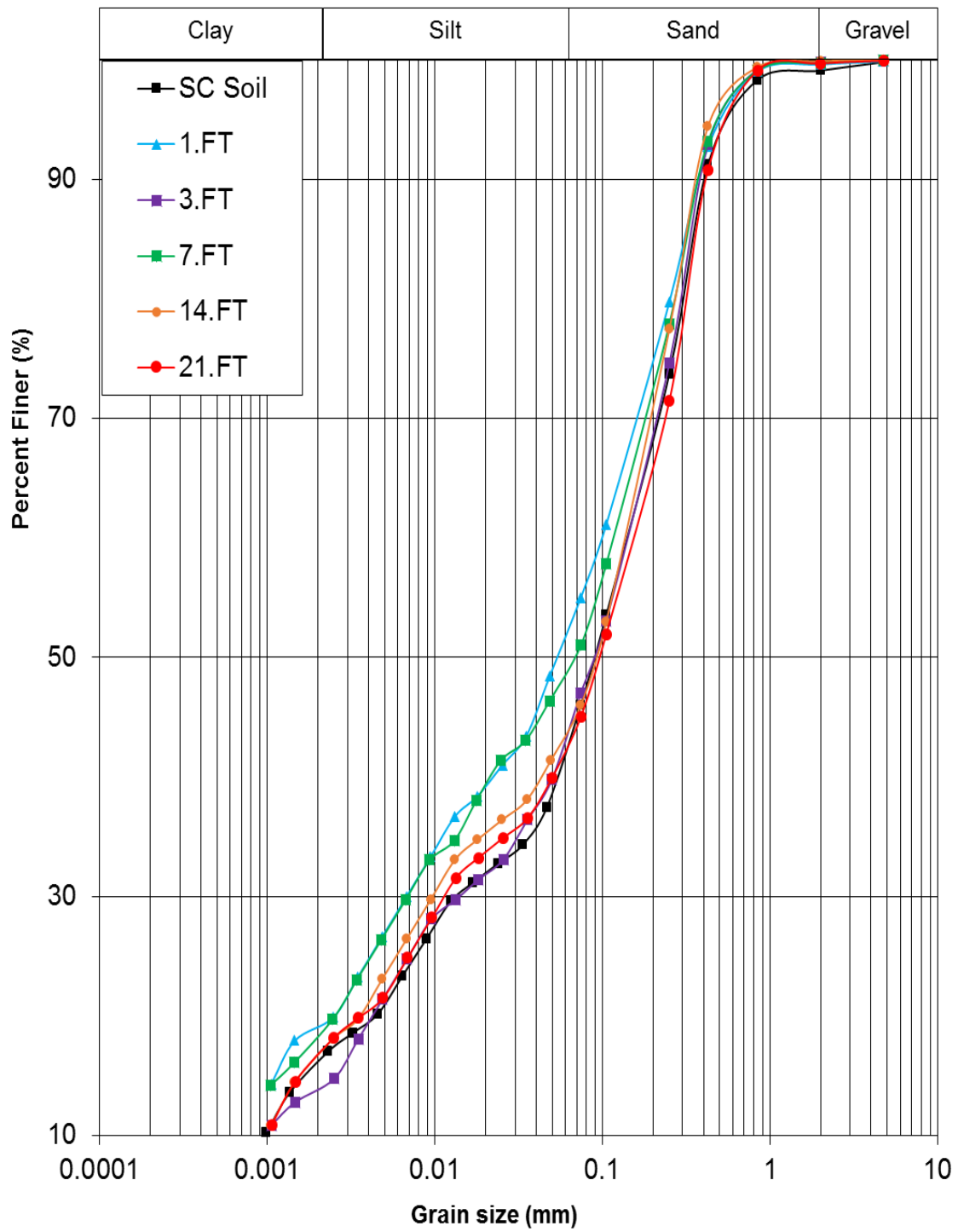


Figure 5.11. Grain size distribution for SC soil

As to FT cycles, the grain size compositions of samples were changed, especially; the amount of clay size particles decreases up to 14 FT cycles, then; it starts to increase (Fig. 5.12a). The opposite behavior was observed on silt size particles. It begins to decrease after 14 FT cycles (Fig. 5.12b).

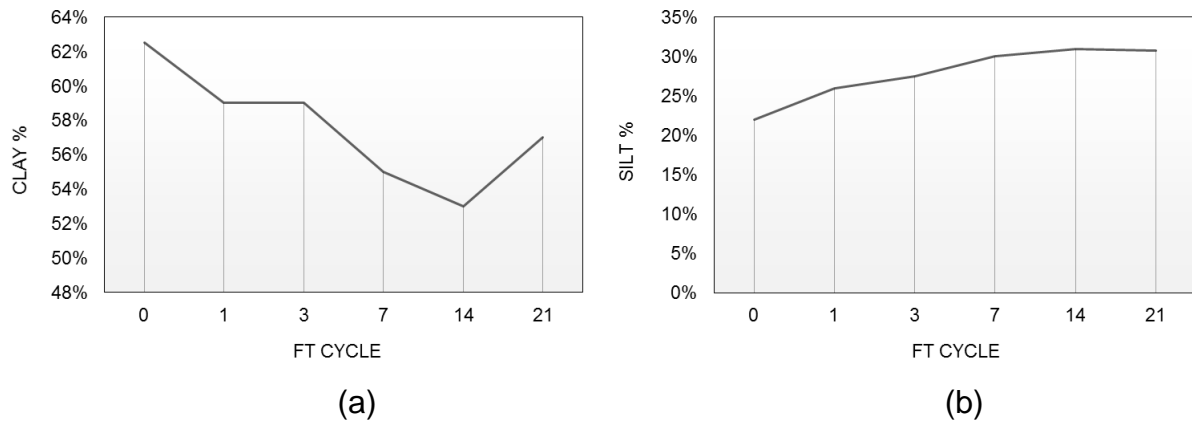


Figure 5.12. Variation of fine particles (a) Clay, (b) Silt

For coarse grain size, more change was seen in the sand size than gravel size. Sand size particle increases until 14 FT cycles, then, decreases (Fig. 5.13a). There is no exact behavior was determined on the gravel size particles (Fig. 5.13b).

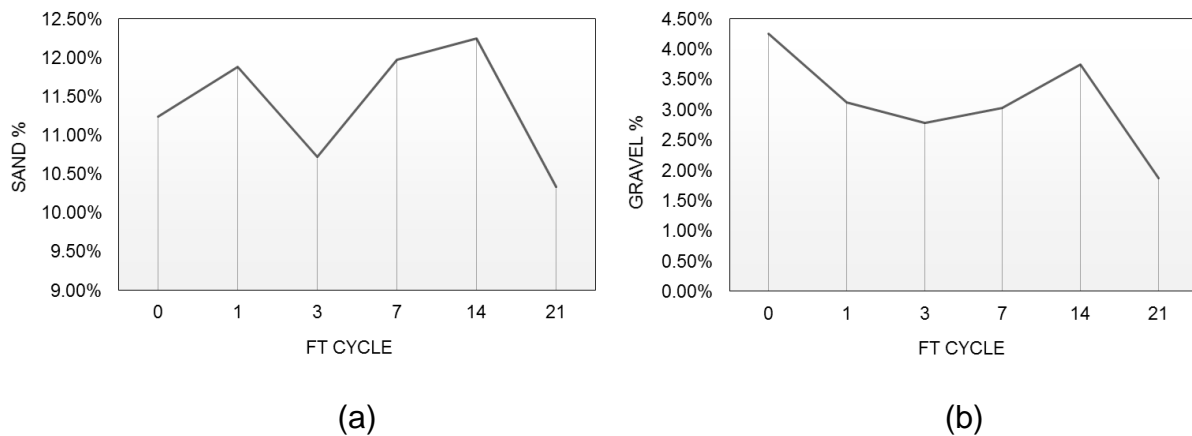
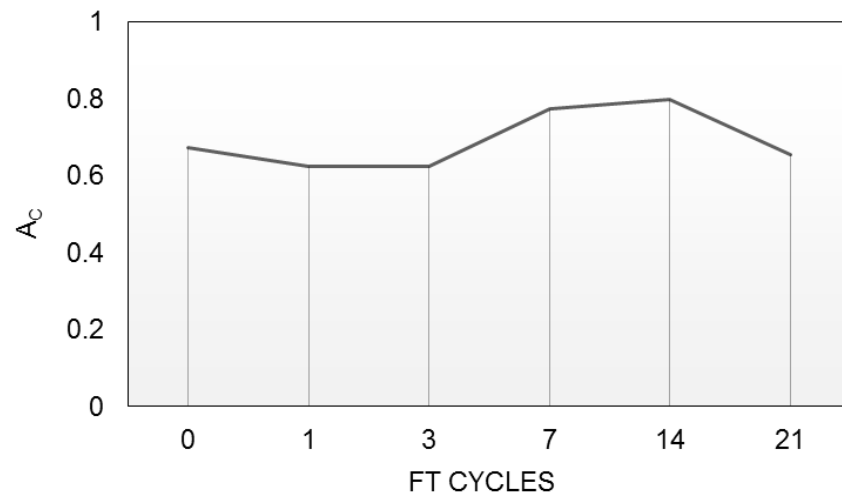


Figure 5.13. Variation of coarse particles (a) Sand, (b) Gravel

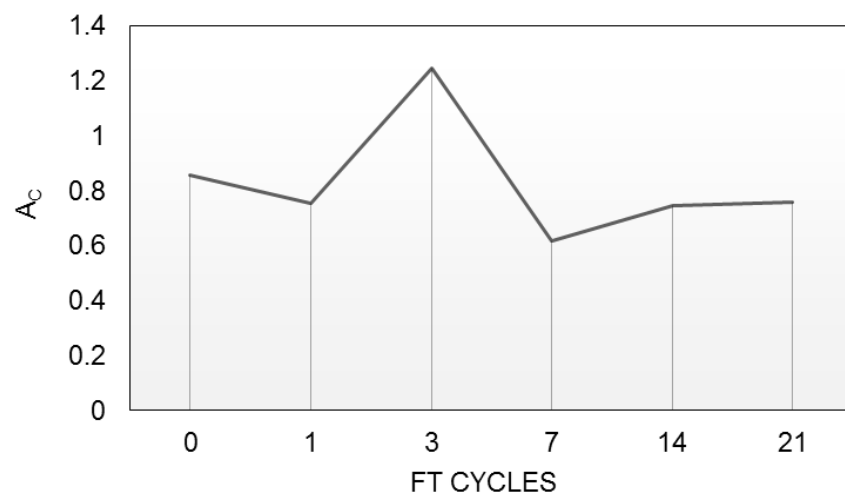
5.4. Clay Activity

The activity (A_c) of a soil is the plasticity index divided by the percent of clay-sized particles (less than 2 μm). Different types of clays have different specific surface areas which controls how much wetting is required to move a soil from one phase to another such as across the liquid limit or the plastic limit. From the activity, one can predict the dominant clay type present in a soil sample. High activity signifies large volume change when wetted and large shrinkage when dried. Soils with high activity are very reactive chemically. Generally the activity of clay is between 0.75 and 1.25 and in this range clay is called normal. It is assumed that the plasticity index is approximately equal to the clay fraction ($A_c = 1$). When A_c is less than 0.75, it is considered inactive. When it is greater than 1.25, it is considered active (Bowles J.E. 1984).

Activities of soil samples were determined after FT cycles. The activity of CH soil showed that there was a relationship between FT cycles and activity values. The original activity value of CH soil was 0.67. However, that value has increased until 14 FT cycles, and a classification of CH soil was changed from inactive to normal active. After 14th FT cycle, it was started to go down, and it has returned the level of inactive clay (Fig. 5.14a). Conversely, the same behavior was not mentioned for SC soil because of the low clay content (Fig. 5.14b). These inferences supported the evaluation of effects of freezing and thawing on grain size.



(a)



(b)

Figure 5.14. Clay activity for (a) CH and (b) SC soils.

5.5. Shear Strength

5.5.1. Sample Preparation

As mentioned before two soil samples were used in this study. All samples were placed into the mold for saturation process. The molded samples were located in the shear box filled with distilled water and waited in it under the 20 kg load for 24 hours. After saturation stage, the other stage on freezing and thawing process explained before has been passed.

5.5.2. Test Results

As it was shown in Fig. 5.15a-16a for CH soil after first FT cycle, cohesion (c) increased as well as internal friction angle (ϕ°) decreased. However, the shear strength parameters start to increase then three FT cycles. Cohesion was increased 36.99% as well as internal friction angle was inclined 22.23% (Table 5.6).

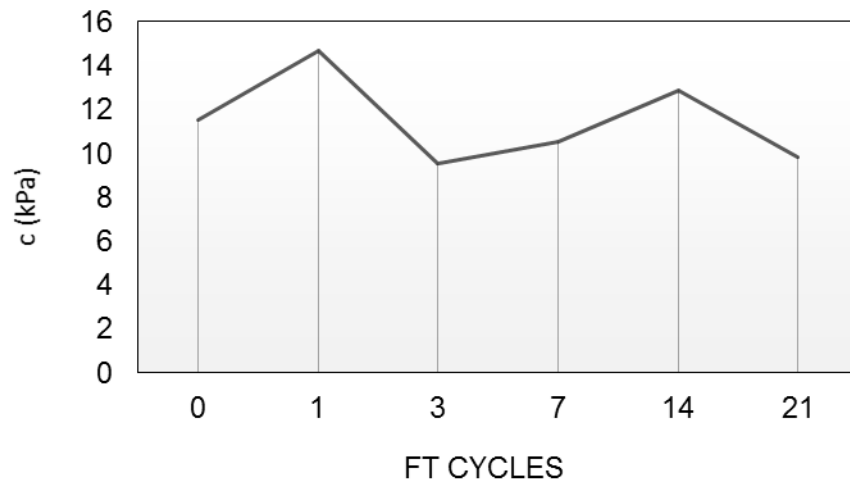
For SC soil after first FT cycles both cohesion (c) and internal friction angle (ϕ°) decreased and as well as CH soil, the shear strength parameters start to increase after three FT cycles (Fig 5.15b-16b). SC soil's cohesion was decreased 95.90% as well as internal friction angle was declined -9.05% (Table 5.7).

Table 5.6. Shear strength parameters

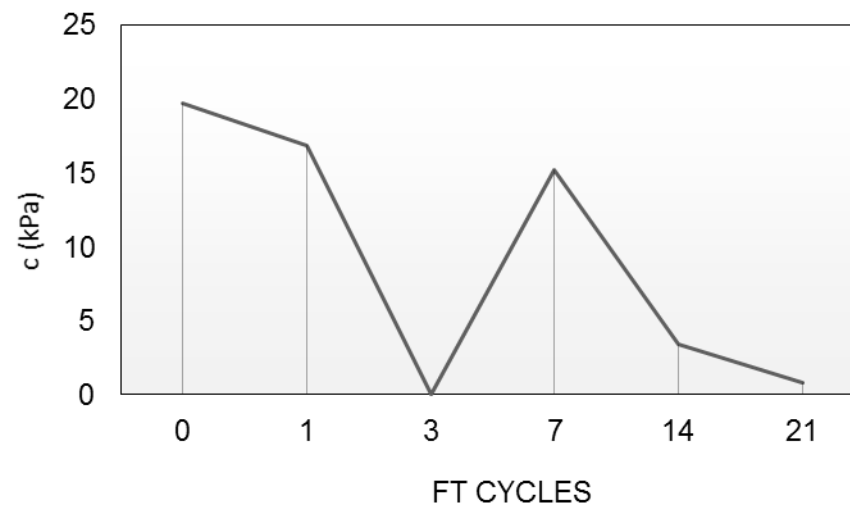
FT Cycles	CH SOIL		SC SOIL	
	c (kPa)	ϕ^0	c (kPa)	ϕ^0
0	27.71	10.95	37.79	19.68
1	18.90	12.48	30.62	16.82
3	18.03	11.99	37.79	0,01
7	19.60	13.58	26.10	15.15
14	21.79	13.41	34.76	3.40
21	21.55	15.00	37.43	0.81

Table 5.7. Change (%) in shear strength parameters

FT Cycles	CH SOIL		SC SOIL	
	c	ϕ	c	ϕ
1	13.94	-31.79	-14.54	18.99
3	9.48	-34.91	-104.42	0.00
7	24.05	-29.26	-23.01	30.95
14	22.44	-21.35	-82.74	8.04
21	36.99	-22.23	-95.90	0.97

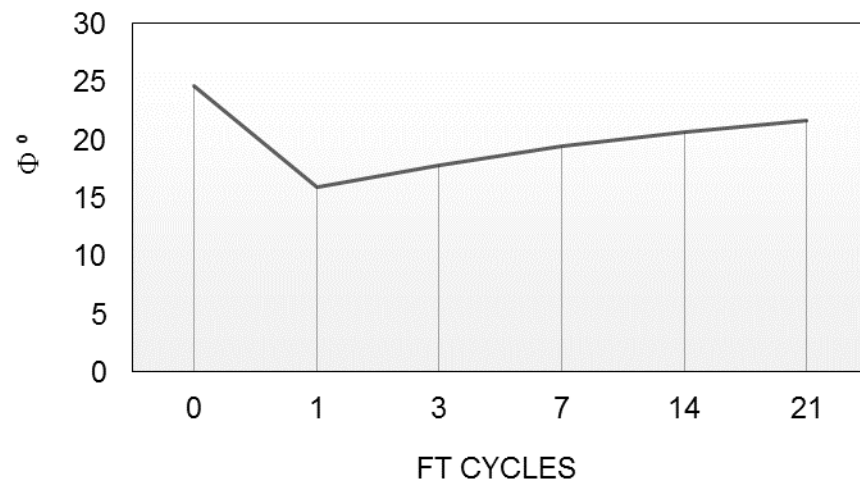


(a)

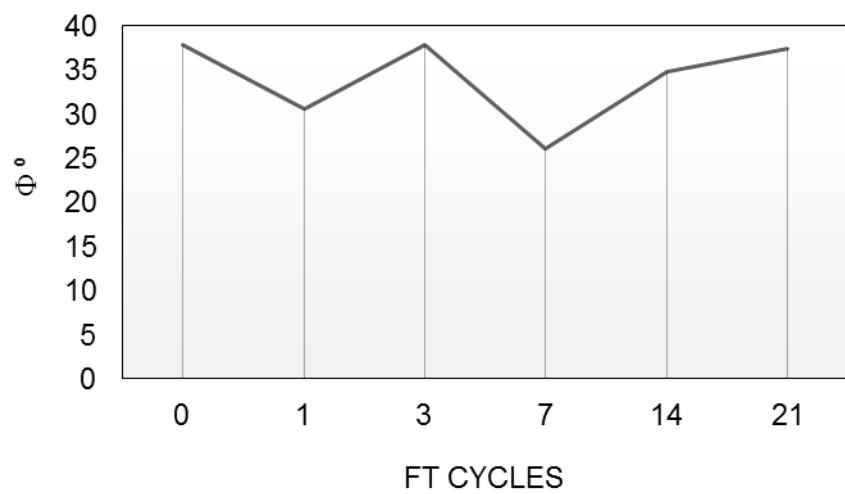


(b)

Figure 5.15. Cohesion (c) of (a) CH and
(b) SC soils after FT cycles.



(a)



(b)

Figure 5.16. Internal friction angle (Φ) of (a) CH and
(b) SC soils after FT cycles.

5.6. Consolidation

This test has been carried out to determine the magnitude and rate of volume decrease that a laterally restricted soil specimen sustains when subjected to various vertical pressures. From the measured data, the consolidation curve (relationship of pressure-void ratio) can be plotted. This data is useful in measuring the compression index, the recompression index and the pre-consolidation pressure (or maximum past pressure) of the soil. Moreover, the data obtained can be used to determine the coefficient of consolidation and the coefficient of secondary compression of the soil samples.

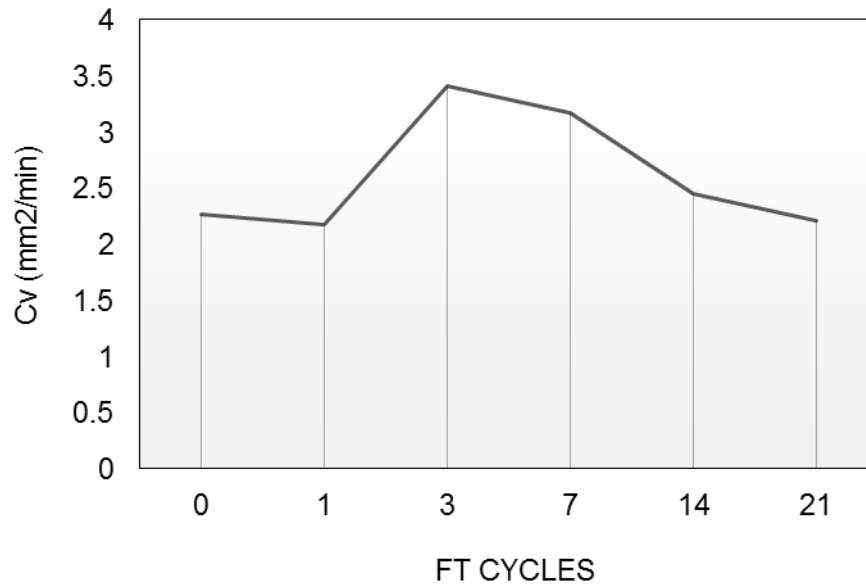
5.6.1. Sample Preparation

As direct shear test, two soil samples were settled into consolidation ring and excess soil from the top of the ring was cautiously trimmed level with the top of the ring. The height, diameter and mass of the consolidation ring should be measured. The initial wet mass of the specimen and ring and the height of the sample were measured. For saturation process the specimen in the consolidation ring was placed in the oedometer and the oedometer was placed in the loading device and waited in it under the 20 kg load for 24 hours.

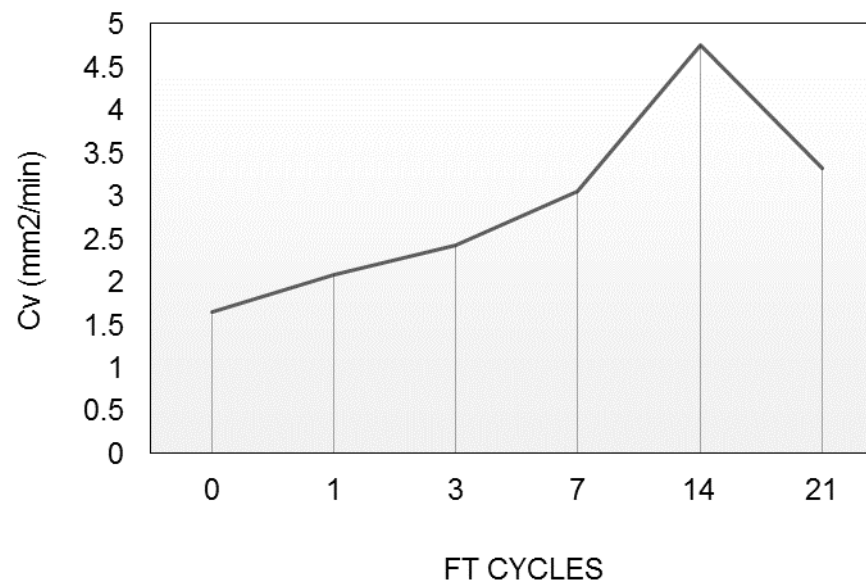
5.6.2. Test Results

The results of total 12 consolidation tests have been used in this study. The tests have been carried out on “undisturbed” CH soil samples that were collected by means of thin metal wall tubes with sharpened cutting edge.

The changes in C_v (Coefficient of Consolidation) of soils which were examined as shown in Figure 5.17a-b, where C_v was plotted on logarithmic scale and FT cycle number on arithmetic scale. Low plasticity soils display an increasing C_v with increasing stress level while high plasticity soils display a decreasing C_v .



(a)

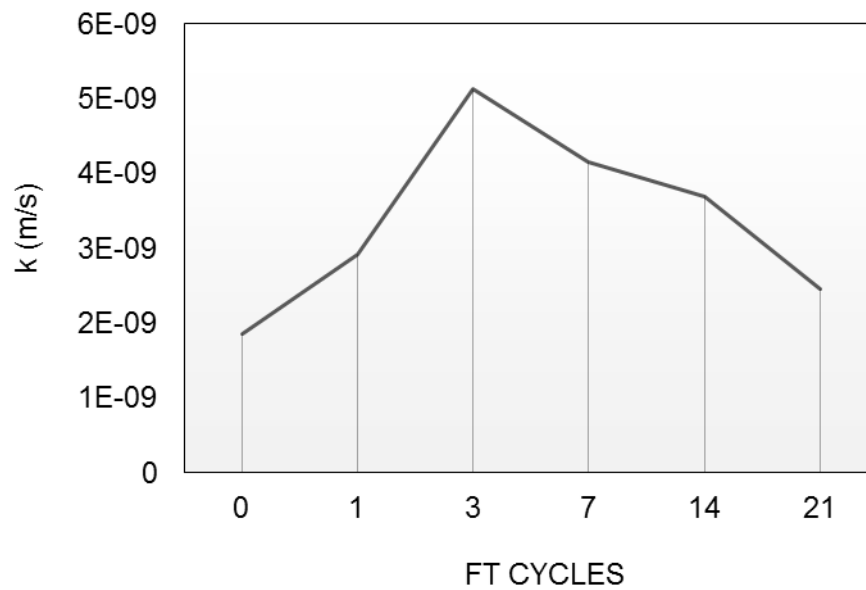


(b)

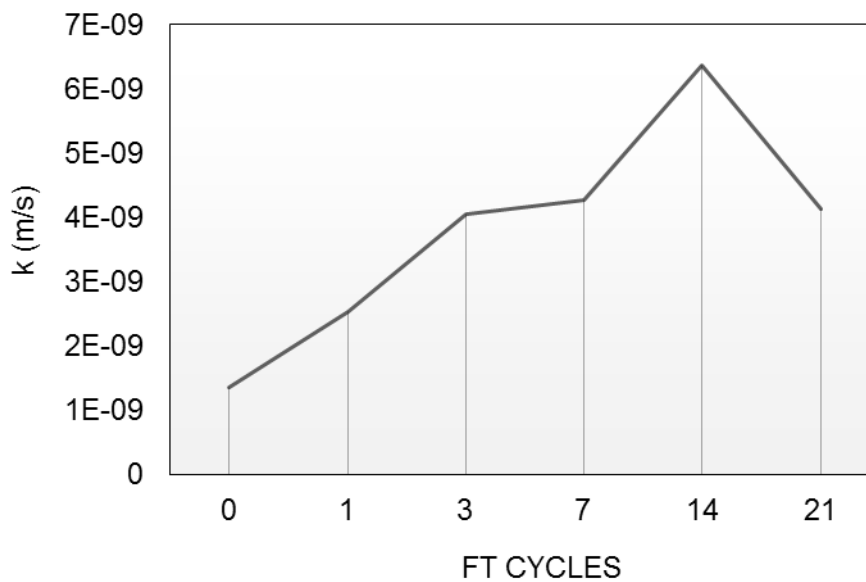
Figure 5.17. Coefficient of Consolidation (C_v) of a) CH and b) SC soils.

The coefficient of permeability of clays is controlled by variety of factors which can be classified as a mechanical and physico-chemical. The mechanical factors of the main items includes size of main item are the size, shape, and the geometrical arrangement of the clay particles.

Here it was observed for CH soil that at first k increased and after 3rd FT cycle decreased as well as clayey sand, which decreased after 14th FT cycle (Fig 5.18a-b).



(a)



(b)

Figure 5.18. Coefficients of permeability (k) of
a) CH and b) SC soils.

5.7. XRD Analyses

After FT cycles, the XRD analyses of fresh, 7th and 21st FT samples were carried out with using a Philips PW-1140 model diffraction with a goniometer speed of 20/minute. A standard method offered by Gundogdu (1982) was used for quantitative estimates of the minerals. In this method, the minerals are calculated in the same way, and the characteristic peak intensities (I) of the minerals are normalized to reflection of dolomite (Ulusay and Erguler, 2003). The mineral contents were determined by the equation 5.3.

$$\text{Percentage of the mineral} = 100 K_a I_a / (K_a I_a + K_b I_b + \dots + K_n I_n) \quad \text{Equation 5.3.}$$

K: constant for mineral type, I: intensity of each mineral

The results of the whole sample mineralogy obtained from diffractograms showed that both soil samples are mainly consisted of quartz, clay, calcite and feldspar minerals. The percentages of minerals were determined by Eq. 5.3 and presented in table 5.8-9.

Table 5.8. The percentages of CH soil's minerals

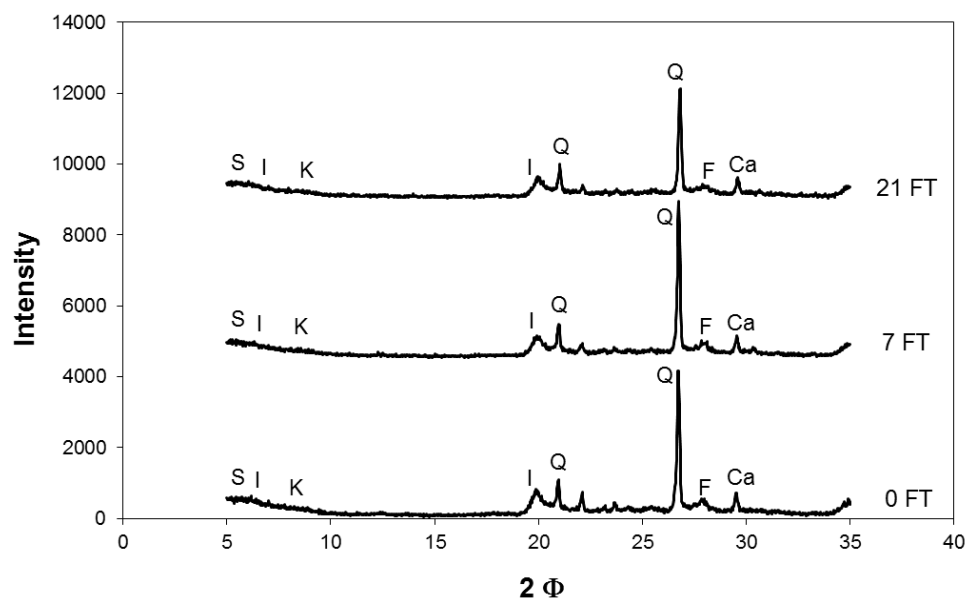
	Quartz (%)	Calcite (%)	Feldspar (%)	Clay (%)
original	11.36	3.22	3.92	81.5
7. cycle	14.47	3.68	4.05	77.52
21. cycle	11.17	3.53	3.94	81.36

Table 5.9. The percentages of SC soil's minerals

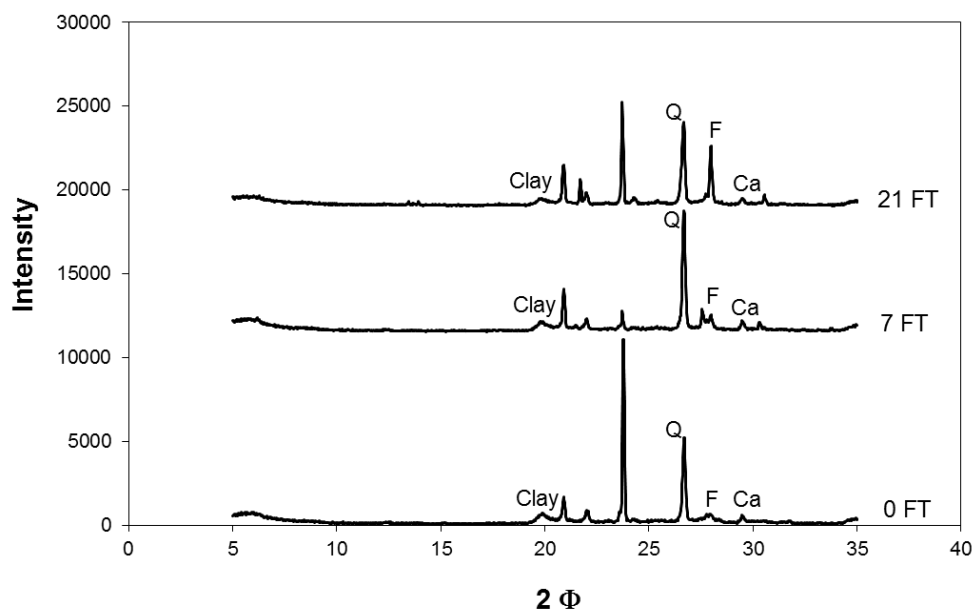
	Quartz (%)	Calcite (%)	Feldspar (%)	Clay (%)
original	12.88	41.29	2.22	43.61
7. cycle	20.65	6.97	3.18	69.2
21. cycle	16.31	5.9	3.2	74.58

The peak intensities of minerals of the original sample were compared to other samples exposed to freezing and thawing. In the diffractograms of CH soil, feldspar mineral content varies between 3.92% and 3.94%. There is no consistent change in the calcite content. The little decrease was occurred up to 7th FT cycle on clay content. However, clay content was increased in a few amounts after 21st FT cycle (Fig. 5.19a).

In the XRD analyses of SC soil, no more changes were observed in mineral contents (Fig. 5.19b).



(a)



(b)

Figure 5.19. XRD analyses of (a) CH and (b) SC soils (Q: Quartz, F: Feldspar, Ca: Calcite)

5.8. Scanning Electron Microscopy (SEM) Studies

Fresh and samples exposed FT cycles were also subjected to SEM analyses with using Zeiss EVO 50 EP scanning microscope under 100– 200 Pa vacuum. SEM micrographs of the both types of specimens were presented in Fig. 5.20-21. The view magnification was selected as 3000X to observe the changes of both of mineral and cracks.

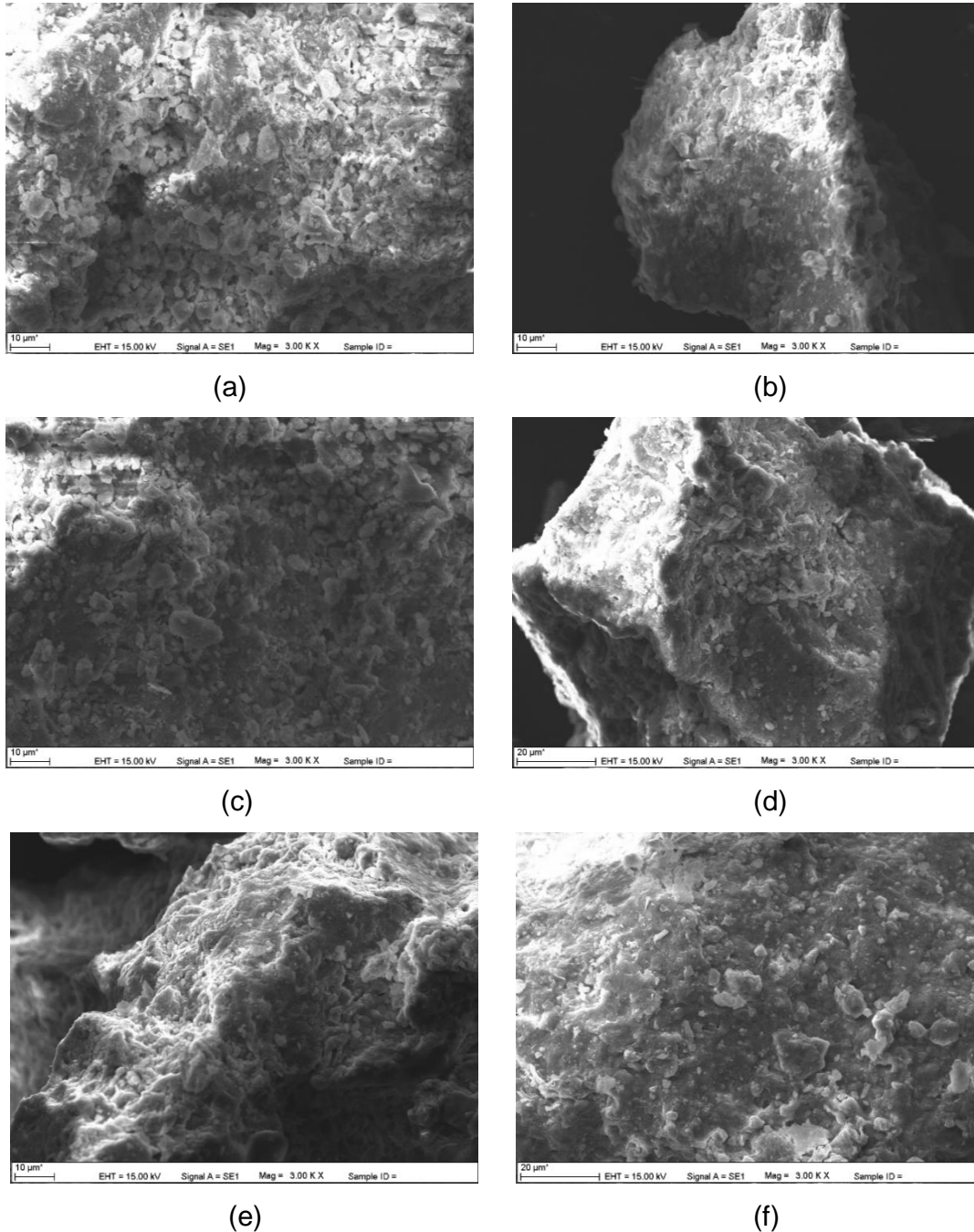
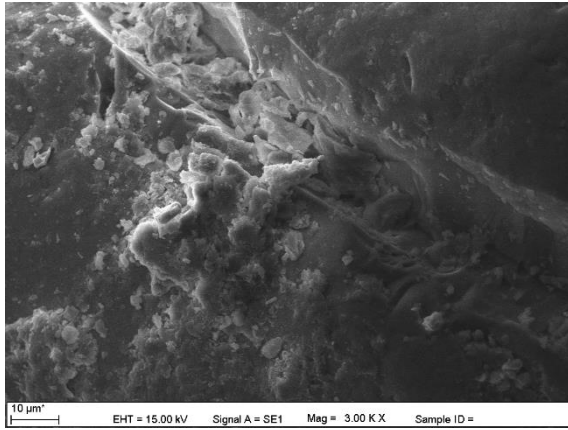
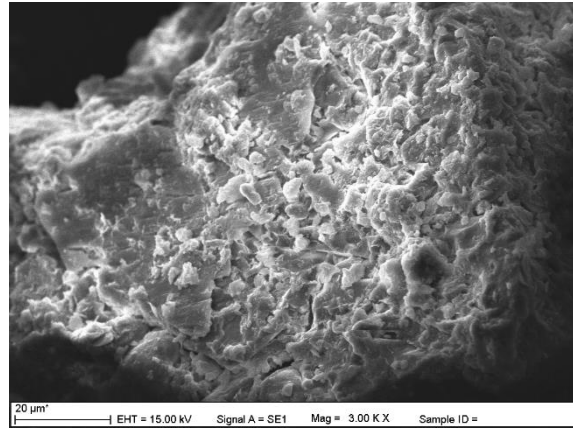


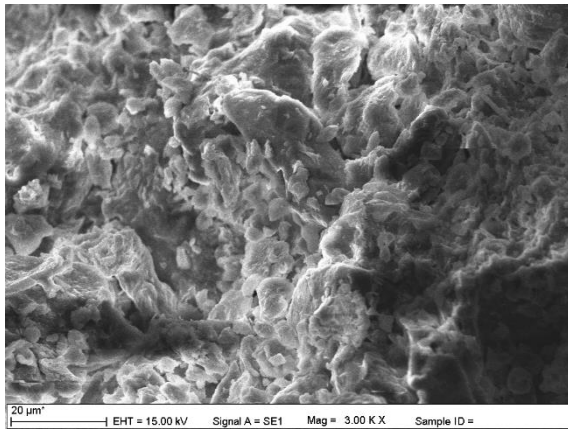
Figure 5.20. SEM micrographs of CH a) Fresh, b) one FT cycle, c) 3 FT cycles, d) 7 FT cycles, e) 14 FT cycles and f) 21 FT cycles.



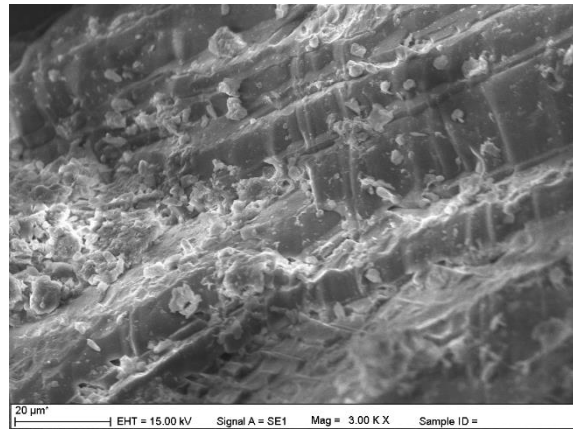
(a)



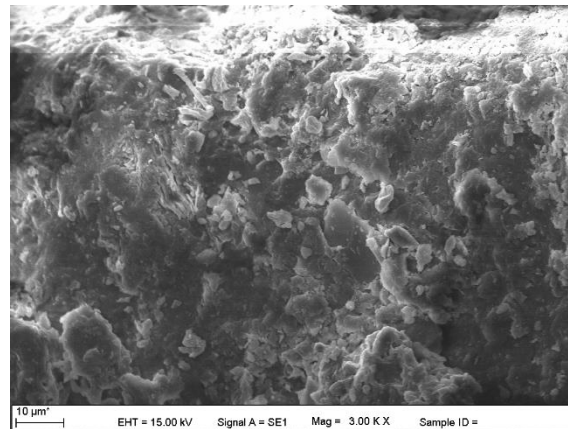
(b)



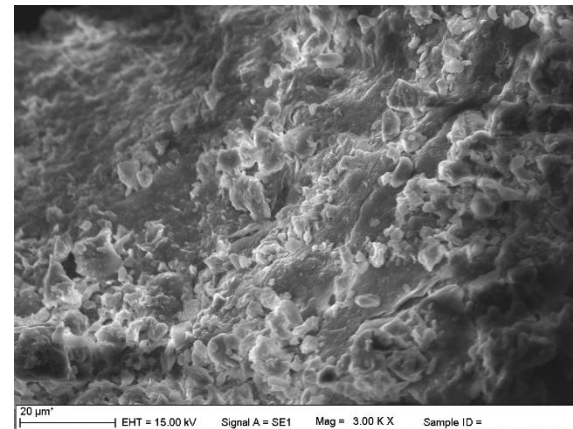
(c)



(d)



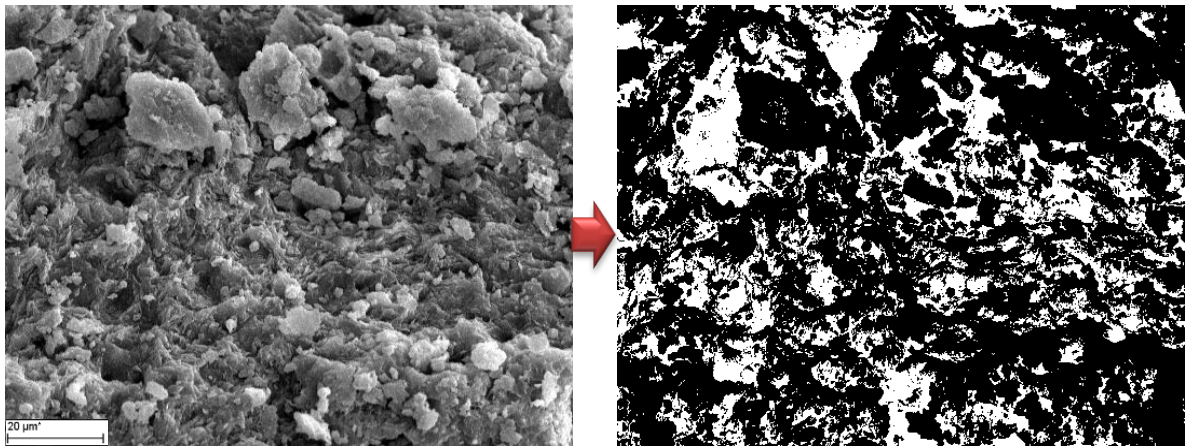
(e)



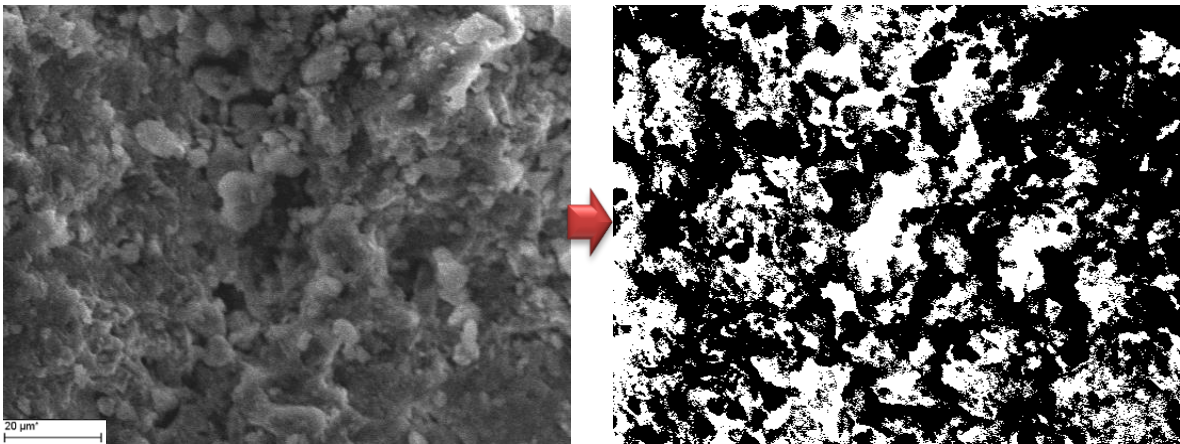
(f)

Figure 5.21. SEM micrographs of SC a) Fresh, b) one FT cycle, c) 3 FT cycles, d) 7 FT cycles, e) 14 FT cycles and f) 21 FT cycles.

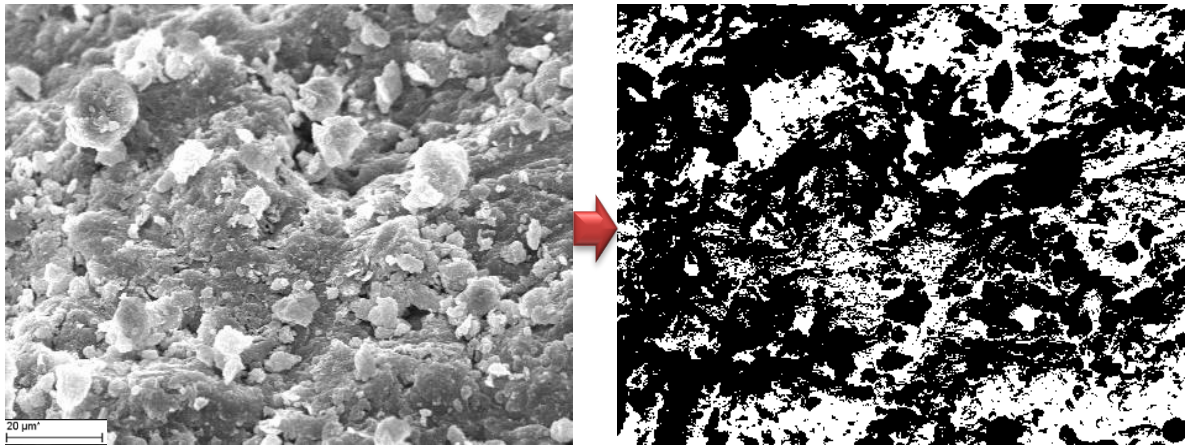
After SEM viewing, the photos were converted into 2bit black-and-white picture format to examine crack propagations and void occurrences in CH soil. This examination was realized as to the study of Cui et al. (2014). Voids were turned into white color, and minerals and matrix were colored as black. The colors of percentages were determined by the histogram analysis of Corel Photo-Paint X3.



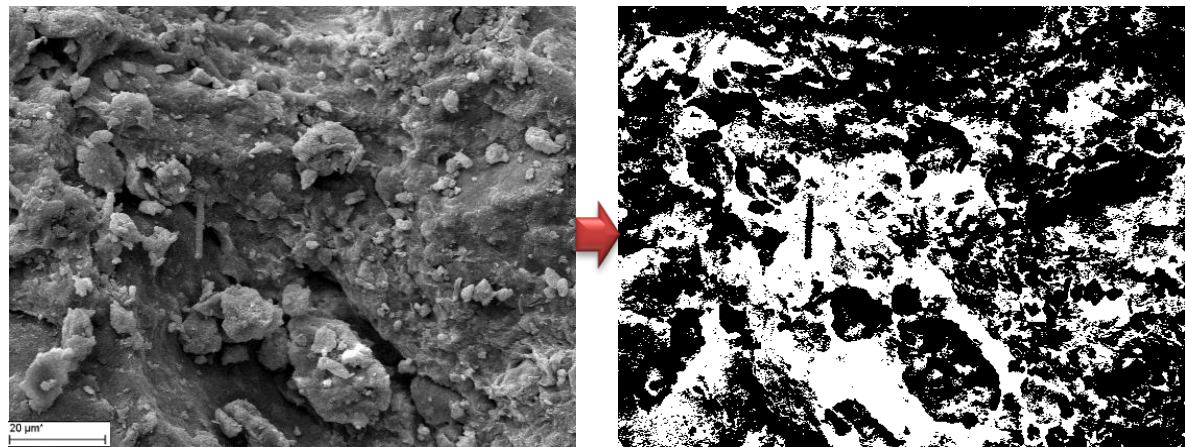
(a)



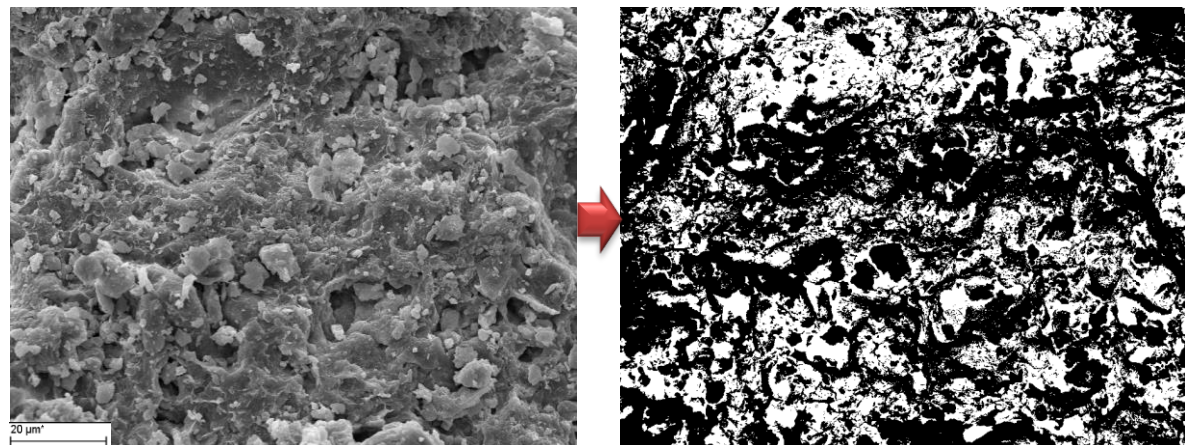
(b)



(c)



(d)



(e)

Figure 5.22. Converting the SEM views of CH soil into black and white color; a) for fresh sample, b) for sample exposed 3 FT cycles, c) after 7 FT cycles, d) 14 FT cycles e) 21 FT cycles.

The result shows similar character as observed in the CH soil properties like (grain size, Atterberg limits, etc.) were seen in these examinations. The white color symbolized voids has increased until 14th FT cycle, then started to decrease. Conversely, the black color represented particles has declined up to 14th cycle, afterwards, inclined (Fig. 5.23). Freezing and thawing process has disintegrated particles in CH soil till 14th cycle, then, particle fragments start to fill cracks and the volume of voids to be reduced.

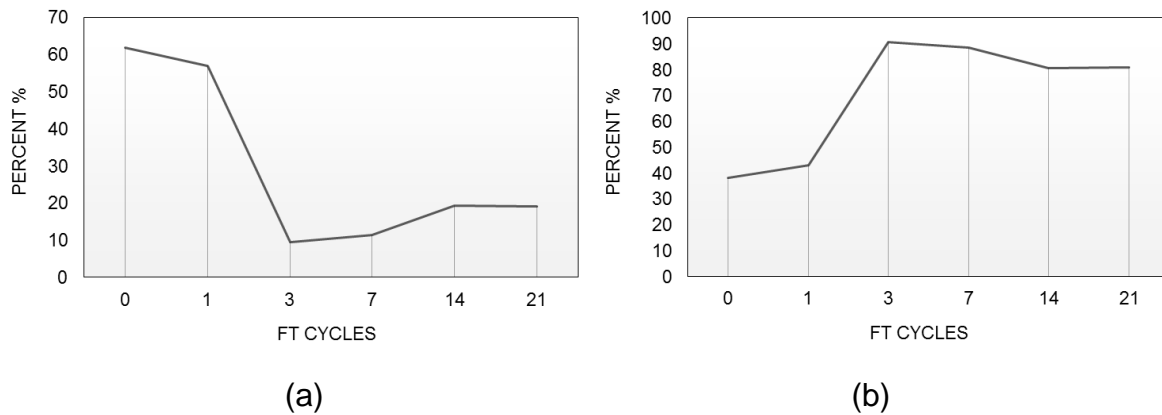


Figure 5.23. The determination of white and black colors to investigate cracks propagation in CH soil; a) for white color represented voids, b) for black color symbolized particles.

However, voids determination by SEM micrograms was not shown the good performance on SC soil (Fig. 5.24). Sand include more big voids in nature. Therefore, this technique is not suitable for sand size particles.

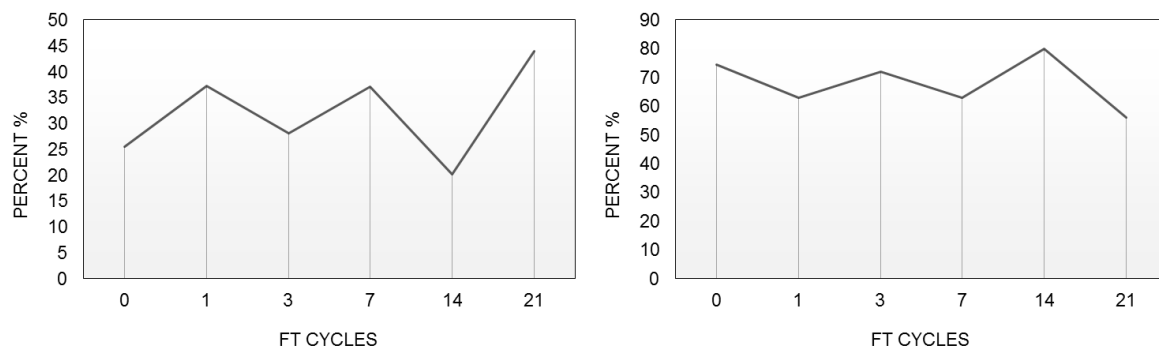


Figure 5.24. The determination of white and black colors to investigate cracks propagation in SC soil; a) for white color represented voids, b) for black color symbolized particles.

6. CONCLUSIONS AND RECOMMENDATIONS

The objective of this study is to find a framework for the frozen Ankara Clay relating the engineering properties of this material to its structure in cold seasons. Samples from the same depth were tested, belonging to different lithological strata of the Ankara Clay. A comparison between the mechanical responses of samples and FT cycles allowed the identification of a relationship between the engineering properties and the structure of frozen Ankara Clay.

Based on the analysis and results, the following conclusions have been drawn:

- 1) Ankara Clay (AC) is very expansive soil due to higher smectite mineral content. As well, the big part of Ankara was founded on the lacustrine sediments. Therefore, AC causes deformations and failures in the urban roads after winter months.
- 2) All test data show that the physical and strength properties, suddenly, decreased after first freezing and thawing cycle. This state sign of the clay mineral orientation due to freezing and thawing process. It is also observed that the soil classification of Ankara Clay was changed from "CH" to "MH" after first FT cycle.
- 3) Specific gravity and density values of CH soil have decreased up to 3 FT cycles, then, starts to incline. However, the same inference was not correct for clayey sand. They have shown a fluctuation trend between 2.49 and 2.46.
- 4) After seven FT cycles, soil consistency limits of CH soil started to incline because sand particles of soil commence disintegration and getting small particles. Conversely, these values of SC soil showed increasing trend up to 7th FT cycle, then; they started to decrease.
- 5) In sieve analyses, the grain size of CH soil changed with the number of FT cycles. Fine grains have decreased until 14th FT cycle, then, they have increased. An opposite behavior was observed on sand and gravel particles. They decreased after 14th FT cycle. These results showed that clay particles were accumulated by FT cycles. Therefore, silt size particles increased after third FT cycle.
- 6) The activity of CH soil was changed by FT cycles. The activity classification was changed from inactive to normal active in the 14th FT cycle, and it returned inactive degree after this point.

- 7) Depending on the FT cycles, the shear strength of CH soil, have dropped until 7th FT cycle, then, they have gone up. The values of internal friction angle and cohesion of the clayey sand soil, commonly, have increased.
- 8) The coefficients of consolidation and permeability of both soil samples were calculated for stress range of 100 and 200 kPa. Similar behavior have been observed during consolidation tests. All values were increased up to 14th cycle, then, decreased.
- 9) During electron microscopy studies, void's increment of CH soil samples was determined because of FT cycles. Later, voids were filled with clay particles. The same Behavior was not observed on the clayey sand soil specimens, clearly.
- 10) About 14th FT cycle can be a threshold value for cohesive soils for observing distinct physico-mechanical properties. Therefore, number of FT cycles of the site must be determined before the construction of light structures (road, concrete covering, etc.) because of variable soil conditions depending on FT cycles. Also, freezing and thawing tests must be realized as to this number of cycle and artificial slope stability analyses must be carried out according to these results.

REFERENCES

- [1] Czurda K.A., and Hohmann M., Freezing Effect on Shear Strength of Clayey Soils, *Applied Clay Science*, 12, 165-187, **1997**.
- [2] Huang WX., Soils Engineering Properties China Water Power Press, Beijing, **1983**.
- [3] Chen Zh Y., Zhou JX., Wang HJ., Soil Mechanics. *Qinghua University Press*, **1994**.
- [4] Thevanayagam S., Shenthann T., Mohan S., Liang J., Undrained Fragility of Clean Sands, Silty Sands and Sand Silts. *Journal of Geotechnical and Geoenvironmental Engineering*, ASCE 128, 10, 849-859, **2002**.
- [5] Coop M.R., The Mechanics of Uncemented Carbonate Sands, *Geotechnique*, 40, 4, 607-662, **1991**.
- [6] Allmar M.A. and Atkinson J.H., Mechanical Properties of Reconstituted Bothkenner Soil, *Geotechnique*, 42, 2, 289-301, **1992**.
- [7] Georgiannou V.N., Burland J.B., Hight D.W., The Undrained Behavior of Clayey Sands in Triaxial Compression and Extension, *Geotechnique*, 40, 3, 431-449, **1990**.
- [8] Jafari M.K. and Shafiee A., Mechanical Behavior of Compacted Composite Clays, *Canadian Geotechnical Journal*, 41, 6, 1152-1167, **2004**.
- [9] Turetsky M.R., Wieder R. K., Vitt D. H., Evans R.J., Scott K. D., The disappearance of relict permafrost in boreal North America: Effects on peatland carbon storage and fluxes. *Global Change Biology*, 13, 1922–1934, **2007**.

- [10] Oztas T., Fayetorba F., Effect of freezing and thawing processes on soil aggregate stability. *Catena*, 52, 1– 8. **2003**.
- [11] Wang D.Y., Zhu Y.L., Ma W., Niu YH., Application of Ultrasonic Technology for Physical-Mechanical Properties of Frozen Soils. *Cold Regions Science and Technology*, 44 ,12-19, **2006**.
- [12] Wang D.Y., Niu YH., Ma W., Effects of Cyclic Freezing and Thawing on Mechanical Properties of Qinghai-Tibet Clay. *Cold Regions Science and Technology*, 48, 34-43, **2007**.
- [13] Paudel B., Wang B., Freeze-thaw effect on consolidation properties of fine grained soils from the Mackenzie valley, Canada , *Geo*, **2010**.
- [14] Guo Y., Shan W., Monitoring and Experiment on the Effect of Freeze-Thaw on Soil Cutting Slope Stability, *Procedia Environmental Sciences*, 10, 1115 – 1121, **2011**.
- [15] Yıldız M., Soğancı A.S., Effect of freezing and thawing on strength and permeability of lime-stabilized clays, *Scientia Iranica*, 19 , 4, 1013–1017, **2012**.
- [16] Aubert J.E., Gasc-Barbier. M., hardening of clayey soil blocks during freezing and thawing cycles. *Applied Clay Science*, 65–66, **2012**.
- [17] Wang T.L., Yue Z.R., Ma CH., Wu Z., An experimental study on the frost heave properties of coarse grained soils. *Transportation Geotechnics*, 1, 137–144, **2014**.

- [18] Aldaood A., Bouasker. M., Al-Mukhtar. M., Impact of freeze–thaw cycles on mechanical behaviour of lime stabilized gypseous soils. *Cold Regions Science and Technology*, 99, 38–45, **2014**.
- [19] Cui Z-D., He P-P., Yang W-H., Mechanical properties of a silty clay subjected to freezing–thawing, *Cold Regions Science and Technology*, 98, 26–34, **2014**.
- [20] Wang TL., Liu Y-J., Yan H., Xua L., An experimental study on the mechanical properties of silty soils under repeated freeze–thaw cycles, *Cold Regions Science and Technology*, 112, 51–65, **2015**.
- [21] Flerchinger G.N., Lehrs G.A., McCool D.K., *Freezing and thawing processes, Encyclopedia of Soils in the Environment*, 104-110, Elsevier, Ltd, Oxford, U.K., **2005**.
- [22] Lehrs G.A., Sojka R.E., Carter D.L., Jolley P.M., *Freezing effects on aggregate stability affected by texture, mineralogy, and organic matter, Soil Science Society of America Journal*, 55, 1401-1406, **1991**.
- [23] Oztas T., Fayetorbay F., Jungqvist G., Oni S.K., Teutschbein C., Futter M.N., Effect of freezing and thawing processes on soil aggregate stability, *Catena*, 52, 1–8, **2003**.
- [24] Watanabe D., Nogami S., Ohya Y., Kanno Y., Zhou Y., Akao T., Shimoi H., Ethanol fermentation driven by elevated expression of the G1 cyclin gene CLN3 in sake yeast, *J Biosci Bioeng* 112, 6, 577-82, **2011**.
- [25] Anonim., Ankara ili 1944-2006 yılları aylık sıcaklık, yağış ve nem ortalama grafikleri, *Devlet Meteoroloji İşleri Genel Müdürlüğü*, Ankara, **2006**.
- [26] Republic of Turkey General Director of Highways, **2008**.

- [27] Turkish State Meteorological Survives, **2006.**
- [28] Kiper O. B., Etimesgut-Batıkent Yöresindeki Üst Pliyosen Çökellerinin Jeo-Mühendislik Özellikleri ve Konsolidasyonu, *Doktora Tezi, Hacettepe Üniversitesi, Jeoloji Mühendisliği Bölümü*, Ankara, 160 s, **1983.**
- [29] Kasapoğlu K.E., Ankara kenti zeminlerinin jeo-mühendislik özellikleri, *Doçentlik Tezi, Hacettepe Üniversitesi, Yerbilimleri Enstitüsü*, Ankara, 206 s, **1980.**
- [30] Batman B, Kulaksız S, Görmüş S., Alacaatlı Yöresinde (SW Ankara) Jura-Kretase Yaşlı İstifin Deformasyon Özelliklerine İlişkin Bir İnceleme, *Yerbilimleri, H.Ü.Y.B.E. Yayın Organı*, Cilt 4, Sayı No. 1-2, 135-153, **1978.**
- [31] Erol O., Ankara ve civarının jeolojisi hakkında rapor. *MTA Enstitüsü Bilimsel Dökümantasyon Şubesi, Derleme*, No: 2491, 238 s, **1954.**
- [32] Erol O., Yurdakul E., Algan Ü., Gürel N., Herece E., Tekirli E., Ünsal Y. ve Yüksel M., Ankara metropoliten arazi kullanım haritası. *MTA Genel Müdürlüğü Raporu*, 99 s, **1980.**
- [33] Akyürek B., Bilginer E., Akbaş B., Hepşen N., Pehlivan Ş., Sunu O., Soysal Y., Dağ Z., Çatal E., Sözeri B., Yıldırım H. ve Hakyemez Y., Ankara – Elmadağ – Kalecik Dolayının Temel Jeoloji Özellikleri, *Jeoloji Mühendisliği*, 20, 31-46, **1984.**
- [34] Dağ Z., Öztümer E., Sirel E., Yazlak Ö., Ankara civarında birkaç stratigrafik kesit: *T.J.K. Bült.*, 8, s. 1-2, 84-95, **1963.**
- [35] Akyürek B., vd., 1/100,000 ölçekli ve açınıma nitelikli Türkiye Jeoloji Haritaları Serisi Ankara-F15 Paftası, *MTA Yayını*, **1997.**

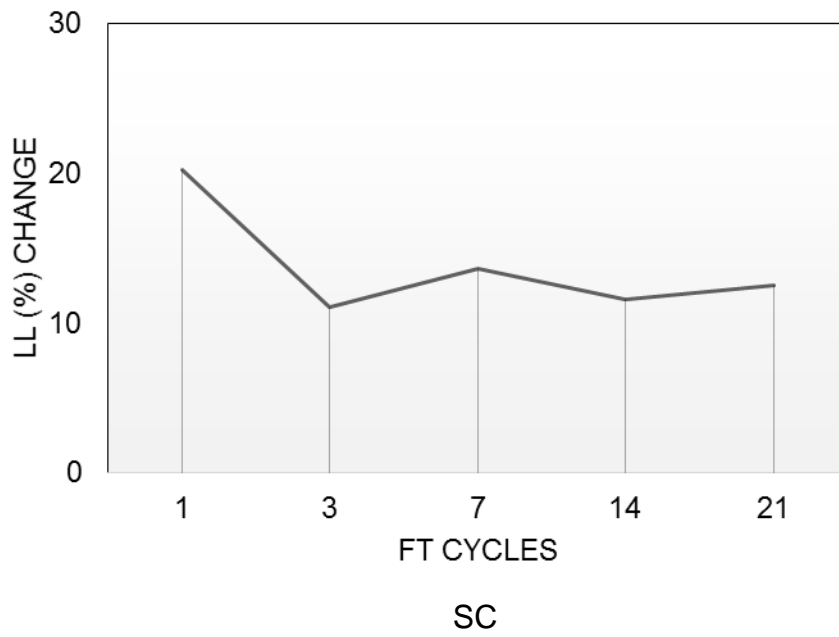
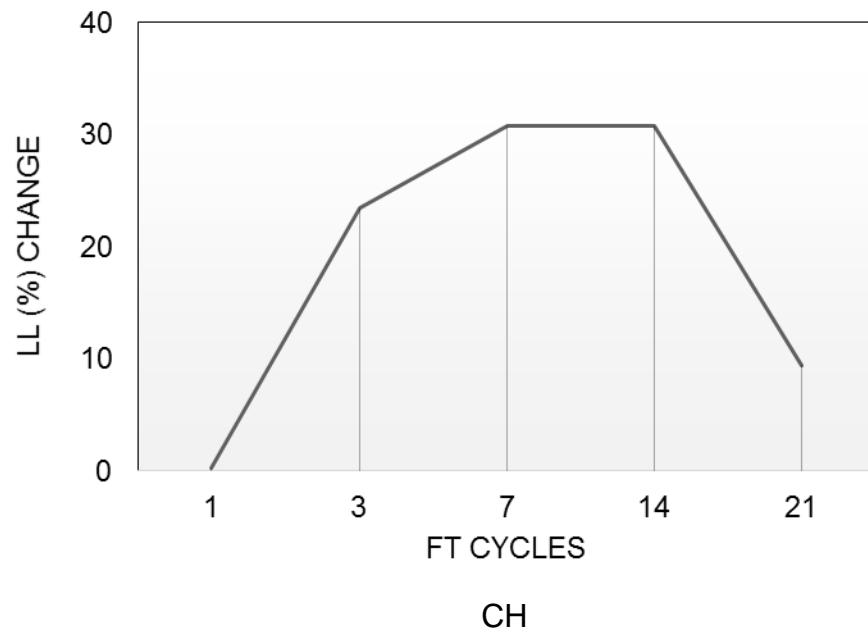
- [36] Erentöz C., 1/15.000 ölçekli Türkiye Jeoloji Haritası derlemesi, Ankara paftası: *M.T.A. Enistitüsü Yayını*, 111 s, **1975**.
- [37] Çalgın R., Pehlivanoğlu H., Ercan T., VE Şengül M., Ankara Civarı Jeolojisi MTA Derleme, No:6487, **1973**.
- [38] Norman T., Ankara Yahşiyen bölgesinde Üst Kretase-Alt Tersiyer istifinin stratigrafisi, *Türkiye Jeol*, Kur, Bült, XV/2, **1972**.
- [39] Avsar E., Ulusay R., Erguler Z.A., Swelling properties of Ankara (Turkey) clay with carbonate concentrations, *Environmental and Engineering Geoscience* 11, 1, 73–93, **2005**.
- [40] Ordemir I., Soydemir C., Birand A., Swelling Problems of Ankara Clays, *9th. Intentional Conference of Soil Mechanics and Foundation Engineering*, Tokyo, Vol.1, 243-247, **1977**.
- [41] Binal A., A new laboratory rock test based on freeze-thaw using a steel chamber, *Quarterly Journal of Engineering Geology and Hydrogeology*, 42, 179-198, **2008**.
- [42] Bowles J.E., Physical and geotechnical properties of soils, *Civil engineering series*, **1984**.
- [43] Gundogdu M.N.G., Neojen yasli Bigadic sedimanter base- ninin jeolojik, mineralojik ve jeokimyasal incelenmesi, PhD Thesis, Department of *Geological Engineering, Hacettepe University*, Ankara, Turkey, **1982**.

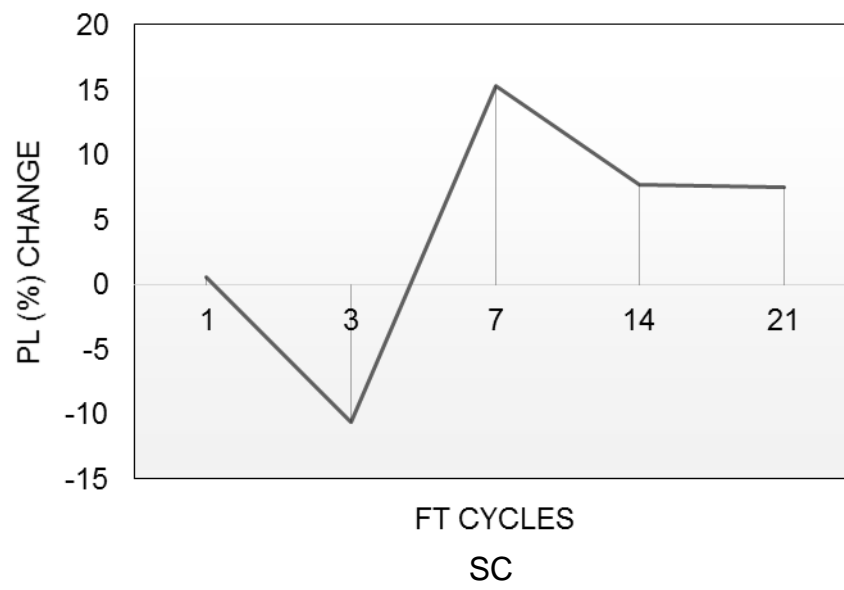
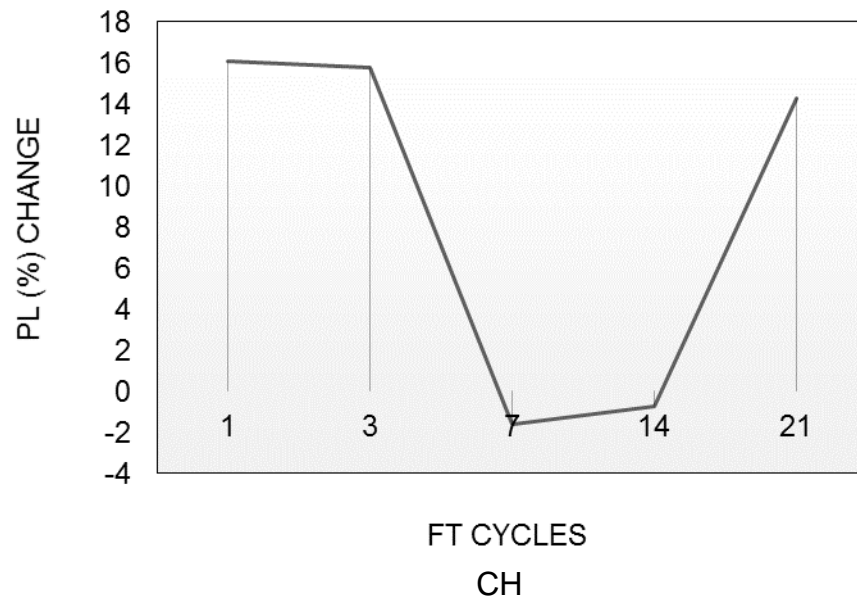
- [44] Erguler Z.A., Ulusay R., simple test and predictive models for assessing swell potential of Ankara (Turkey) Clay, *Department of Geological Engineering, Faculty of Engineering, Applied Geology Division*, Hacettepe University, Ankara, **2002**.

Appendix A. Unified Soil Classification System (USCS)

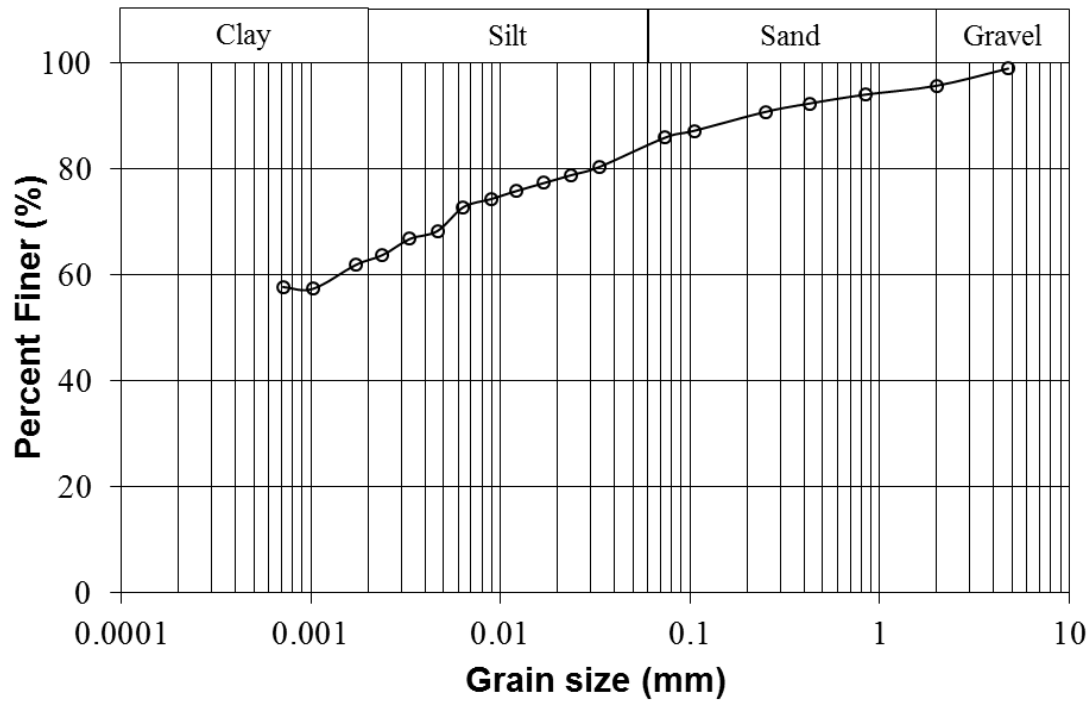
Description		Laboratory criteria				Notes
		Group Symbols	Fines (%)	Grading	Plasticity	
Coarse Grained (more than 50% larger than 63µm BS or No. 200 US sieve size)	Gravels (more than 50% fractions of gravel size)	Well graded gravels, sandy gravels, with little or no fines	GW	0-5	$C_u > 4$ $1 < C_c < 3$	Dual symbols if 5-12% fines. Dual symbols if above A-line and $4 < P_l < 7$
		Poorly graded gravels, sandy gravels, with little or no fines	GP	0-5	Not satisfying GW requirements	
		Silty gravels, silty sandy gravels	GM	>12	Below A-line or $P_l < 4$	
		Clayey gravels, clayey sandy gravels	GC	>12	Above A-line and $P_l > 7$	
	Sands (more than 50% of coarse fraction of sand size)	Well graded sands, gravelly sands, with little or fines	SW	0-5	$C_u > 6$ $1 < C_c < 3$	
		Poorly graded sands, gravelly sands, with little or fines	SP	0-5	Not satisfying SW requirements	
		Silty sands	SM	>12	Below A-line or $P_l < 4$	
		Clayey sands	SC	>12	Above A-line and $P_l > 7$	

Appendix B. Atterberg Limit Changes

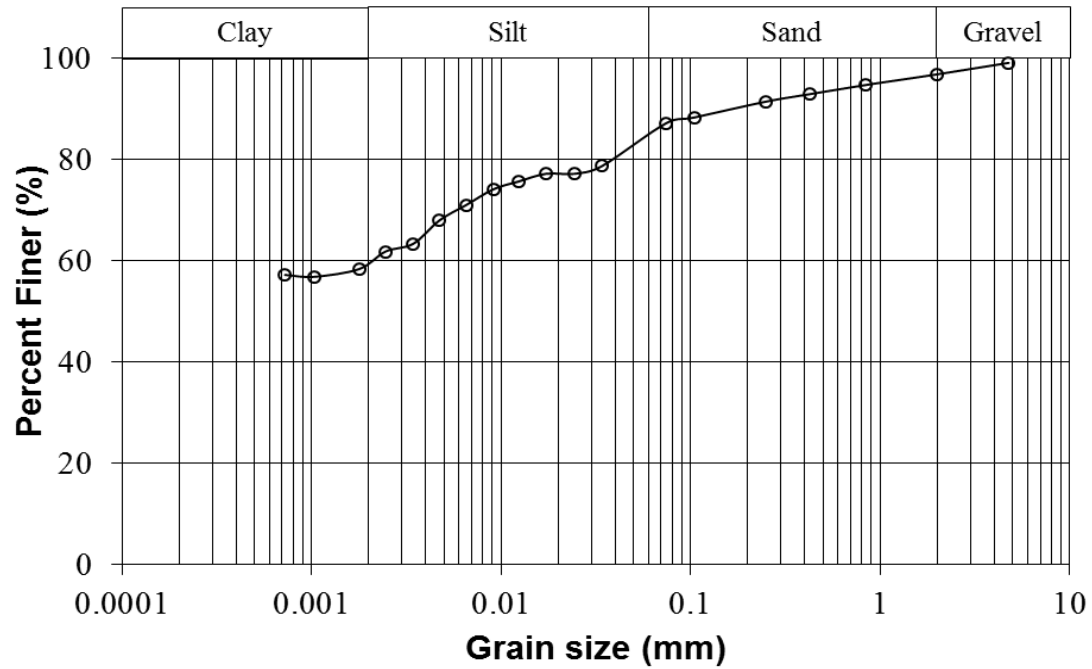




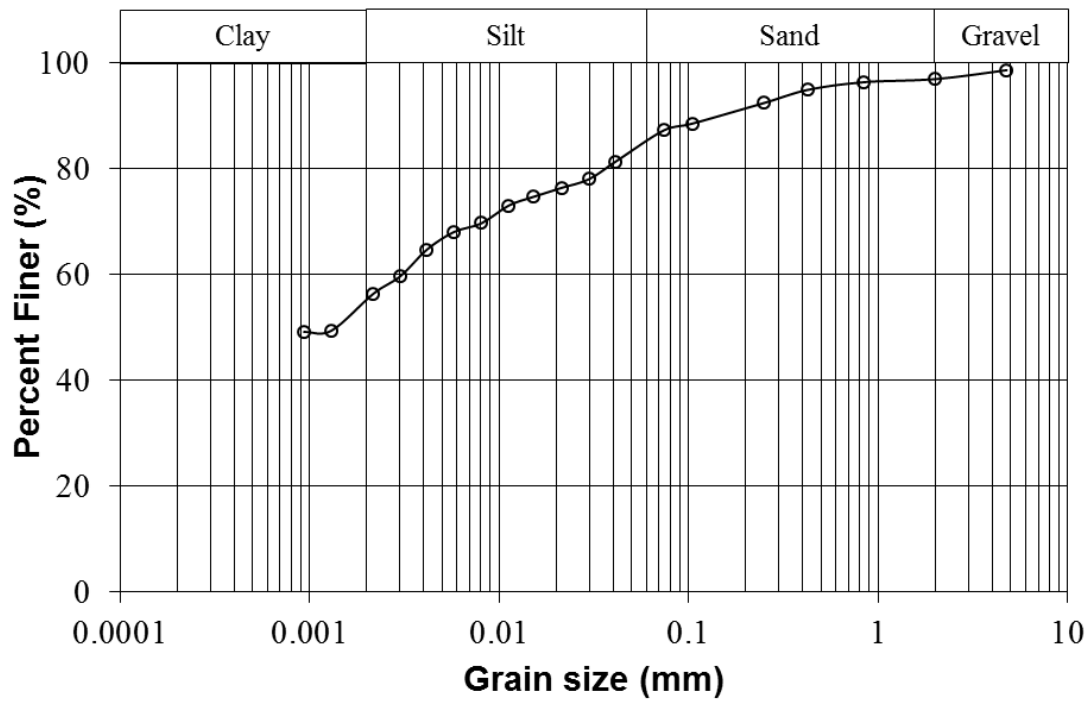
Appendix C. Grain size distribution



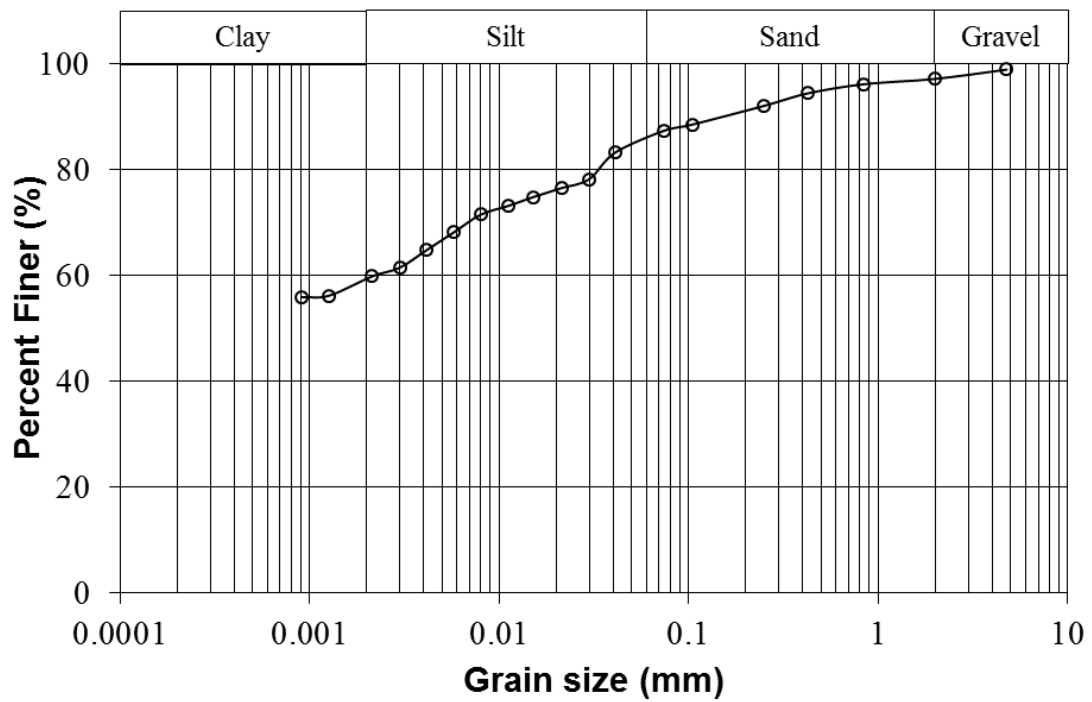
Original CH



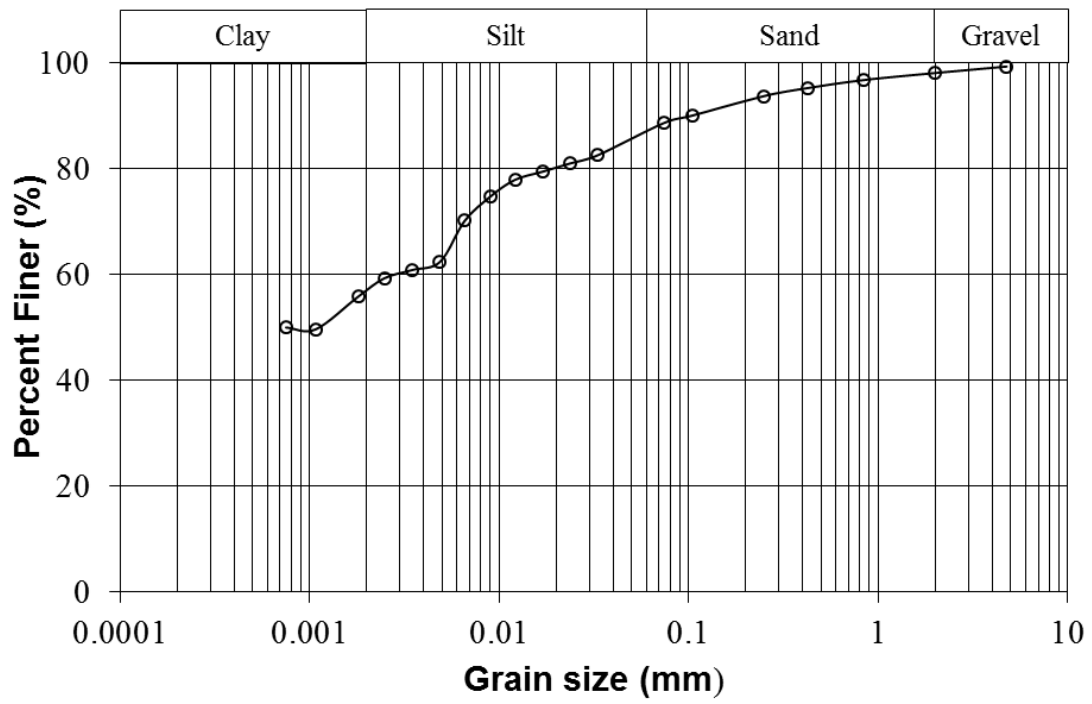
CH, 1. FT cycles



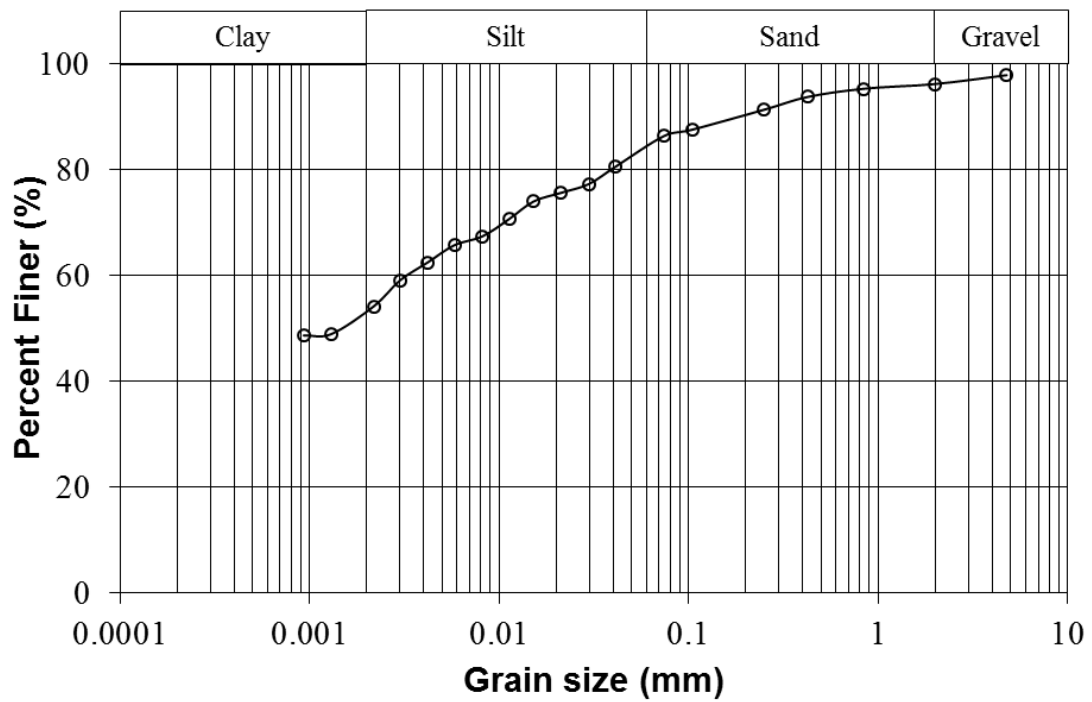
CH, 3. FT cycles



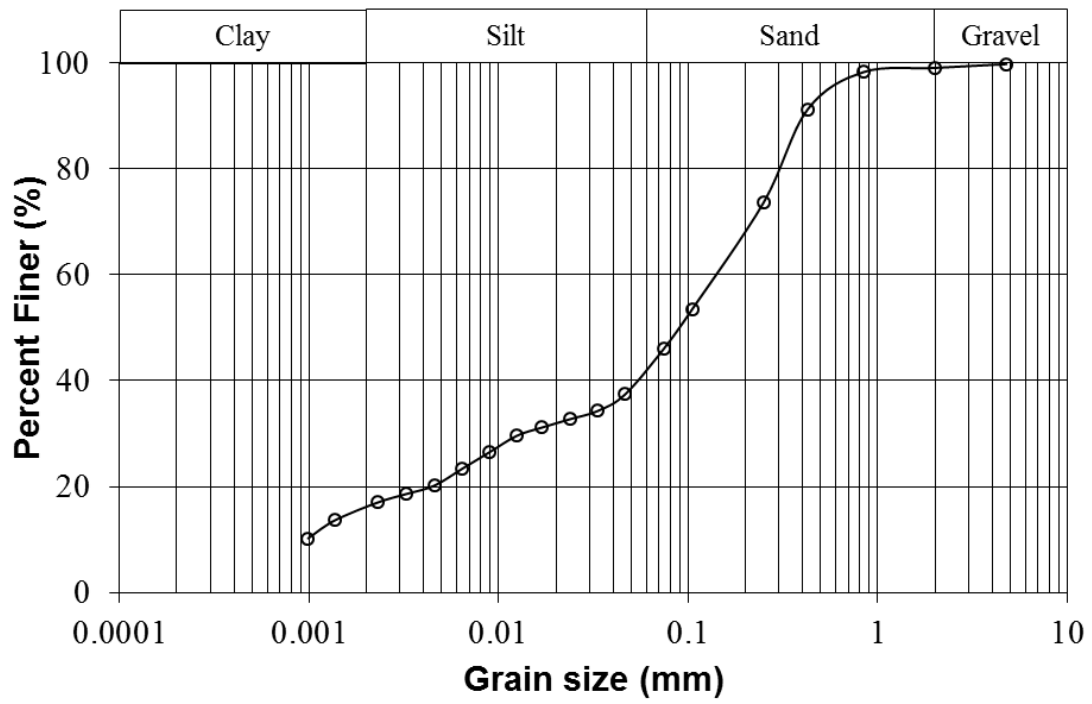
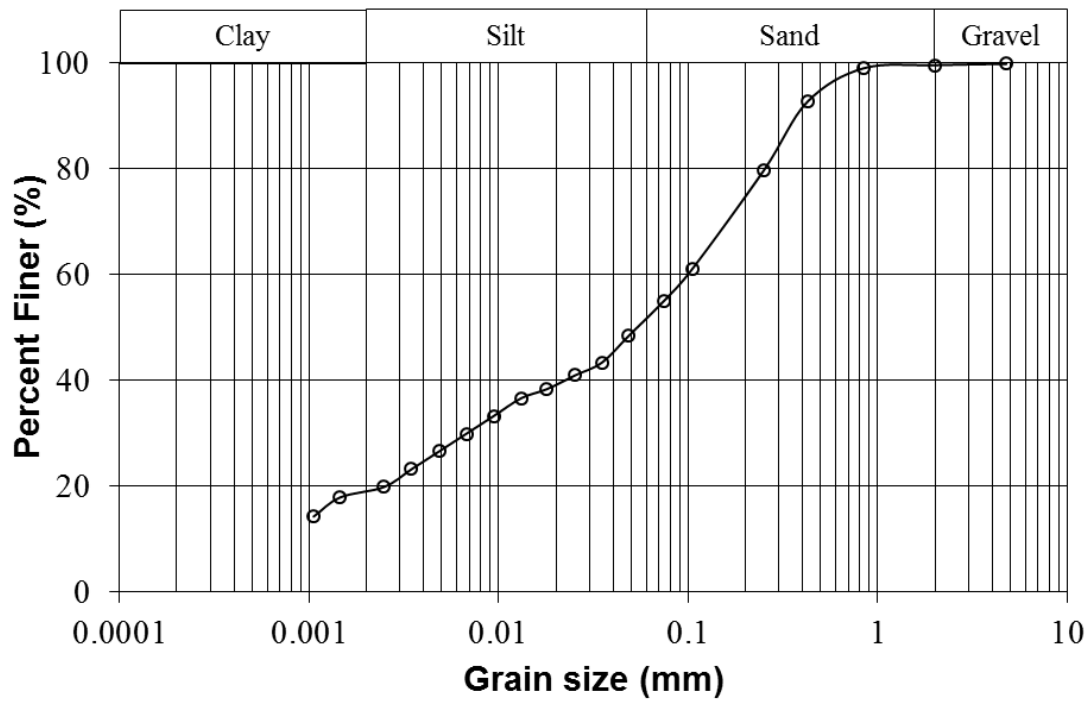
CH, 7. FT cycles

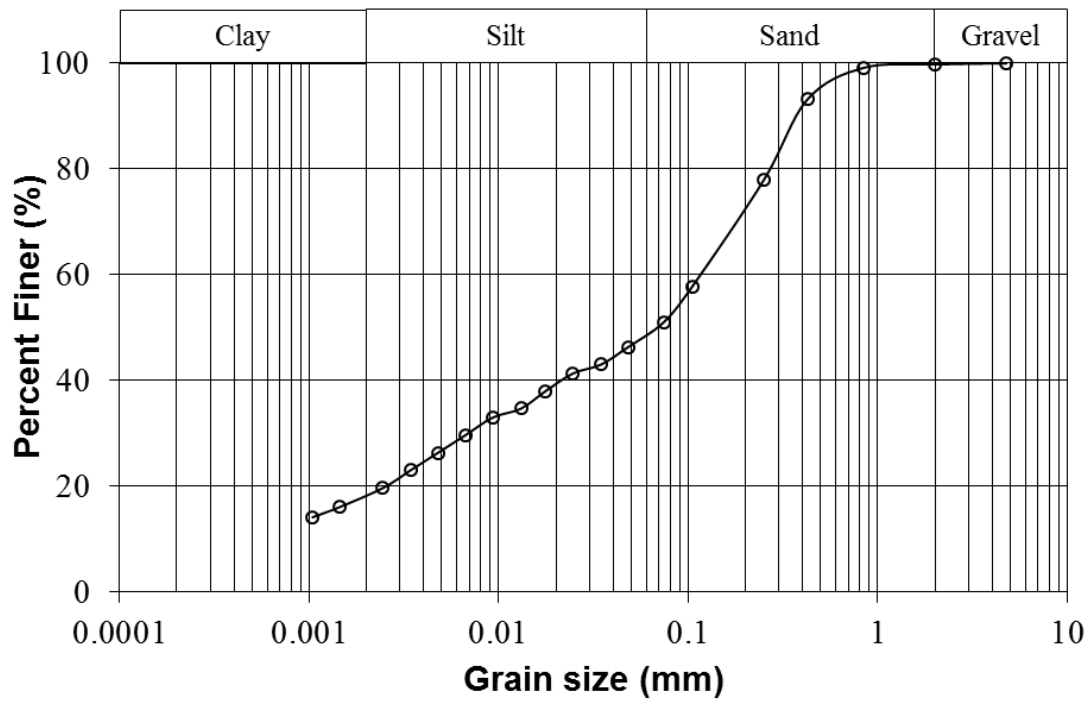


CH, 14. FT cycles

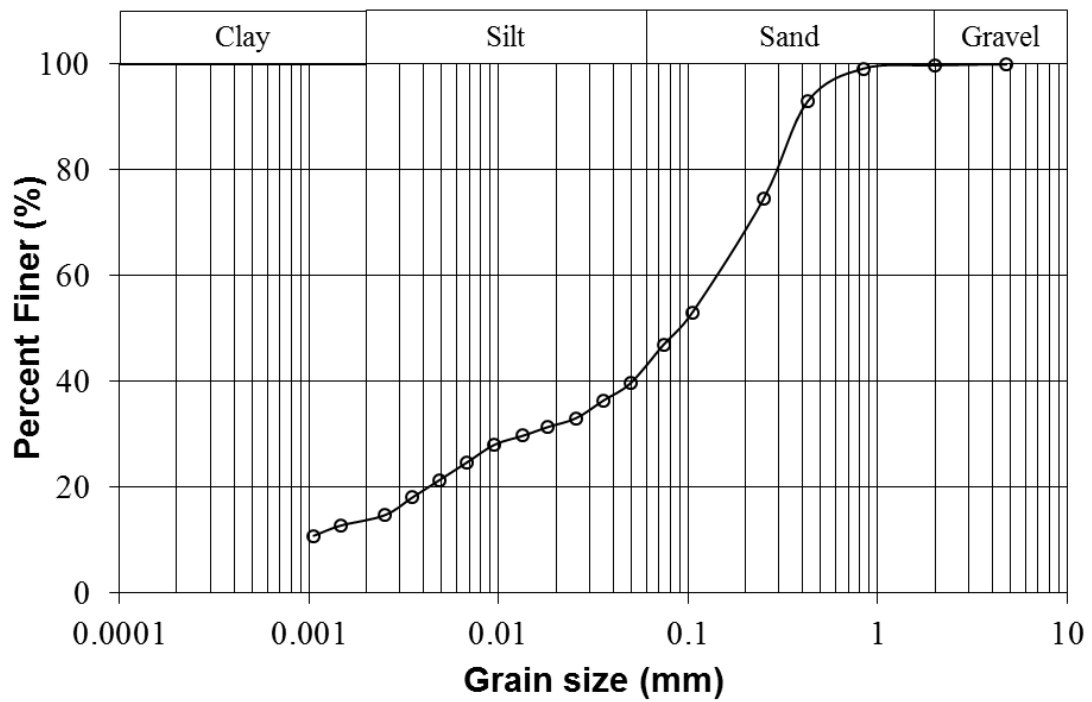


CH, 21. FT cycles

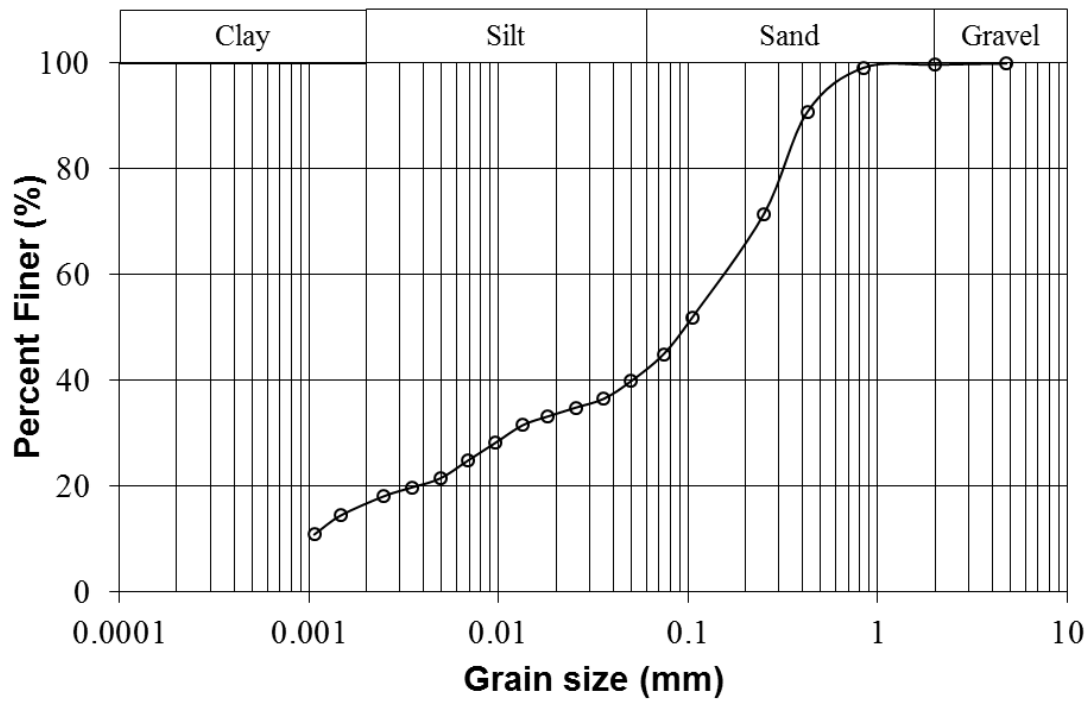




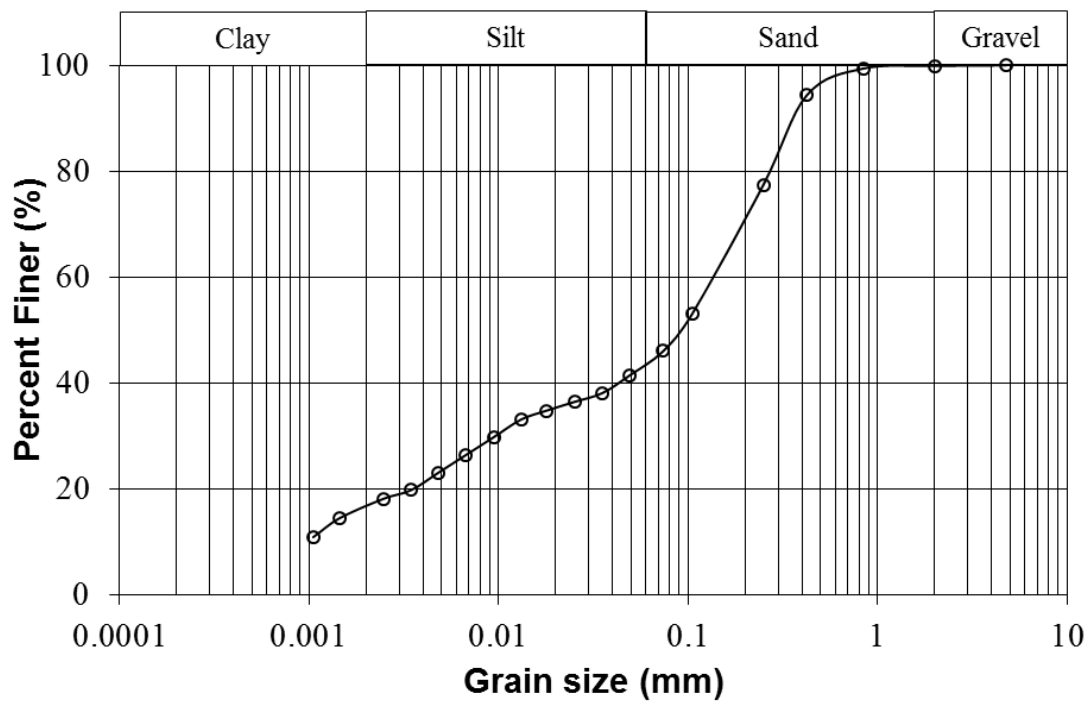
SC, 3. FT cycles



SC, 7. FT cycles

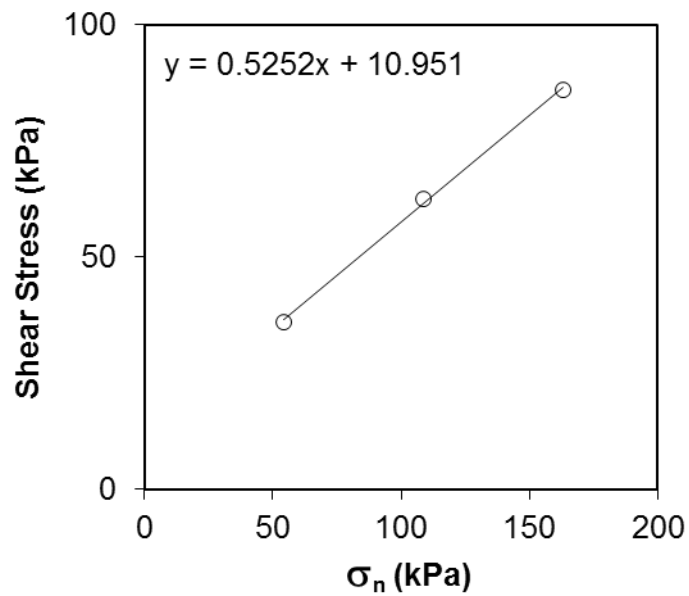
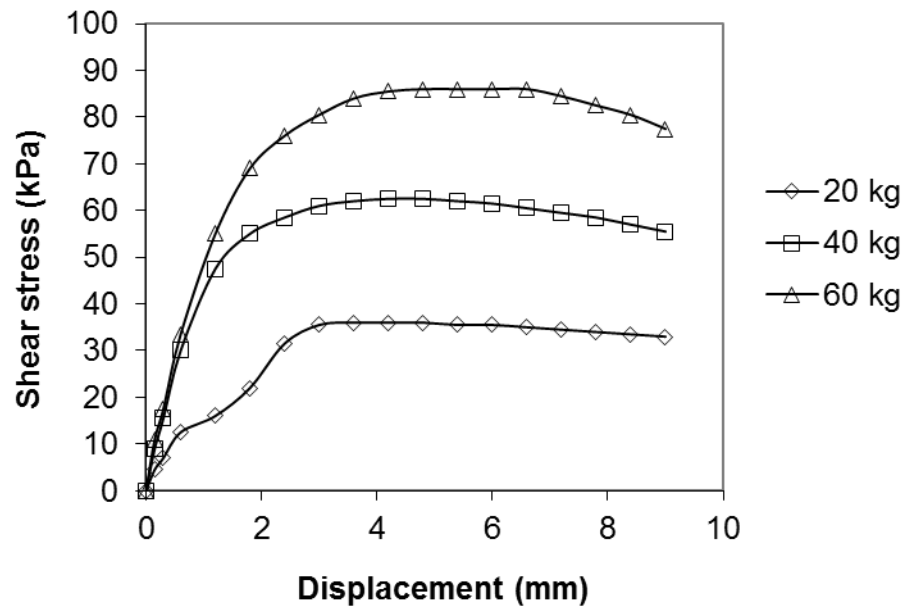


SC, 14. FT cycles

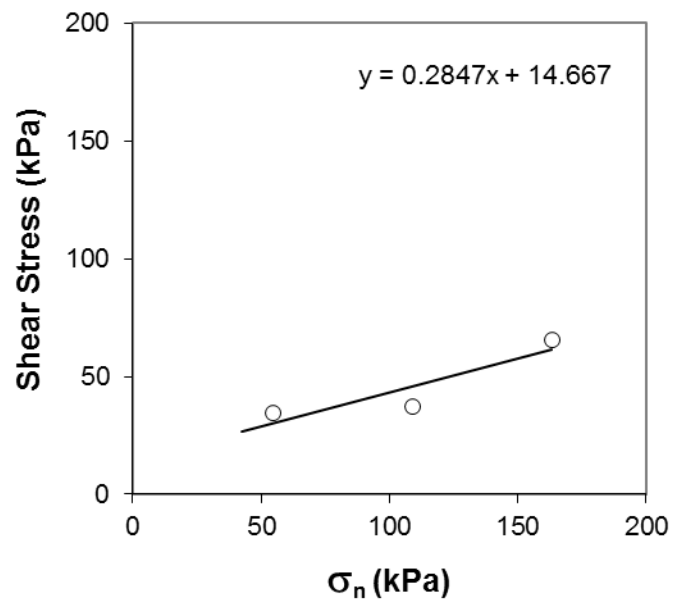
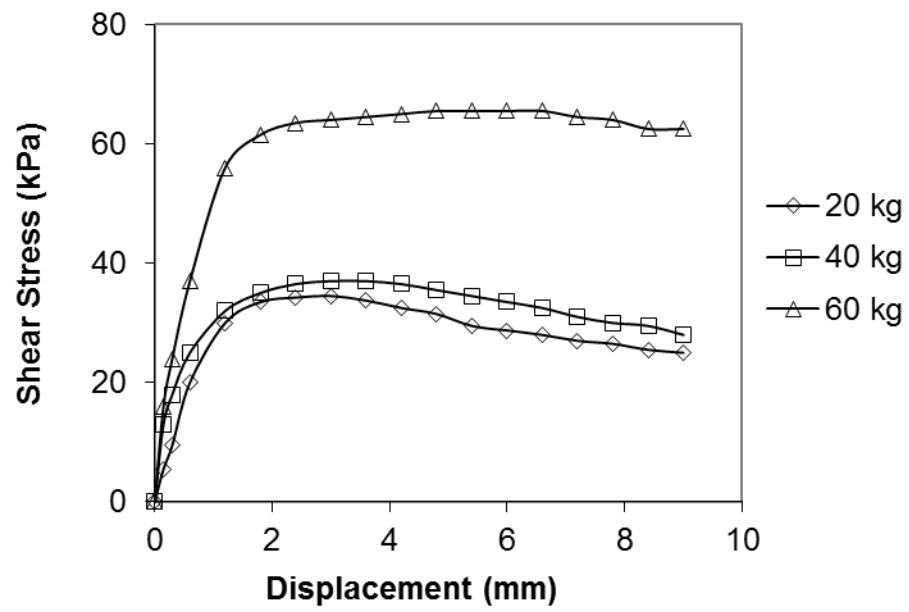


SC, 21. FT cycles

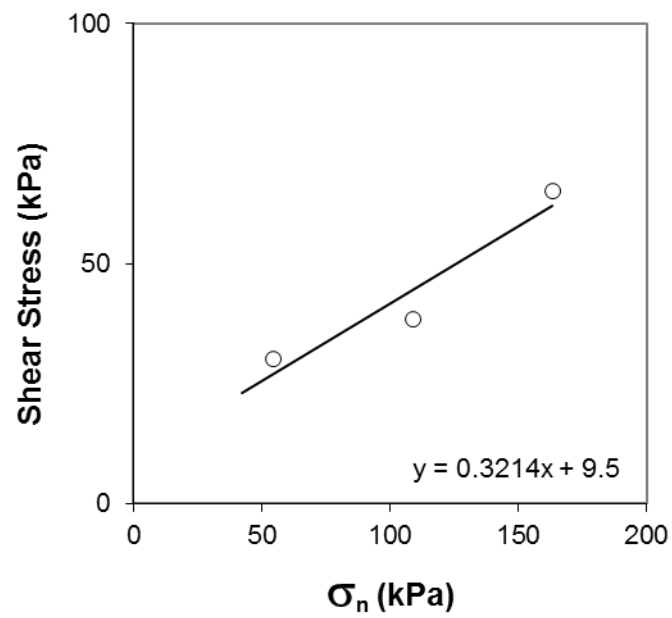
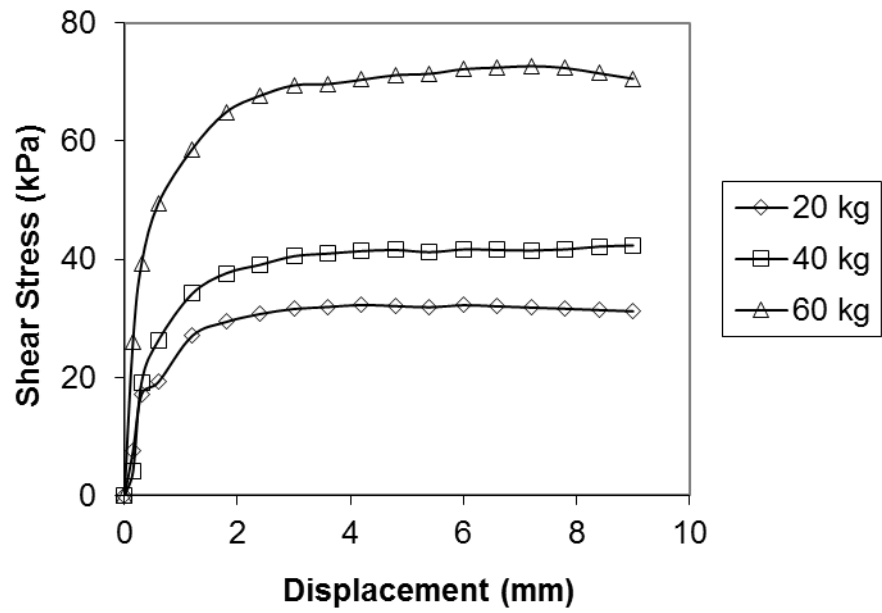
Appendix D. Direct Shear Box Test



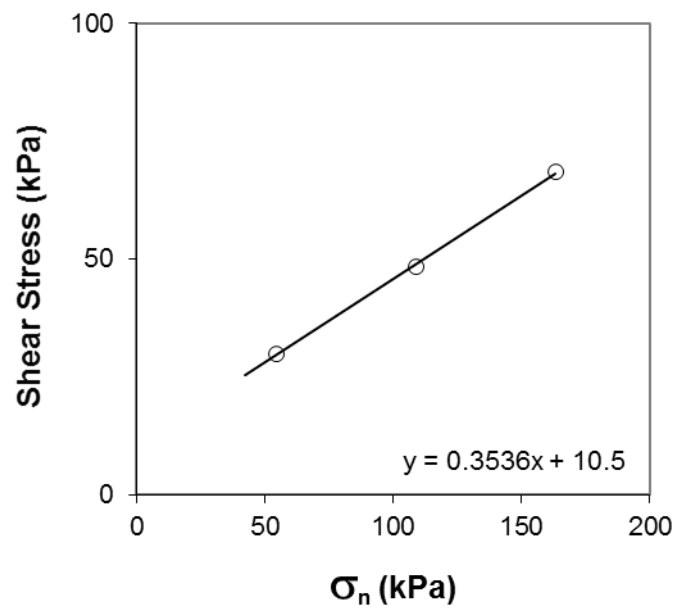
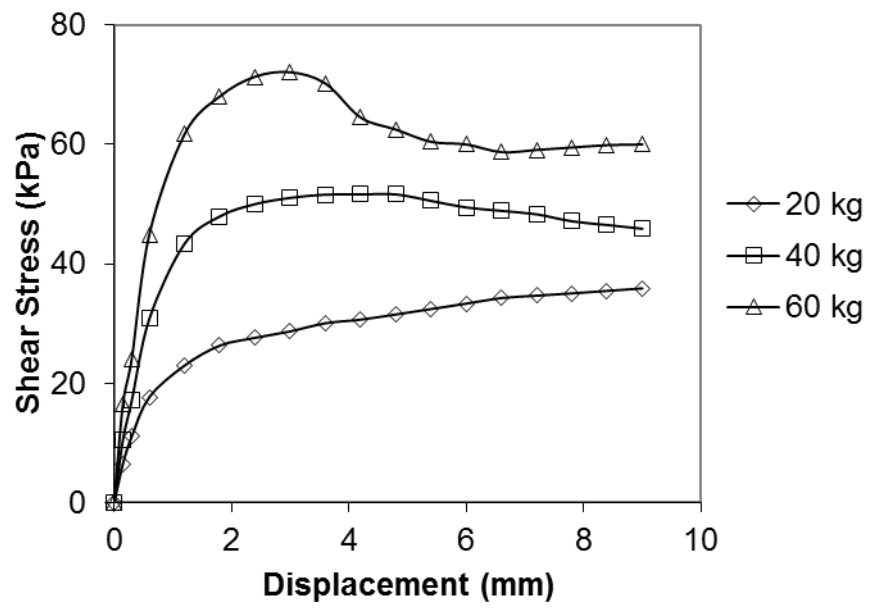
Original CH



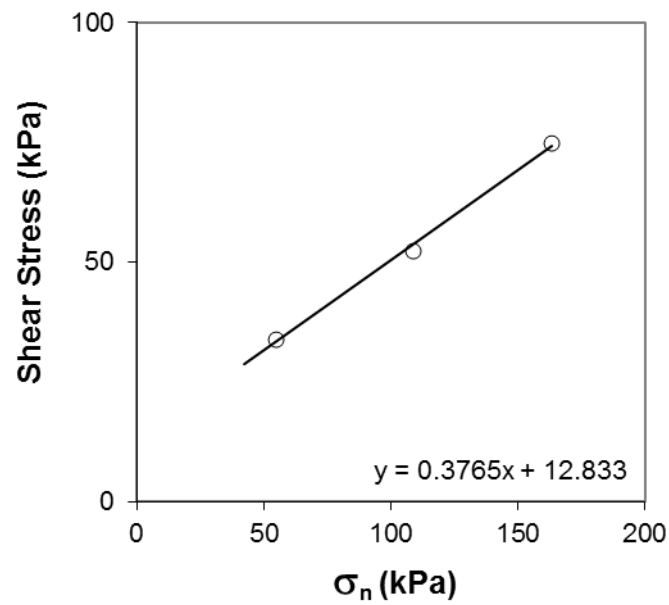
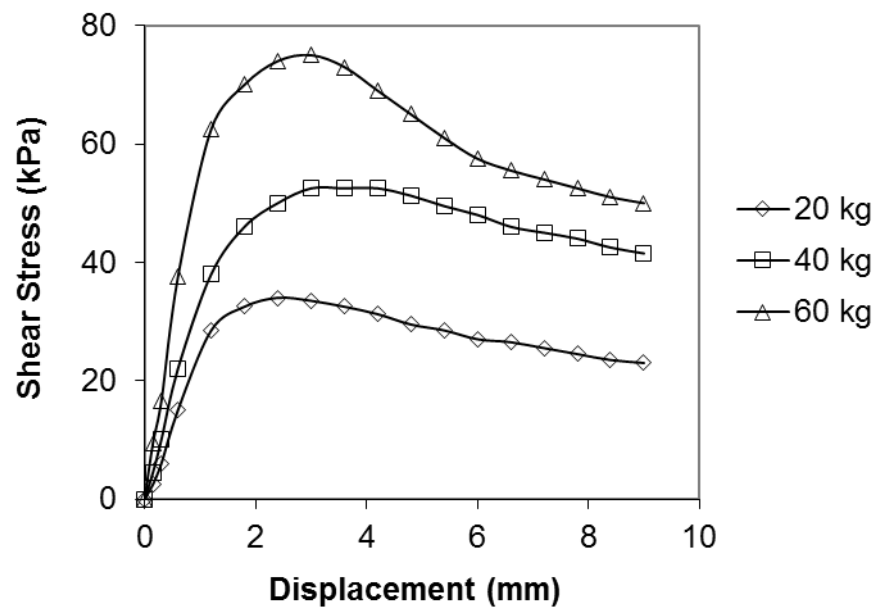
CH, 1. FT Cycle



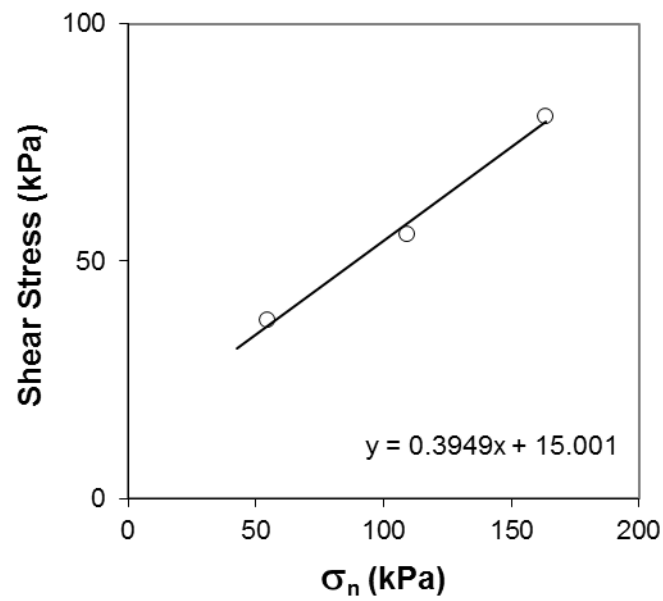
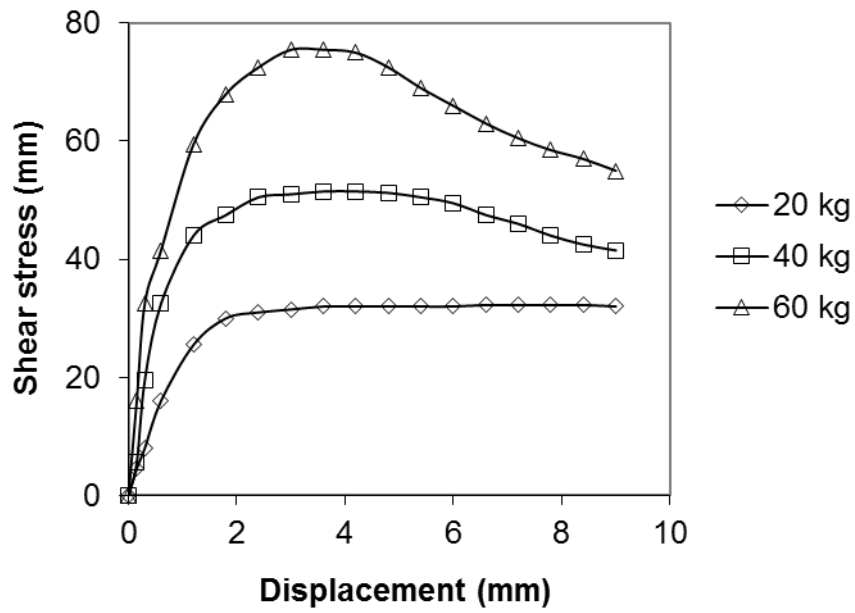
CH, 3. FT Cycle



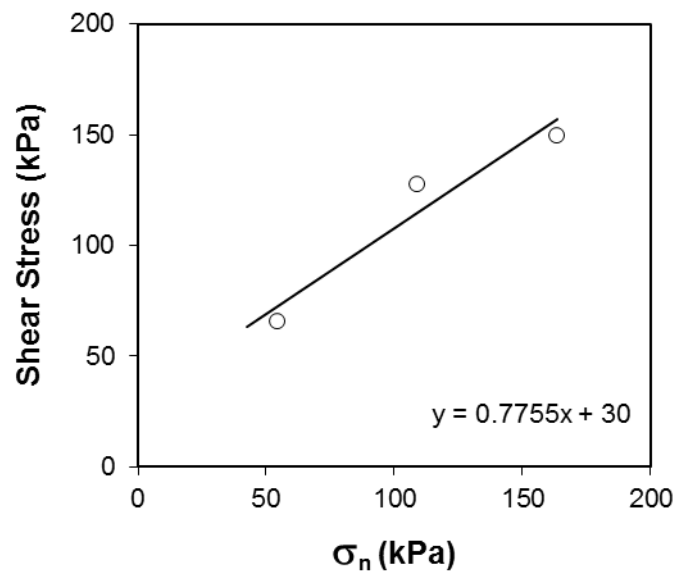
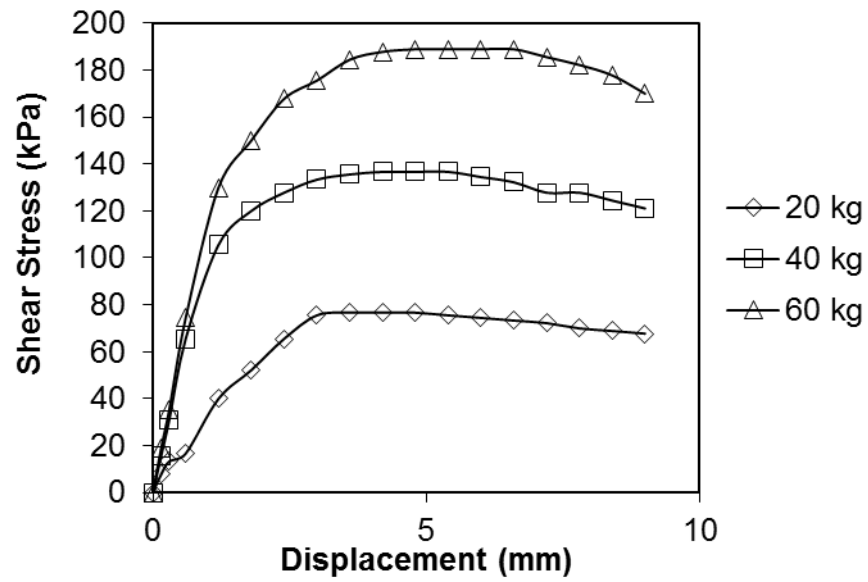
CH, 7. FT Cycle



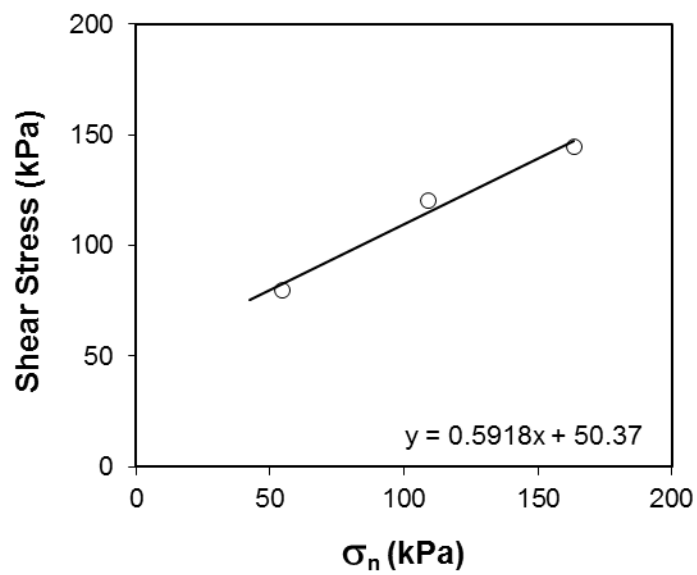
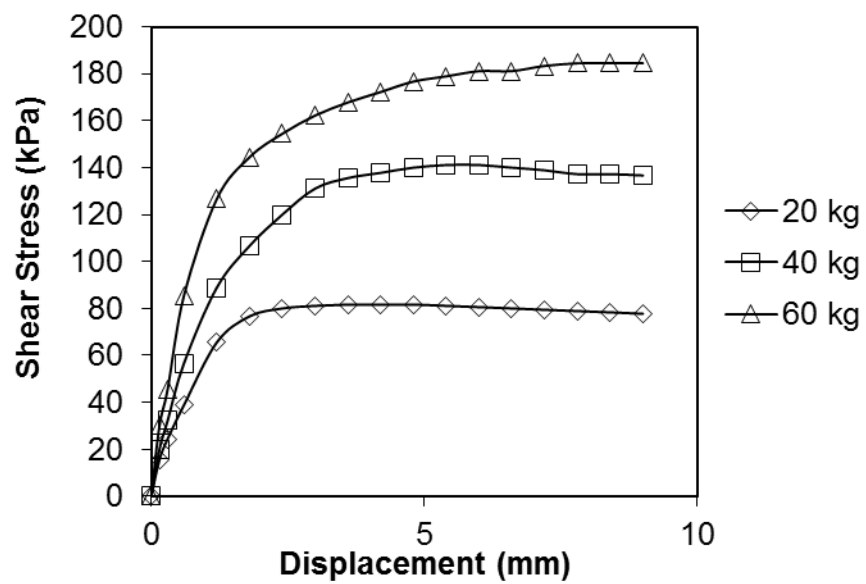
CH, 14. FT Cycle



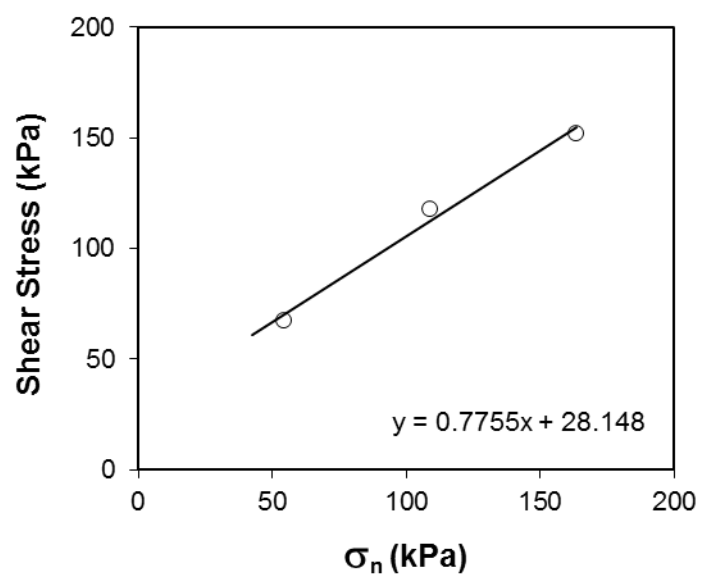
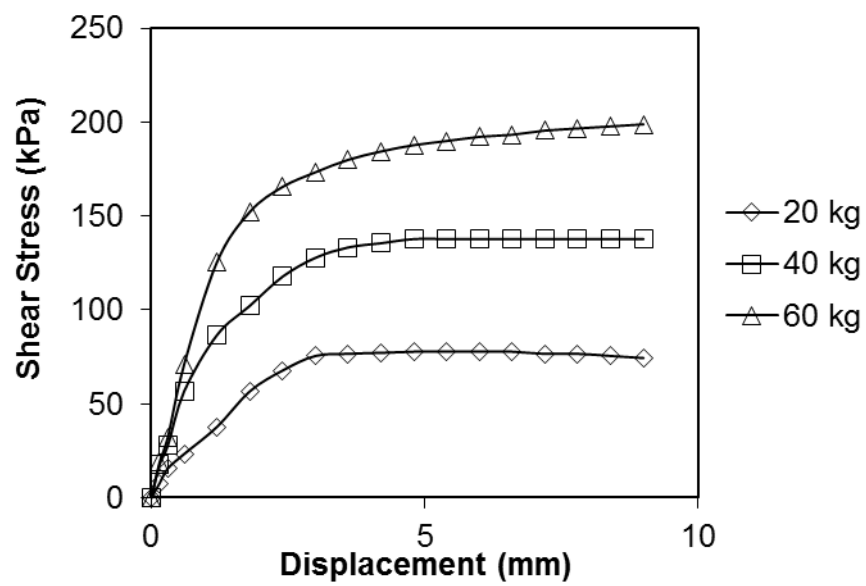
CH, 21. FT Cycle



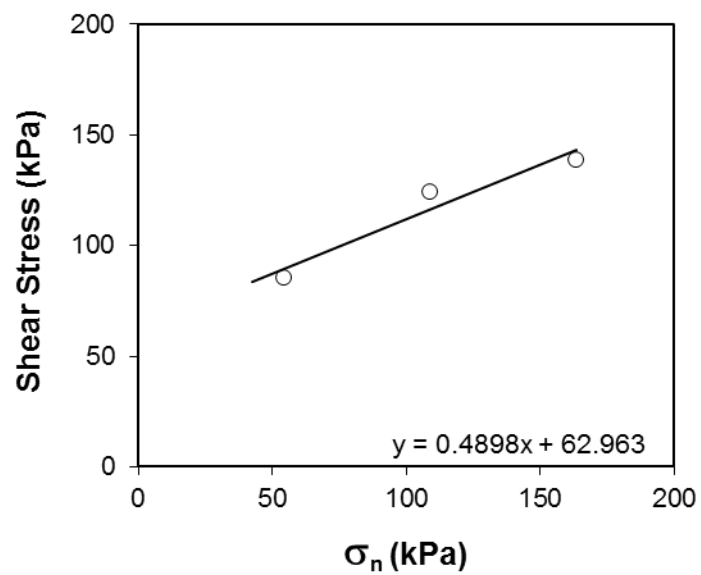
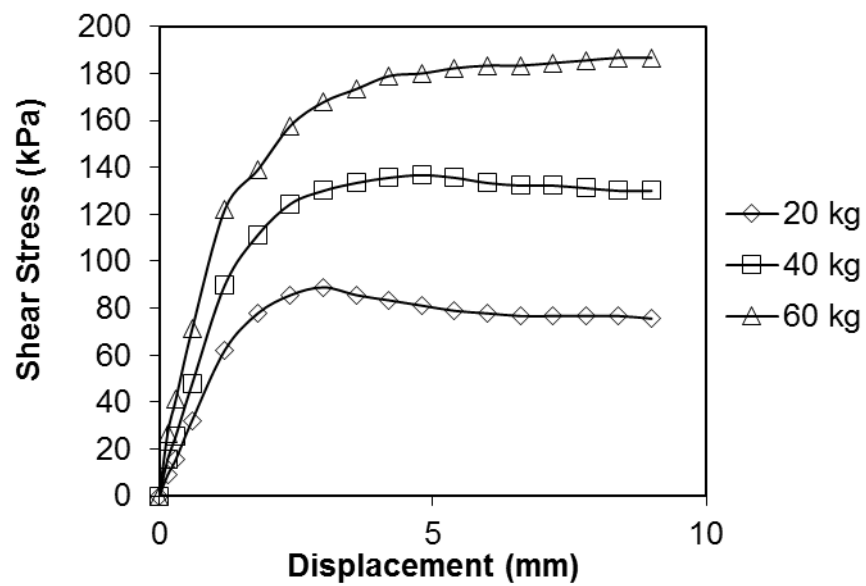
Original SC



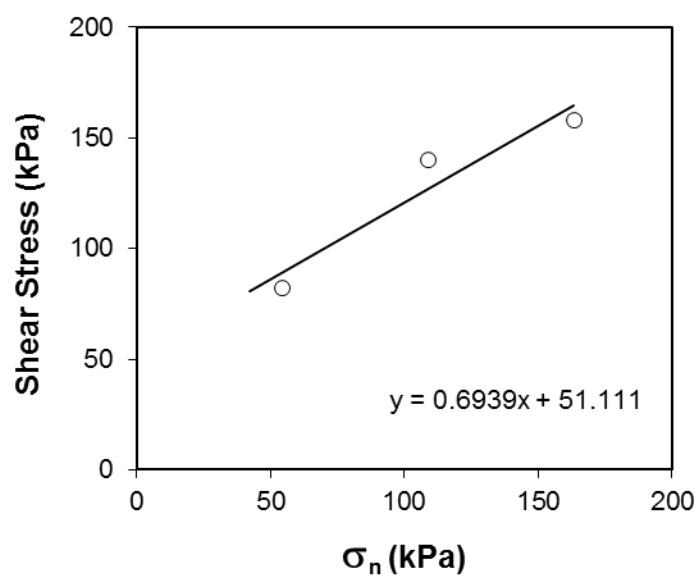
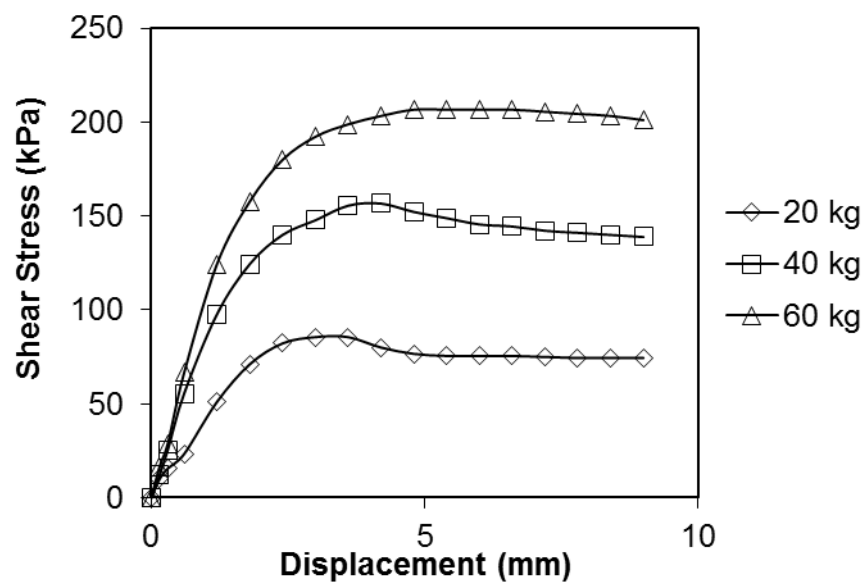
SC, 1. FT Cycle



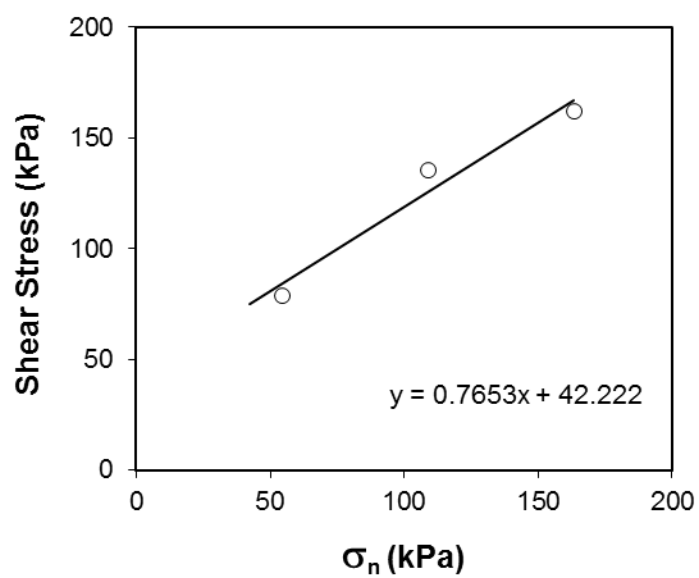
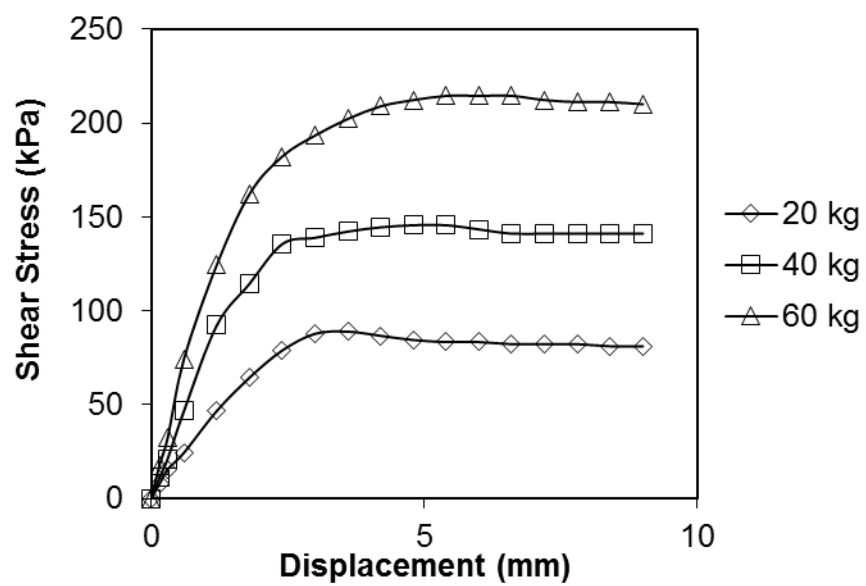
SC, 3. FT Cycle



SC, 7. FT Cycle



SC, 14. FT Cycle



SC, 21. FT Cycle

Curriculum vitae

Credentials

Name, Surname : Parisa ADELİ GHAREH VİRAN

Place of Birth : IRAN

Marital Status : Single

E-mail : parisa.adeli1989@gmail.com

Address : Seyran Street, No. 87/14

Education

High School : Parvine Etesami

BSc. : University of Urmia

Foreign Languages

Persian, English

Work Experiences

Areas of Experiences

Geological engineering, soil mechanics

Projects and Budgets

Donma-çözülme toprak zeminlerin deformasyon ve dayanım karakteristikleri üzerine etkisinin incelenmesi, Tübitak Proje No.114Y0888

Publications

Oral and Poster Presentations

2015, 10th International Congress on Civil Engineering, Iran (Investigation of Freezing and Thawing Effects on the Physico-mechanical Properties of Ankara Clay)

2015, European Geoscience Union, Austria (Effects of Freezing and Thawing on Consolidation Behavior of Clayey Soils)